CAR-EBD: Modular Polypeptide Devices for the Small Molecule Regulation of Chimeric Antigen Receptor T cell Activity

Ian Blumenthal

A dissertation

submitted in partial fulfillment of the

requirements for the degree of

Doctor of Philosophy

University of Washington

2023

Reading Committee:

Suzie H. Pun, Chair

Michael C.V. Jensen

Patrick S. Stayton

Hao Yuan Kueh

Program Authorized to Offer Degree:

Bioengineering

University of Washington

Abstract

CAR-EBD: Modular Polypeptide Devices for the Small Molecule Regulation of Chimeric Antigen Receptor T cell Activity

Ian Blumenthal

Chair of Supervisory Committee:

Suzie H. Pun

Department of Bioengineering

The advent of chimeric antigen receptor (CAR) T cell therapies holds immense promise for the future of cancer treatment. However, the vast majority of current CAR T cell therapies are self-guided, relying on endogenous programming to interpret novel receptor signaling, which may lead to poorly regulated and undesirable functional outputs ranging from cytokine release syndrome and neurotoxicity to incomplete tumor control and immunological exhaustion. These failures at both ends of the functional spectrum (hyperfunction and hypofunction, respectively) are the result of an incomplete mastering of the biological underpinnings of T cell activity and differentiation, combined with the inherent complexity of treating tumors with a patient-derived product – each with their own unique genetic background, immunological history, and target-tumor state. I aim to address these limitations by modifying CAR T cells so their activity may be directly regulated through the use of small molecule drugs. I have pursued several design iterations to accomplish this goal.

Regulation is most successfully achieved by genetic fusion of a CAR to an estrogen-analog binding protein domain (EBD) to create CAR-EBD. These EBD regulators are small in size, highly drug-sensitive, exhibit rapid switching kinetics, are transferable between different CARs and other proteins of interest, function *in vivo* and may be engineered to be selectively responsive to different estrogen analogs (e.g., tamoxifen, CMP8, ES8) to provide orthogonal regulation of multiple transgenes. Having successfully demonstrated the advantageous traits of this system, there are many future applications for this technology.

To my friends – for keeping me sane through the long years (and accepting my enthusiastic blathering about T cells).

To my family – for teaching, helping, and trusting me to find and follow my passion.

To my wife, Leila – for your unconditional love, support, and patience that made this all possible.

You all inspire me to achieve.

Table of Contents

Table of Figures

Chapter 1. Introduction

1.1 From TCRs to CARs: A History of Design

The 1980s heralded a rapid expansion in our understanding of immune function with the identification of the T cell receptor (TCR) as the surface protein that defined T cell clonality and mediated T cell recognition of foreign vs self [1, 2]. By the end of that decade, appreciation of the TCR as the gateway to unlocking T cell agency over other cells sparked the dream of altering this specificity to generate exquisitely targeted, self-propagating, long-lasting, anti-microbial and anti-cancer therapies – 'living drugs' [3]. It has taken over 25 years, hundreds of millions of dollars, and many, many millions of work hours to translate these insights to the clinic, but the advances of the last two decades have finally brought adoptive T cell therapies into the medical limelight.

Efforts to redirect T cells have adopted several formats. The first is direct engineering of the variable regions of the TCRα and ß chains to generate *de novo* or selected binders. Once a stable TCR with a given specificity is created, it may then be transferred to T cells through a variety of genetic engineering approaches [4]. While engineered TCRs have the advantage of surveying the entire array of intracellular proteins through interaction with MHC-peptide complexes, they are also limited to targeting antigens amenable to MHC presentation, and generating TCRs with arbitrary specificity poses a technical challenge due to the intricacy of TCR complex interactions in T cell activation (Figure 1). In

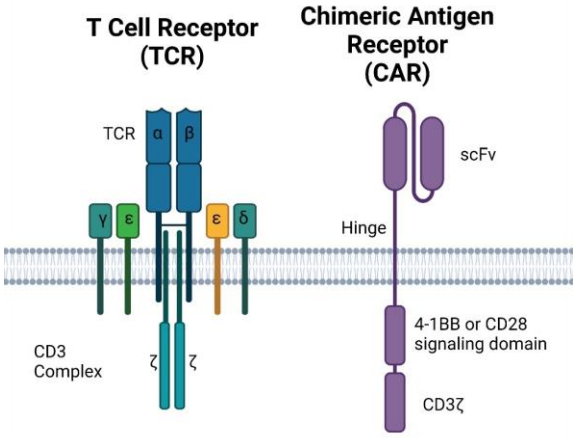

Figure 1. *Comparison of TCR and CAR composition. Produced with BioRender.*

contrast to this are synthetic receptors created through protein fusions, such as chimeric antigen receptors (CARs). CARs are composed of multiple human protein parts, including a targeting domain, a hinge region, a transmembrane domain, and one or more intracellular signal transducers (Figure 1). Antigen recognition is most often achieved with a single-chain variable fragment (scFv) derived from an antibody. By design, this allows for MHC-independent T cell activation, greatly increasing the flexibility in target selection. This is then connected to a hinge region that acts as a spacer between the scFv and the transmembrane domain. This spacer increases the conformational flexibility for antigen binding, and there is a growing body of evidence highlighting the importance of this region in modulating CAR activity [5]. The cytoplasmic signaling domain is typically comprised of a CD3ζ activation motif (immunoreceptor tyrosine-based activation motifs -- ITAMs) borrowed from the TCR. Additional signaling domains may also be included, with second and third generation CARs daisy-chaining co-stimulatory domains (e.g., CD28/4-1BB) in series with CD3ζ to improve T cell activity and longevity. As described, both engineered TCRs and CARs have distinct advantages, however, the ease of design and testing of CARs has enabled rapid iteration and some of the first unequivocally successful applications of adoptive T cell therapies in the clinic. This success has been underscored by hundreds of clinical trials in the United States for the treatment of a wide variety of tumors, and six FDA-approved CAR T cell therapies for the treatment of leukemia or lymphoma through the targeting of CD19 or CD269 (B-cell Maturation Antigen)[6].

However, along with these remarkable successes have arrived some sobering realities. Therapeutic variability, incomplete tumor control, and severe side effects have plagued both CAR T cell clinical trials and post-approval applications. Notably, Kymriah (tisagenlecleucel) and Yescarta (axicabtagene ciloleucel), representing the first cohort of FDA-approved CAR T

cell therapies to market, result in high rates of cytokine release syndrome (CRS) and central nervous system toxicity [7, 8]. These conditions have proven common in many CAR T cell trials treating hematological malignancies and can be life-threatening, preventing the ascension of these therapies to standard-of-care over conventional treatments (e.g., chemotherapy, radiation, immune checkpoint blockade) in spite of the high remission rates they generate [6].

Further limitations of modern CAR T cells have also been observed in trials to treat solid tumors. In comparison to leukemia, solid tumors are typically both densely localized and exhibit much greater agency over their local microenvironment, actively recruiting immunosuppressive cell types, expressing immune checkpoint ligands, manipulating local metabolism, and impeding immune trafficking [9]. Each of these individually interferes with a CAR T cell's antitumor activity, and this enhanced resistance to treatment results directly in CAR T cell dysfunction, as well as demanding longer treatment times to successfully eradicate a solid tumor. Subsequently, protracted treatment timelines can result in T cell differentiation into an "exhausted" phenotype, wherein T cells experiencing chronic antigen exposure undergo changes to their gene expression profiles and chromatin architecture to become progressively hypo-functional – losing proliferative potential and killing capacity, becoming increasingly sensitive to immune inhibition, and finally resulting in cell death [10-12]. T cell exhaustion has been identified as a primary contributor to failure to treat solid tumors with CAR T cells, and while strategies to prevent it have been proposed, clinical success remains elusive [13].

Compounding both of these challenges – high levels of activity leading to CRS/neurotoxicity and low levels leading to failure to treat tumor and exhaustion – are the inherent difficulties in producing bespoke therapies to treat a patient's unique tumor. In order to avoid immune

rejection of the therapy, each CAR T cell patient donates their own T cells to be manufactured into their therapy. As a result, each therapy is singular (reflecting the unique genetic background and immunological history of the patient) and is set with a unique challenge (the specific characteristics of a patient's tumor – tumor burden, target antigen density, mutational profile) [14]. Variable T cell differentiation state following manufacturing, variable engraftment and expansion rates after administration, and variable per-cell anti-tumor activity all result from an incomplete understanding of the immunological processes being manipulating and can contribute to inconsistent patient outcomes [15, 16]. While our understanding of the underlying biological determinants of therapeutic success are rapidly evolving, it is a complicated process that will take decades to elucidate in full [17].

Presently, the potential of CAR T cells remains much greater than we are able to access. In the absence of comprehensive understanding and prediction, the next best thing is control. Current clinical protocols for the treatment of CRS/neurotoxicity involve the administration of high dose corticosteroids or IL-6 inhibitors (e.g., tocilizumab), which may interfere with the therapy's ability to function and target tumor [18]. These interventions function as an effective stopgap for patients experiencing runaway immune reactions, yet the field remains unable to selectively augment CAR T cell activity when and where necessary to achieve positive clinical outcomes against solid tumors. Recent research has highlighted the potential value in transiently resting of CAR T cells to prevent epigenetic changes associated with exhaustion and improve anti-tumor activity [19, 20]. We hypothesize that a pharmacologically regulated system capable of reversibly shielding CAR T cells from target antigen would enable a next generation CAR T cell that is both safer – by providing reversible activity reduction in the event of CRS/neurotoxicity – and more potent – by enhancing the therapeutic longevity through periodic rest. Furthermore, such regulatory capabilities, could

permit the use of CAR T cell potency enhancers that may pose a risk with constitutive activity [21-23].

To address the described needs of a next generation CAR T cell, such a regulation platform would have a number of important traits:

- Stringent on and off states
- Rapid kinetics
- Small genetic payload
- Human-derived to reduce immunogenicity
- Minimal novel elements to reduce FDA regulatory burden
- Easily transferable regulatibility between different CARs or other proteins of interest
- Ability to be multiplexed to allow for the parallel or orthogonal regulation of multiple transgenes

To this end, we have investigated several enabling technologies for such a system. First, we assessed the suitability of small molecule regulated degradation domains ("degrons") for the regulation of CARs and TCR-signaling adapter proteins (Chapter 2). Following a thorough assessment, we ultimately moved on to a related system utilizing endogenous interactions of a human hormone receptor with cytoplasmic chaperone proteins to sterically occlude CAR signaling until the addition of steroid analogs (Chapters 3-7).

Chapter 2. Degron regulation of CARs and TCR signaling adapter proteins

2.1 Introduction

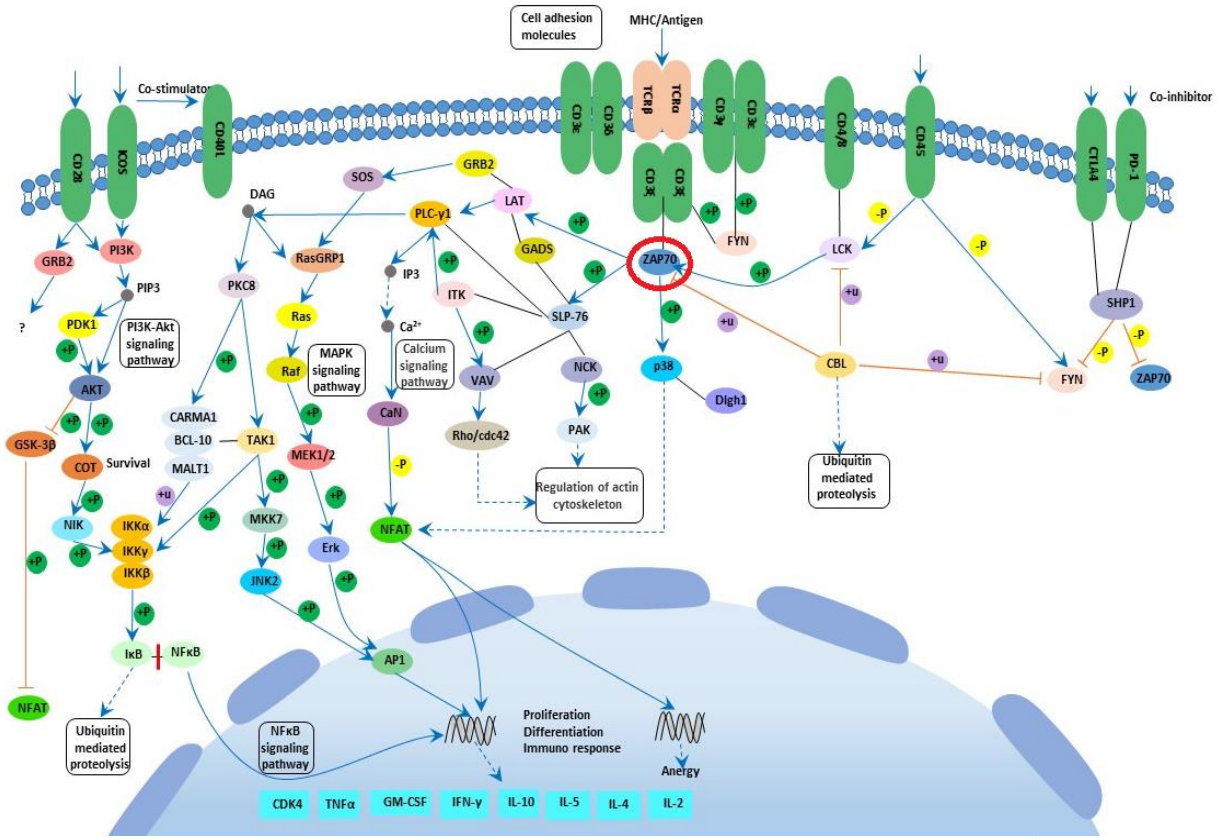

Figure 3. *TCR signaling cascade. Note the TCR in the upper right as well as the adapter kinase Zap70 (circled in red). Produced with BioRender.*

The intracellular signaling network that regulates T cell activation is a highly branched set of recursive and amplifying kinase cascades capable of producing transformative changes in T cells in response to as few as 10 agonist ligands [24]. The extreme sensitivity and fine tuning of these interlaced systems complicates attempts to modify its endogenous function. Indeed, it has been observed that even functional CARs exhibit differences in their signaling properties compared to TCRs (including reduced antigen-sensitivity and altered downstream phosphorylation patterns), which has been hypothesized to contribute to CAR T cells' current

limitations [25]. Importantly, if one's goal is to regulate the full signaling pathway – as ours is – there are limited options available, namely the CAR/TCR itself and a CAR/TCR-proximal tyrosine kinase, Zap70, which serves as the final unified pathway member before divergence (Figure 2)[26]. In contrast to a CAR, which is already an exogenous protein, for the regulation of Zap70, we rely on inactivating mutations to the kinase domain of ZAP70 that have been previously demonstrated to inhibit TCR signaling in a dominant negative manner through constitutive occupation of the phosphotyrosine moieties on activated CD3ζ [27].

Originally identified as important mediators of steroid signaling in plant development, degradation domains exhibit ligand-dependent stability, granting control over the expression of an arbitrary protein through direct fusion [28]. In this regulatory paradigm, constitutive promoters produce constant levels of mRNA resulting in continual translation of the protein of interest (POI), however, rapid ubiquitination of the degradation domain and subsequent elimination by the proteasome prevents accumulation and activity until it is stabilized by ligand (Figure 3, top) [29]. The opposite is also possible, where ligand binding causes degradation. This is known as a ligand-induced degradation domain (LID) (Figure 3, bottom) [30]. Many of the features of these degron systems align with the desirable properties of a CAR T cell regulatory system as outlined previously: rapid kinetics (~6hrs on; ~10hrs off), small genetic payload (12kDa to 30kDA), easily transferable to new POIs, and

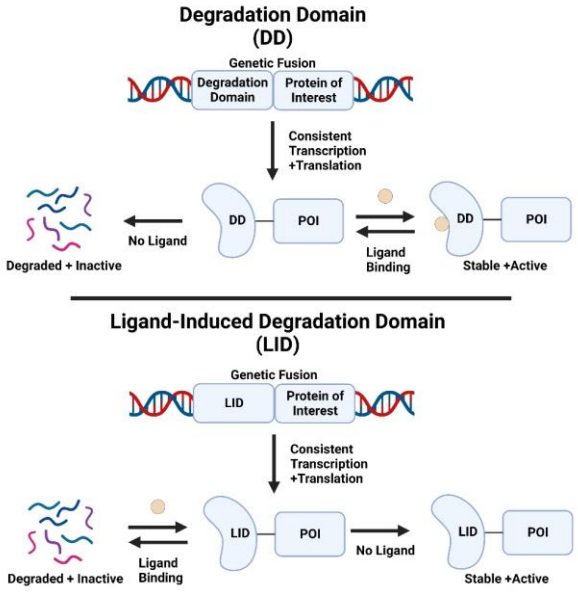

Figure 5. *Depiction of the function of degradation domains (DD; "ligand-on") and ligand induced degrons (LID; "ligand-off"). POI = protein of interest. Produced with BioRender.*

multiple degron variants (human FKBP12, e coli DHFR, human ER1α) and associated inducer molecules (SHIELD-1, Trimethoprim, 4-hydroxitamoxifen/CMP8, respectively) [31, 32]. Of particular interest to us was the use of engineered human estrogen receptor 1 alpha ligand binding domain (ERαLBD) degrons (huERdd and huERLID) with estrogen analogs. Importantly, this combination is composed of human parts, reducing the likelihood of construct immunogenicity. Also, the ERαLBD has FDA-approved ligands that are well tolerated in patients to micromolar concentrations [33]. Specifically, Tamoxifen – and its active metabolite 4-hydroxytamoxifen (4-OHT) – is an estrogen receptor antagonist indicated for use in breast and ovarian cancers. Finally, there are published mutations to the binding pocket of the ERαLBD which dramatically reduce affinity for endogenous hormones while maintaining high affinity for (Z)-4-OHT [34]. This allows for a regulation platform that is half-orthogonal to patient biology (since (Z)-4-OHT still interacts with wild type estrogen receptors). Full orthogonality is further achievable through the introduction of additional mutations which enable the binding of CMP8, a novel estrogen analog that does not bind unmodified estrogen receptor [34].

In this study, we aimed to validate degron functionality (which had previously only be tested in mouse embryonic fibroblasts) in human T cells through genetic fusion to fluorescent proteins. Subsequently, we tested whether degron-based regulation was sufficient to modulate CAR receptor signaling through genetic fusion to the FMC63 CD19CAR as well as genetic fusion to a dominant negative version of Zap70 [27]. We found that degrons function similarly in human T cells as they do in mouse fibroblasts. However, the stringency of these systems varied significantly, especially in T cells. Unexpectedly, we found some T cell functional outputs were more amenable to regulation than others. Ultimately, external forces

resulted in the abandonment of this regulatory strategy during optimization, however, the lessons we learned have proven invaluable in our future pursuits.

2.2. Results

2.2.1 Degradation domains derived from the human ERαLBD regulate protein expression in human T cells.

Previous studies exclusively tested the huERdd and huERLID in 3T3 mouse embryonic fibroblasts. In order to demonstrate feasibility and achieve a better understanding of the function of this system in human T cells, we created a fluorescent protein reporter system composed of eBFP2 fused to huERdd and mCherry2 fused to huERLID (Figure 4A). Jurkat T cells were transduced using lentivirus containing these constructs, and were magnetically sorted for expression of a truncated EGFR reporter gene (EFGRt) (Figure 4B – see Methods for details). Jurkat cells expressing these constructs and treated with 5 micromolar inducer molecule (either (Z)-4-OHT or CMP8) for 24 hours exhibited more than a 6-fold increase in median fluorescence intensity (MFI) as measured by flow cytometry (Figure 4C) (huERLID data similar, but not shown). To determine the range of sensitivity of these constructs to induction, dose response curves were generated using serial dilution of inducer molecules (Figure 4D-F). eBFP2-huERdd exhibited a maximum 5.95x increase in MFI from baseline upon addition of increasing concentrations of (Z)-4-OHT, with an EC50 of 52nM. The same construct exhibited a maximum 11.9x increase in MFI from baseline upon addition of increasing concentrations of CMP8, with an EC50 of 48nM. mCherry2-huERLID exhibited a 7x decrease in MFI from baseline to maximum destabilization. These changes reflect a dose

response over 2 full orders of magnitude of drug concentration, and highlight the use of multiple inducer molecules to alter gene expression both up and down using degradation domains in Jurkat T cells. Of note, the huERdd system demonstrated a greater dynamic range than the huERLID domain, though neither degron system was particularly stringent in the "off" state. eBFP2-huERdd maintained low but significant eBFP2 expression in the absence of induction (compare the light blue histograms in Figure 4B and 4C), and mCherry2-huERLID maintained strong mCherry expression even when fully induced. To investigate this phenomena, we tested the interaction between multiplicity of infection (MOI) and MFI fold change of the eBFP2-huERdd construct (Figure 4G). This identified a consistent relationship between the average copy number of the construct and the baseline expression of our fluorescent protein in the off state, with concomitant increases in maximum induction that max out around an MOI of 5. Given the degree of leaky expression even at the lowest MOIs, this highlights the need for fine tuning, both of copy number and of the promoter driving gene expression, if off-state stringency is to be achieved.

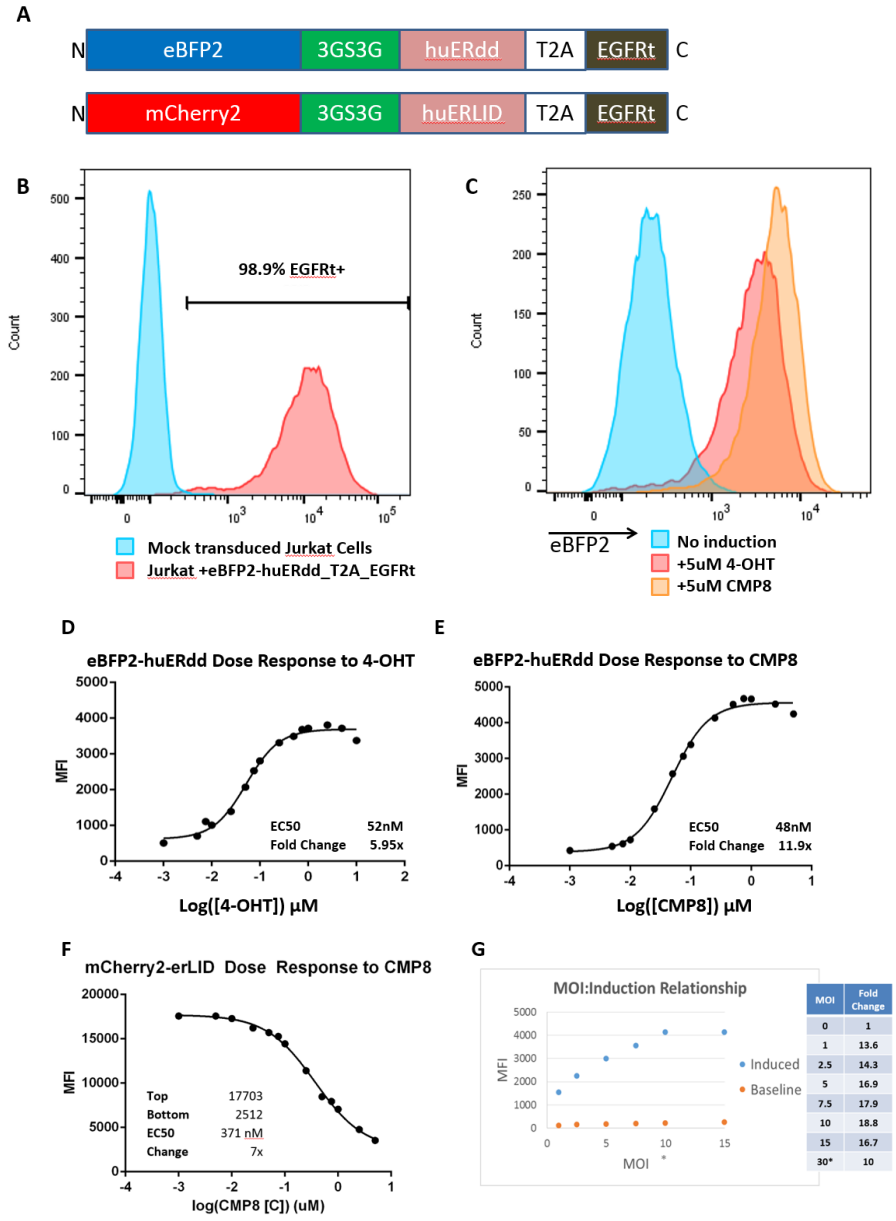

Figure 8. *Degradation domains derived from the human ERαLBD regulate protein expression in human T cells.*

A) Construct schema – fluorescent proteins were genetically fused to their respective degrons by a 3GS3G linker. Each construct contained a transduction marker (EGFRt) following a ribosomal skip sequence. Constructs were packaged in engineered lentivirus (see Methods) and expressed by an EF1a promoter. B) Jurkats were magnetically sorted based on the presence of the transduction marker (EGFRt)(huERLID was also >95% pure – not shown). C) eBFP2-huERdd positive Jurkat T cells were cultured in the presence or absence of 5 micromolar inducer molecule (as described) for 24hours, then fixed and run on a flow cytometer. D-F) Dose response curves of eBFP2-huERdd and mCherry2-huERLID to inducer molecules. Cells were cultured in the relevant concentration of drug for 24 hours before being fixed and run on a flow cytometer. G) Investigation into the effect of viral multiplicity of infection (MOI) on the inducibility of the eBFP2-huERdd system in Jurkat T cells.

2.2.2 The success of regulation of T cell activation with the huERdd degron depends on degradation target and functional output

The existing literature on degrons suggests that cytoplasmic proteins are more tightly regulated than membrane bound ones [31]. Following this lead, the first construct we tested was a dominant negative version of the tyrosine kinase Zap70 regulated by the huERdd degron domain (dnZap70-huERdd). Early testing in transduced and purified Jurkat cells exposed to CD3/CD28 stimulation beads demonstrated this construct has no ability to shield T cells from receiving activation signals (Figure 5). In spite of this setback, our success in the regulation of fluorescent proteins drove us to further test the huERdd degron in the regulation of the activity of the "gold-standard" FMC63 CD19CAR (Figure 6A). In similar fashion to the fluorescent protein constructs discussed previously, the CD19CAR-huERdd constructs are under the control of an EF1a promoter and include a truncated EGFR as a transduction and sorting marker (Figure 6B). Expression of both the CD19CAR control (~50kDa) and CD19CAR-huERdd (~75kDa) in primary CD8 T cells was confirmed by western blot by staining for the CD3ζ domain of both constructs (Figure 6C). Construct expression was quantified relative to endogenous CD3ζ allowing for relative comparisons between the constitutively active (ca) construct at an MOI of 1 and the degron construct at a range of MOIs (1, 3, 6). At baseline without induction, the expression of the CD19CAR-huERdd was 4.1-7.4% (depending on MOI) of the expression of the caCD19CAR under the same promoter. Upon induction with 5 micromolar CMP8 for 24hrs, this increased to 11.7-22.1% of the caCD19CAR (NB: expression of the caCD19CAR does not change in response to incubation with CMP8; data not shown). These data are in accordance with our observations of the fluorescent reporter system in Jurkat cells, though the fold change over baseline is less (~3-fold). That the baseline and induced transgene expression levels are so much less than the caCD19CAR under the same promoter was a surprise and not reported in the literature,

however the difference in expression observed between the huERdd and huERLID systems helps place this difference in context.

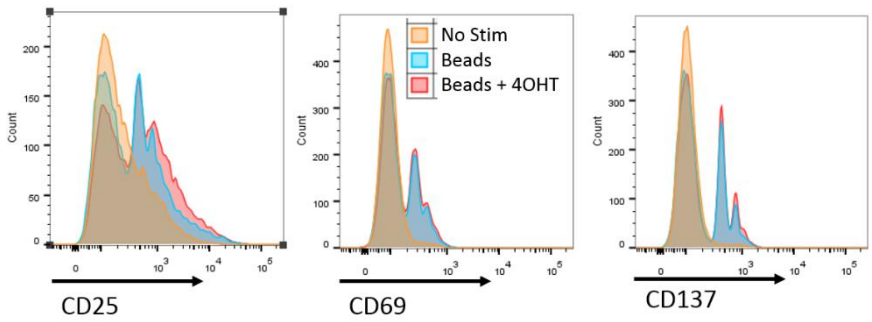

Figure 11. *Regulation of TCR activation in Jurkat T cells expressing dnZap70-huERdd.* Jurkat T cells purified for the expression of a dnZap70-huERdd_T2A_EGFRt construct were incubated with or without 1 micromolar (Z)-4-OHT for 24hrs, then exposed to CD3/CD28 stimulation beads for 12 hours before being stained for expression of CD25, CD69, and CD137 (early markers of TCR activation).

Functional studies were performed on primary human CD8 T cells expressing either the caCD19CAR or the CD19CAR-huERdd. A cytokine release assay was performed against K562 tumor cell lines expressing either CD19 (experimental condition), OKT3 (positive control), or parental (negative control) (Figures 7A and B). While there was anomalous variability within the experiment (e.g., mock and caCAR T cells producing greater cytokine in the presence of 1 micromolar (Z)-4-OHT), the CD19CAR-huERdd T cells evidently increased their IFN-γ cytokine production upon induction with both (Z)-4-OHT and CMP8. IL-2 and TNF-α production responded significantly less to exposure to antigen under induction with both molecules, though this is expected of CD8 T cells. A chromium release assay was also performed against the same K562 tumor lines to assess the ability of huERdd regulation to control target-specific lysis in the absence of induction (Figures 7C and D). In contrast to our observations with cytokine release, we saw no ability to regulate target-specific lysis in the off-state. Though importantly, the addition of a genetic fusion to huERdd

did not impede the functionally of the T cells in this assay. Unexpectedly, we did see a marked drop in cytolytic ability in all cells in the 1 micromolar CMP8 condition for which we do not currently have an explaination (Figure 6D). These results clearly illustrate the complexity of CAR signaling in the determination of activity, demonstrating differential regulation between different functional outputs. They also suggest that CAR T cell cytokine production and target-specific lysis are robust to large changes in CAR expression.

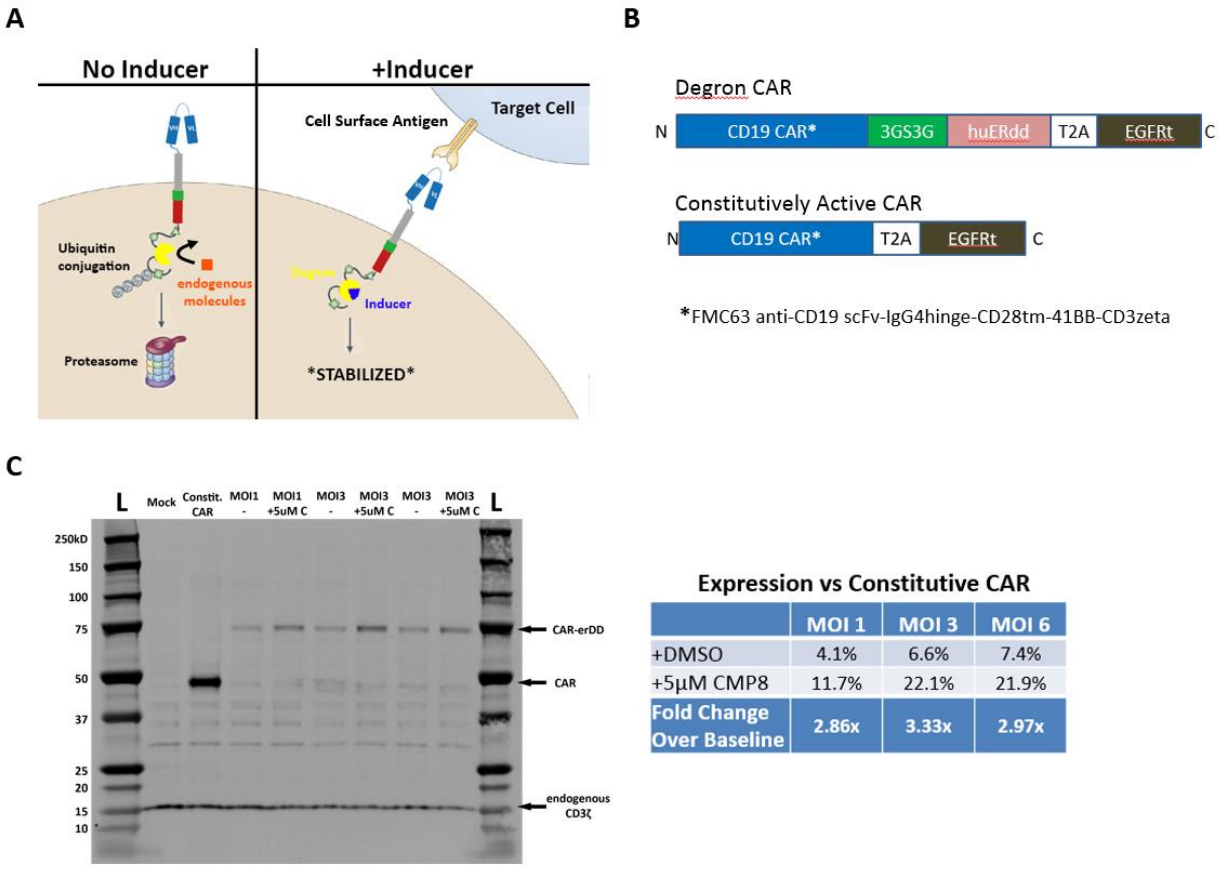

Expression vs Constitutive CAR

	MOI 1	MOI 3	MOI 6
+DMSO	4.1%	6.6%	7.4%
+5µM CMP8	11.7%	22.1%	21.9%
Fold Change Over Baseline	**2.86x**	**3.33x**	**2.97x**

Figure 14. *CD19CAR-huERdd is expressed in primary human T cells.*

A) CD19CAR-huERdd construct function schema. B) Degron-controlled CD19CAR and constitutively active CD19CAR construct composition schema. C) Western blot demonstrating CD19CAR-huERdd expression in primary human CD8 T cells at different MOIs in the presence and absence of 5 micromolar CMP8 (24hr incubation) compared to expression of the constitutive CAR. Companion table showing quantification of CD19CAR/CD19CAR-huERdd bands to each other, after normalization to endogenous CD3ζ expression.

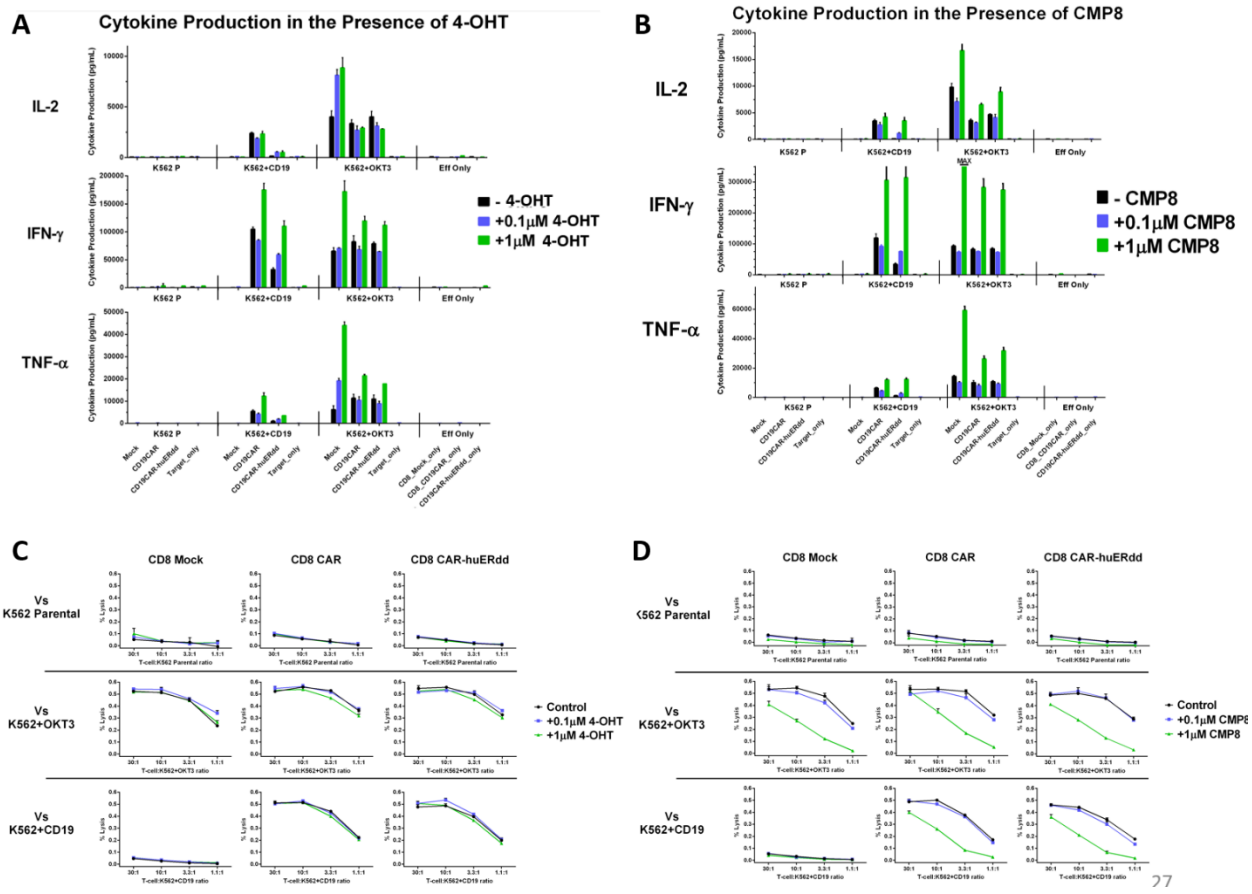

Figure 17. *The success of regulation of the FMC63 CD19CAR with the huERdd degron depends on functional output.*

All T cells were incubated in the relevant drug and concentration for 24hrs prior to the initiation of functional studies. A) A cytokine release assay was performed comparing the cytokine release of CD8 T cells carrying the caCD19CAR to CD8 T cells carrying the CD19CAR-huERdd and exposed to an antigen expressing tumor line (K562+CD19) and appropriate controls in the presence or absence of inducer molecule at the described concentrations. B) A chromium release assay was performed comparing the antigen-specific lysis of CD8 T cells carrying the caCD19CAR to CD8 T cells carrying the CD19CAR-huERdd and exposed to an antigen expressing tumor line (K562+CD19) and appropriate controls in the presence or absence of inducer molecule at the described concentrations.

2.3 Summary and Future Directions

Initial testing in Jurkat T cells was positive. We demonstrated wide dose response ranges for both the huERdd and huERLID systems over multiple orders of magnitude of inducer drug concentration, all in clinically relevant ranges. We also began to investigate the relationship

between transgene copy number and fold induction over baseline, with the goal of optimizing how the constructs were delivered and expressed. However, the limited stringency of the off state for both degrons was concerning from the beginning, and further in vitro testing of the CD19CAR-huERdd system in CD8 T cells raised significant concerns for the platform's viability after demonstrating no ability to regulate antigen-specific killing. While the switching activity we observed in controlling cytokine release demonstrated that there may be potential after optimization of promoter strength, it remains impressive that 5% of caCAR expression is sufficient to achieve equivalent antigen-specific killing in a chromium release assay. While it increases the difficulty of optimizing the huERdd system, it suggests that the amount of CAR we are expressing on CAR T cells may be in vast excess. For CARs known to suffer from tonic signaling, this information may be especially relevant information and provide fruitful impetus for future investigation.

In spite of these early speed bumps, much work was planned for optimization (additional promoters, additional linkers, additional CARs, additional degrons), and initial testing was performed demonstrating repeated on/off cycling of the huERdd and huERLID systems without additional loss of stringency or leakiness (data not shown). Furthermore, a collaboration was started with the Stayton lab at UW, using the eBFP2-huERdd degron reporter system and a FITC-specific CAR in conjunction with CMP8 and FITC loaded polymer-backbone "drugamers" to load T cells with linear "backpacks" that provide local release of degron-stabilizing drug over time (Figure 8). This work resulted in a patent and a publication [35, 36].

The potential applications of this technology to CAR T cells, and adoptive cellular therapies in general, are diverse and exciting. However, after learning of the public announcement of Obsidian Therapeutics – a company based in part on the use of degron technologies, branded

as cytoDRiVE® – the decision was made to pivot to alternative means of cellular control. Subsequent work by the groups degron development and T cell engineers at Stanford and UCSF has been impressive, and I remain excited to see how these technologies develop [20].

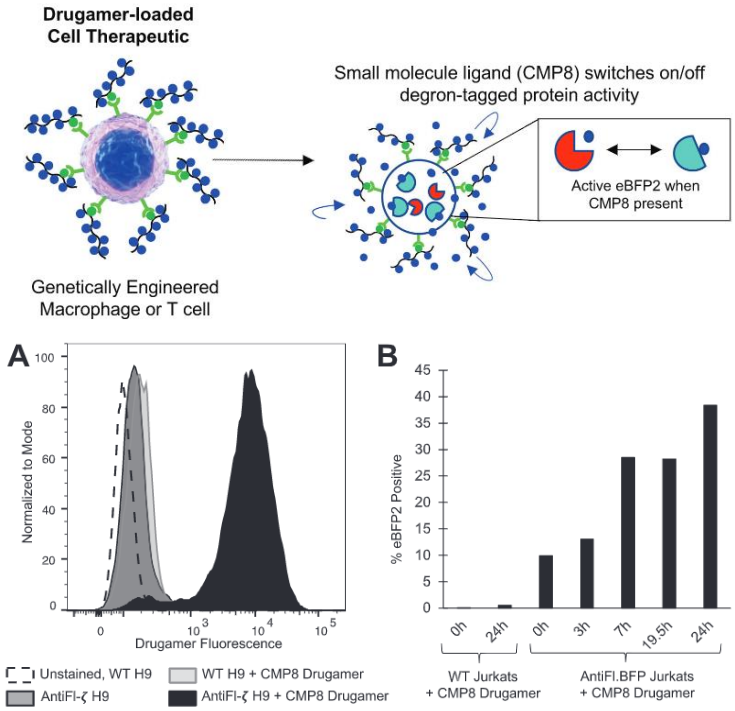

Figure 20. *Arming engineererd T cells with CMP8 drugamer activates the degron-tagged transgene, eBFP2-ERdd, and increases intracellular protein fluorescence activity through sustained local drug release.*

Top) Schematic mechanism of polymeric prodrug "drugamer" loading on engineered cell therapeutics. Immune cells are engineered with a bioorthogonal and humanized scFv receptor that binds to polymeric prodrugs via a high affinity receptor–ligand binding reaction. The polymeric pro-drugs sustain the release of small molecule drug cargo via tunable linker design and selection. The versatility of this platform was demonstrated by arming genetically engineered Tcells with a drugamer A) The immortalized T cell line, H9, was the versatility of AntiFITC expression and function in different immune cell classes. AntiFl H9s were loaded with CMP8 drugamer and drugamer fluorescence was compared against drugamer-loaded wild type (WT) and AntiFl H9 controls with no drugamer loading. B) Jurkat T cells were cotransduced with AntiFl and a transgene encoding for a degron-tagged fluorescent protein, eBFP2 (AntiFl.BFP Jurkats). Arming of AntiFl.BFP Jurkats with CMP8 drugamer resulted in increased eBFP2 fluorescencedetection induced by the gradual release of CMP8 from the drugamer when compared to a CMP8 drugamer-loaded WT Jurkat control. eBFP2 fluorescencedetection from CMP8 drugamer-loaded AntiFl.BFP Jurkats increased steadily over 24h.

Chapter 3. CAR-EBD – Initial forays into leveraging protein-protein interactions to modulate CAR T cell activity

3.1 Introduction

Our experiences with drug-regulated estrogen receptor-derived degradation domains brought to our attention a wide array of existing modifications to and applications of estrogen receptor alpha ligand binding domains (ERαLBD) [37, 38]. Many of these systems have been invaluable to the scientific community for their ability to modulate gene expression, either directly through driving transgene expression (e.g., the HEA3 and HEA4 synthetic transcription factors), or indirectly by using fusions with Cre to control the spatial and temporal expression of target gene(s) in animal models [39]. The majority of these applications leverage the useful intracellular localization characteristics of the estrogen receptor to control the transcription of other genes or transgenes. In brief, endogenous estrogen receptors (ERα and ERß) are expressed in the cytoplasm of a cell in complex with heat shock proteins (HSP), especially HSP90, through their ligand binding domain [40]. Upon encountering an estrogen molecule, the interaction between the estrogen receptor and HSP90 is disrupted, allowing two estrogen receptors to make a homodimer around a molecule of estrogen. This dimer subsequently translocates to the nucleus and binds estrogen-responsive elements in the genome with its DNA-binding domain in order to drive downstream gene expression [41]. By isolating just the ligand binding domain of the estrogen receptor, and expressing it in genetic fusion with other protein domains, novel function can be achieved [34].

While estrogen-binding domain (EBD) use in regulating transcriptional events is common in the literature, as are studies investigating the impact of HSP90 on the trafficking and function of its chaperone partners, there have been few examples of successfully using the binding of HSP90 to EBDs to regulate cytoplasmic processes [42]. However, since HSPs are distributed throughout the cytoplasm, in theory, such sequestering and/or steric interactions should be possible. With our application to CAR T cells in mind, a "CAR-EBD" construct would be constitutively present on the cell surface, but only capable of signaling upon administration of estrogen and the subsequent dissociation of HSP90 (Figure 9A).

Critical to this application is the ability to achieve orthogonality to host biology. As discussed previously, mutations have been identified that prevent binding of endogenous estrogens to mutant ERαLBD. Some of these mutations retain similar affinities for estrogen analogs, while some contain alterations that increase affinity for specific analogs, while still ablating affinity for endogenous estrogens (e.g., the ERT2 domain) [37]. As we saw with degrons, some of these mutations are compatible and may build off of each other, wherein sets of mutations for blocking endogenous estrogen binding may be supplemented with additional mutations that enable binding to novel estrogen-analogs (e.g., CMP8-binding domains) [34]. For use in this study, we have compiled a set of mutated ERαLBDs specific for a variety of estrogen analogs (Figure 9B). These include ERT2 (re-dubbed EBD(4OHT) for use in these studies), a CMP8-responsive EBD (dubbed EBD(CMP8)), and an EBD mutant responsive to a carboxylated estrogen, ES8 (dubbed EBD(ES8)).

We hypothesize that the genetic fusion of these EBDs to the carboxyl-terminus of a CAR will enable drug-regulation of the activities of the CAR through the physical occlusion of the tyrosine kinases (namely, Zap70 and Lck) necessary to transduce activation signals from the cell surface to the cytoplasm. In theory, this regulation would occur in a manner that fulfills

all of the desirable traits outlined previously, including stringent on and off states (constant CAR-EBD expression promotes stable interactions with HSP90), rapid and reversible kinetics (no transcription or translation necessary), small genetic payload (~25kDa for every EBD), utilizing a human-derived protein to reduce construct immunogenicity, having the potential to use already FDA-approved estrogen-analogs for activity regulation (tamoxifen metabolites), readily transferable between different CARs and other proteins of interest, and readily multiplexible for use in the parallel or orthogonal regulation of multiple transgenes.

To this end we have generated a large library of CAR-EBDs composed of different CARs, linkers, and EBDs (Figure 9C). CARs used include a human-derived CD19CAR (huCD19CAR [43]), a B7H3CAR [44], a 806CAR [45], and a CD22CAR [17]. Linkers used include direct fusion ("0Gly"), 1 glycine, 2 glycines, and 3 glycines. This narrow range was chosen in response to early data underlining the importance of proximity to the CD3ζ domain and suggesting that the margin for error between functional and non-functional may be both very small and differ from CAR to CAR. As previously described, we tested 3 EBD domains with differing mutations that confer sensitivity to different drugs (Figure 9B.

So far, we have tested many of these constructs extensively in vitro in both Jurkat T cells and primary human T cells. As predicted, many are highly functional, though this varies between CARs, linkers, and EBDs. Additional optimization may be required to achieve the necessary off-state stringency for some CARs. Our most developed data sets exist for the B7H3CAR regulated by each EBD variant and connected by a 3Gly linker, as well as the huCD19CAR regulated by EBD(4OHT) and connected by a diversity of linkers (0Gly, 1Gly, 2Gly, 3Gly). Most of the data presented here will be of these constructs. In composite, this new "CAR-EBD" platform for the regulation of CAR T cell activity works well and is robust to a wide variety of use cases.

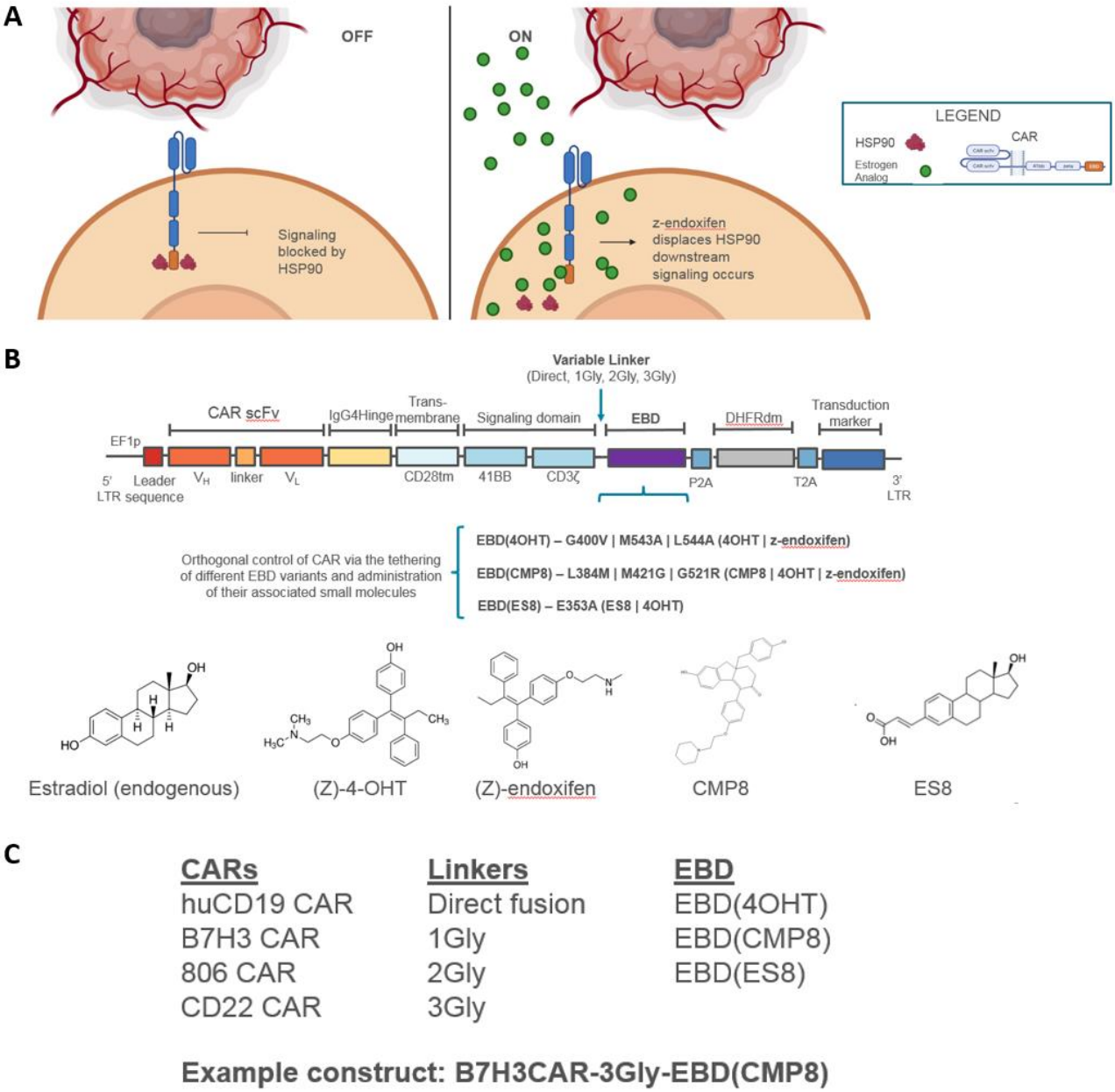

Figure 21. CAR-EBD construct design and proposed mechanics. Produced in BioRender.

A) CAR-EBD functions through interactions with cytoplasmic protein chaperones (such as HSP90) that block CAR signaling until an estrogen-analog is administered, disrupting the interaction. B) CAR-EBD is constructed by taking an existing CAR and adding an EBD, with or without a linker, to the carboxyl-terminus of the CAR. Importantly, CAR specificity and EBD variant may be altered without breaking the system. Each EBD variant contains a different complement of mutations that enable it to bind different drug sets. None of them bind endogenous estrogens. C) To date, we have tested 4 2nd generation CARs with at least a subset of 4 different linker variants and 3 different EBD variants.

3.2 Results

3.2.1 CAR-EBD enables drug-titratable activation in response to antigen in Jurkat T cells

Initial testing was performed in Jurkat T cells and focused on the use of two cohorts of constructs. These included the huCD19CAR-XGly-EBD(4OHT) construct paired with 1Gly, 2Gly, and 3Gly linkers, as well as the B7H3CAR-3Gly-EBD(XXXX) construct paired with the EBD(4OHT) and EBD(CMP8) variants. Jurkat T cells without a CAR and with the appropriate constitutively active CAR were used as controls. The parental Jurkat line used for CAR-EBD transduction and testing had previously been engineered with a T cell activation-sensitive promoter, iSynPro (for "inducible synthetic promoter"), driving expression of a GFP:ffluc fusion protein (iSynPro manuscript in preparation by other members of the Jensen lab). This construct allows us to read out activation signals from the CAR or CAR-EBD with a fluorescent reporter.

In order to test the stringency of the off state of this system, Jurkat T cells containing iSynPro_GFP:ffluc and the huCD19CAR-XGly-EBD(4OHT) linker variants were treated with 0nM, 100nM, and 500nM (Z)-4-OHT for 24 hours and subsequently exposed to a K562+CD19 tumor line at an effector to target ratio of 2:1 for 24 hours. Every linker variant of the huCD19CAR-XGly-EBD(4OHT) system demonstrated increased activity with drug, though there were differences between the linker variants (Figure 10A). While all linker variants produced similar GFP signals at maximum induction, the off state of the huCD19CAR-1Gly-EBD(4OHT) construct was the most stringent, though still resulted in a small amount of GFP expression in the off state when exposed to target antigen (Figure 10B). Compared to the constitutive CAR, the degree of maximal activation (both in %GFP+ and GFP median fluorescence intensity (MFI)) in each of the linker variants was also similar.

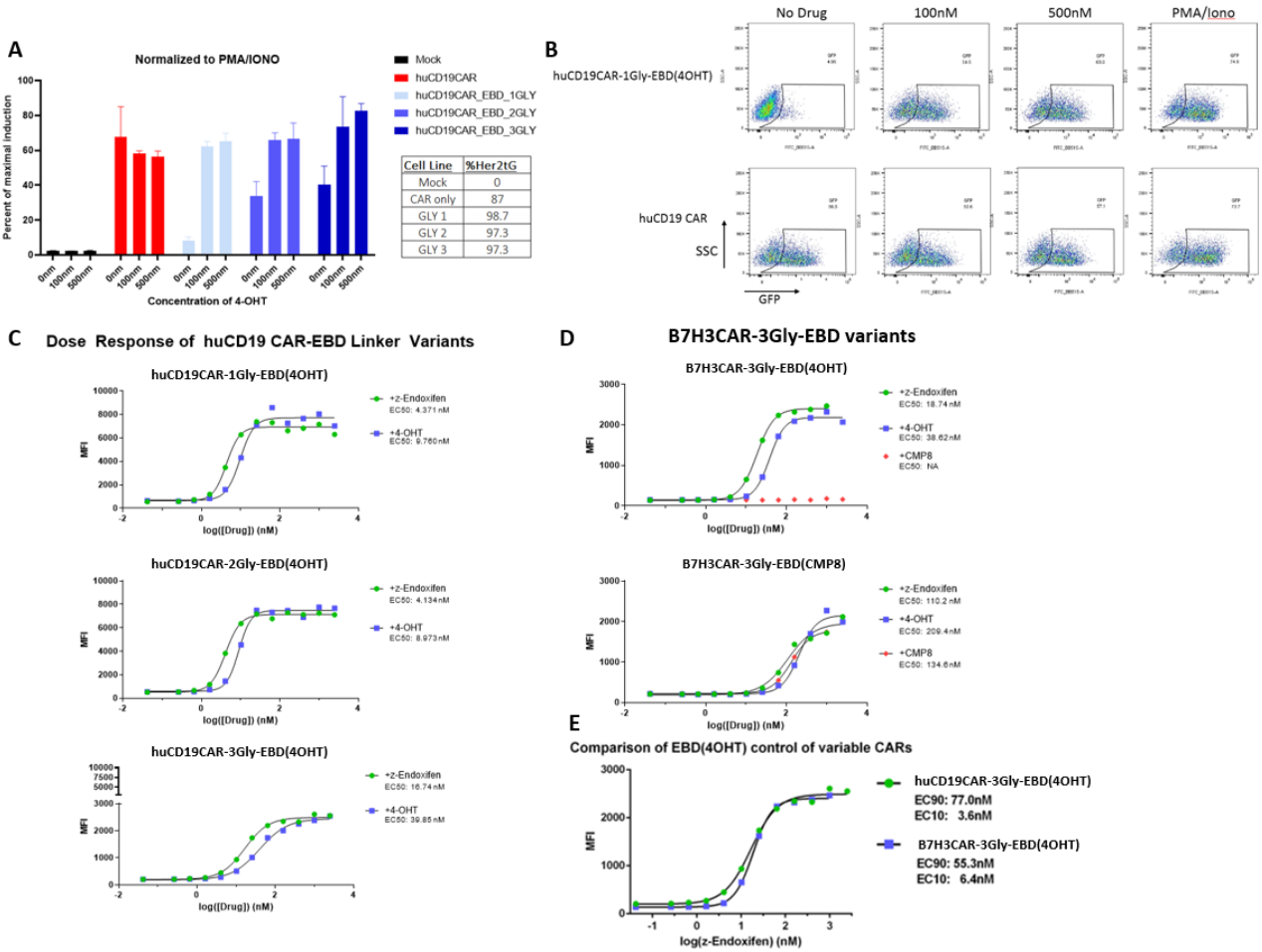

Figure 24. *CAR-EBD enables drug-titratable activation in response to antigen in Jurkat T cells.*

A&B) Jurkat T cells containing the huCD19CAR-XGly-EBD(4OHT) linker variants were pretreated with 0nM, 100nM, or 500nM (Z)-4-OHT for 24hrs before being exposed to target tumor expressing their CAR-targeted antigen (K562+CD19) and GFP was quantified by flow cytometry. Jurkat T cells used in this study were pure for expression of the transduction marker Her2tG after culture in methotrexate for 2 weeks (see Methods). C-E) Construct dose response curves were generated for Jurkat T cells containing the huCD19CAR-XGly-EBD(4OHT) linker variants and the B7H3CAR-3Gly-EBD(XXXX) EBD variants. Cells were treated with a range concentrations of inducer molecules, including (Z)-4-OHT, (Z)-endoxifen, and CMP8 for 24hrs, then were exposed to target tumor expressing their CAR-targeted antigen (K562+CD19) for 24hours, then Jurkat GFP was quantified by flow cytometry.

Having demonstrated the ability of these constructs to turn on and off, we next aimed to determine their dose response to a wider range of drugs and drug concentrations. With the same experimental setup as in Figure 10A&B, we tested the titration of activation over 3 orders of magnitude of drug concentration for several drugs and for both the huCD19CAR-

XGly-EBD(4OHT) linker variant cohort and the B7H3CAR-3Gly-EBD(XXXX) EBD variant cohort. Similar dose response was observed within the huCD19CAR-XGly-EBD(4OHT) linker variant cohort, though the magnitude of induction was less for the 3Gly variant. In this study, the leakiness of the 2Gly and 3Gly linker variants in the linker variant cohort were still greater than the 1Gly variant, but the observed effect was smaller (Figure 10C). This data lead to the huCD19CAR-1Gly-EBD(4OHT) construct becoming our frontrunner construct in future huCD19CAR-EBD studies. Also notable, the EBD(4OHT) EBD domain was sensitive to both (Z)-4-OHT and (Z)-endoxifen (another tamoxifen metabolite currently undergoing FDA approval for standalone use) in both CAR cohorts. In the B7H3CAR-3Gly-EBD(XXXX) EBD variant cohort of constructs, we observed that the EBD(4OHT) exhibits greater drug sensitivity than EBD(CMP8) to (Z)-4-OHT (EC50s of 39nM and 209nM, respectively) (Figure 10D). This is consistent with the mutational goals of the original ERT2 domain that EBD(4OHT) is based on [37]. Furthermore, we see that EBD(CMP8) is sensitive to all three drugs tested, (Z)-4-OHT, (Z)-endoxifen, and CMP8, while EBD(4OHT) does not respond to even high doses of CMP8, highlighting the potential for orthogonal regulation with this system. Finally, an important finding of this experiment was the similarity in dose response for the same EBD and linker, but differing CAR scFv (Figure 10E). EC10, or effective concentration 10%, approximates the highest drug concentration without the turning the construct on, and EC90 approximates the lowest drug concentration while maintaining maximal induction. We can see that there is virtually no difference in the drug-responsiveness between the two CARs regulated by the same EBD and linker architecture in this system.

3.2.2 Cell surface CAR-EBD expression changes after induction, independent of activation

With our earlier experience working with estrogen receptor-derived degron systems, we were interested to see if and how the expression of a CAR-EBD would change upon induction with an inducer molecule. To this end, we cultured Jurkats from both variant cohorts [huCD19CAR-XGly-EBD(4OHT) linker variants and B7H3CAR-3Gly-EBD(XXXX) EBD variants] with inducer molecule for 24hours to compare the cell surface expression of the CAR-EBDs to cells not exposed to inducer molecule (Figure 11). It was observed in both cohorts that culture with drug in the absence of stimulation results in an increase in cell surface CAR-EBD expression. This increase in expression is unlikely to be due to global protein increases, as the transduction marker used in these cells [Figure 10A&B left panels; Her2tG for the huCD19CAR-XGly-EBD(4OHT) linker variants; CD19t for the B7H3CAR-3Gly-EBD(XXXX) EBD variants] did not increase in the CAR-EBD cells, and the expression of the constitutively active CARs (caCAR) did not change after drug addition. Also notable, is that similar changes in expression were observed for different inducer molecules (4-OHT and CMP8) with the B7H3CAR-3Gly-EBD(CMP8) construct. This is an interesting finding, however, in contrast to traditional degron systems, the CAR-EBDs are consistently expressed at high levels in the absence of inducer molecule. The relevance of this change in CAR-EBD expression – while both interesting and sizeable (about a 3-fold increase in MFI upon drug addition) – requires additional investigation, and may not meaningfully impact the functionality of the CAR-EBD system.

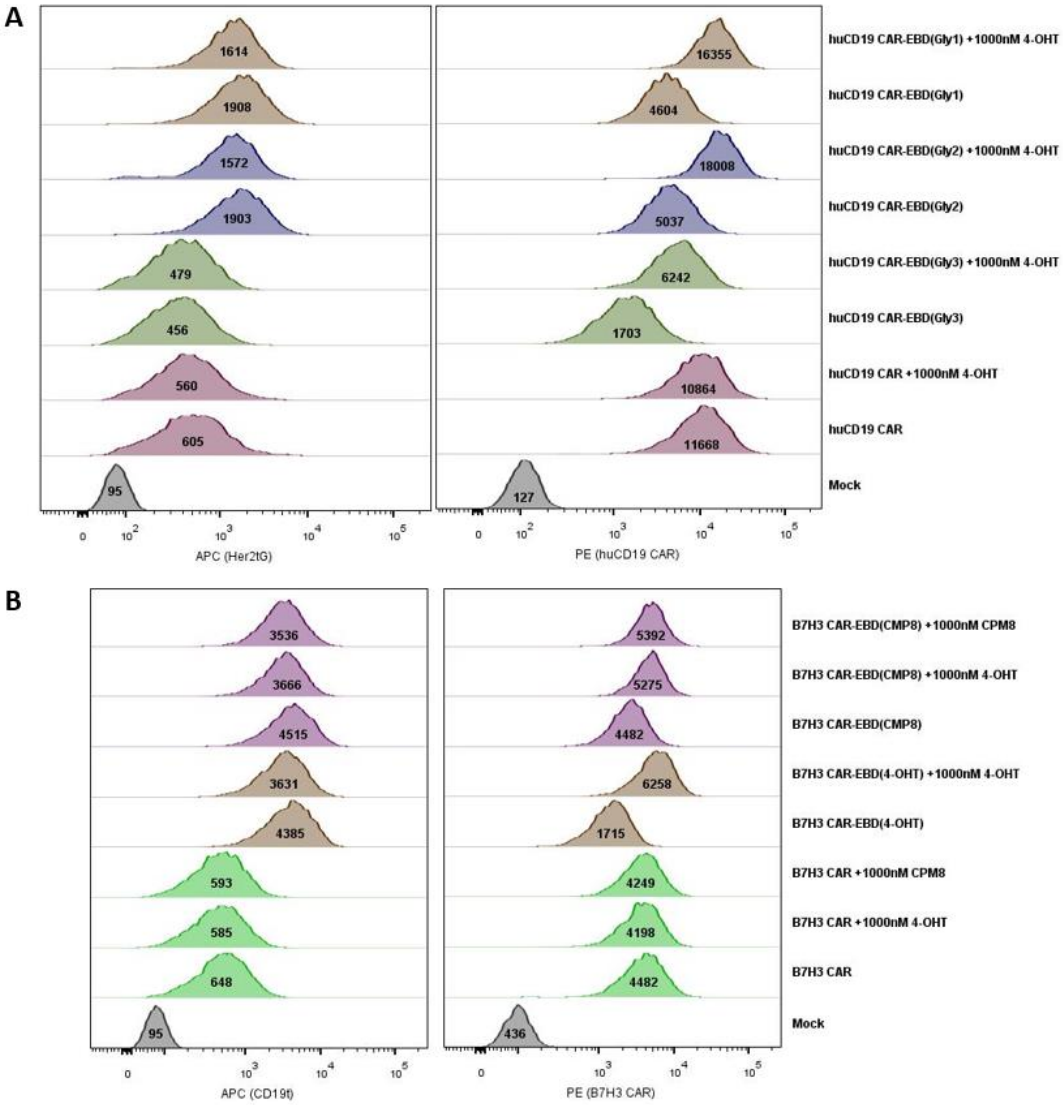

Figure 27. *Cell surface CAR-EBD expression changes after induction, independent of activation.*

A) huCD19CAR-XGly-EBD(4OHT) linker variant Jurkat T cells were cocultured (or not) with (Z)-4-OHT for 24hrs in the absence of stimulation. Cells were subsequently stained for the appropriate transduction marker as well as with an anti-human scFv antibody that binds both the huCD19CAR and the B7H3CAR. B) Same as A for the B7H3CAR-3Gly-EBD(XXXX) EBD variants, and including induction with CMP8.

3.2.3 Jurkat T cells expressing huCD19CAR-1Gly-EBD(4OHT) activate dynamically in response to antigen stimulation upon drug addition.

To begin investigating the kinetics of CAR-EBD activation, we used an Incucyte stimulation assay. 20k Jurkat T cells expressing iSynPro_GFP:ffluc and either no CAR, the huCD19CAR,

or the huCD19CAR-1Gly-EBD(4OHT) construct were cultured alone in a 96 well plate for 12 hours to establish a baseline before 20k K562+CD19 tumor cells were added to each of the the wells (Figure 11). Upon addition of the target cells, the Jurkat cells expressing the caCD19CAR immediately began producing GFP. In contrast to previous findings, the observed baseline GFP levels of the huCD19CAR-1Gly-EBD(4OHT) construct exposed to target-expressing tumor cells was the same as the Jurkat cells without a CAR (Jurkat "Mock"). 24hours after the addition of the tumor cells, (Z)-4-OHT was added to all wells. Upon this addition, the huCD19CAR-1Gly-EBD(4OHT) Jurkats immediately began producing GFP at nearly the same rate as the caCD19CAR Jurkats the day before though the degree of maximum induction was less (rate compares time to relative maximum GFP induction -- slopes diverge because of differences in absolute signal).

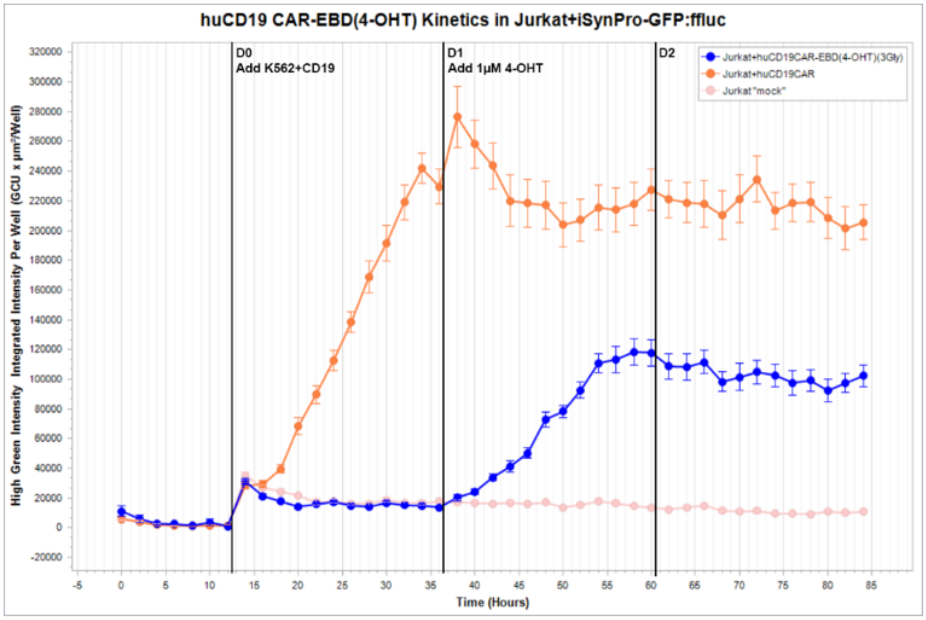

Figure 30. *Jurkat T cells expressing huCD19CAR-1Gly-EBD(4OHT) dynamically activate in response to antigen stimulation upon drug addition.*

Jurkat T cells expressing iSynPro_GFP:ffluc and either no CAR, cahuCD19CAR, or huCD19CAR-1Gly-EBD(4OHT) were cultured in an Incucyte taking images every 2 hours in the green and phase channels. After 12 hours cultured alone, K562+CD19 tumor cells were added to the culture. 24hours later, 1 micromolar (Z)-4-OHT was added to every well.

3.3 Conclusions

Initial testing of the CAR-EBD system in Jurkat T cells with an iSynPro_GFP reporter for activity was both very successful and enabled rapid iteration through a number of initial constructs. We demonstrated nanomolar sensitivity of the EBD domains as well as their transferability between different CARs while preserving similar characteristics. Both the B7H3CAR and huCD19CAR appeared to accept regulation by EBD with stringent off states and on states equal to their constitutive CARs. The linker study with the huCD19CAR-XG-EBD(4OHT) cohort suggests that there may be important impacts to very small changes to receptor physics and spacing. This hypothesis makes sense given our predicted mechanism of action, however the observation that CAR-EBD expression increases substantially following drug administration is unexpected, and may represent an alternative means of regulation. To aid in this this problem, early Incucyte data is very promising in helping our understanding of CAR-EBD switching kinetics. Ultimately, while promising, the data generated in Jurkat T cells is preliminary and much additional testing must be done in primary T cells.

Chapter 4. CAR-EBD – optimization and testing in T cells

4.1. Introduction

Having successfully demonstrated the functionality of two EBD variants with multiple CARs and several linkers in Jurkat T cells, we next aimed to assess the functionality of these constructs in primary T cells to ensure this platform would retain our desired stringency and activation properties in non-immortalized, donor-derived cells. To this end, we moved both construct cohorts (huCD19CAR-XGly-EBD(4OHT) linker variants and B7H3CAR-3Gly-EBD(XXXX) EBD variants including an EBD(ES8) construct) as well as several other CAR-EBDs (EGFR806CAR-3G-EBD(4OHT) and CD22CAR-3G-EBD(4OHT)) into primary human T cells for further testing.

4.2. Results

4.2.1 The expression of CAR-EBD in primary T cells follows similar trends to expression observed in Jurkats

Several batches of T cells were isolated from blood cones and apheresis products from 6 different donors to produce our assorted CAR-EBD T cell lines. Human CD4 and CD8 T cells were cultured at a 1:1 ratio and transduced together with either a relevant constitutively active CAR or an EBD-CAR from one of the mentioned cohorts. Selection for successful transduction was performed with 100nM methotrexate (MTX – see Figure 9B for construct details) to produce high purity engineered T cell populations. Figure 13A represents typical

transgene expression data and CD4:CD8 ratio after selection and culture (See Supplemental Data SD1 for more examples). Expression of the CAR-EBDs was directly assessed by flow cytometry (staining for the CAR scFv) and western blot (staining for the CAR CD3ζ) in the presence and absence of drug induction for 24hrs (Figure 13B&C). Notably, the cell surface expression changes upon culture in drug media (seen in Figure 11 in Jurkats and Figure 13D in T cells) are also reflected in total cell expression seen in the western blot (Figure 13B). Image analysis of the western blot determined the fold change in total-cell CAR-EBD expression to align with the changes in cell-surface expression seen by flow cytometry (about 3-fold).

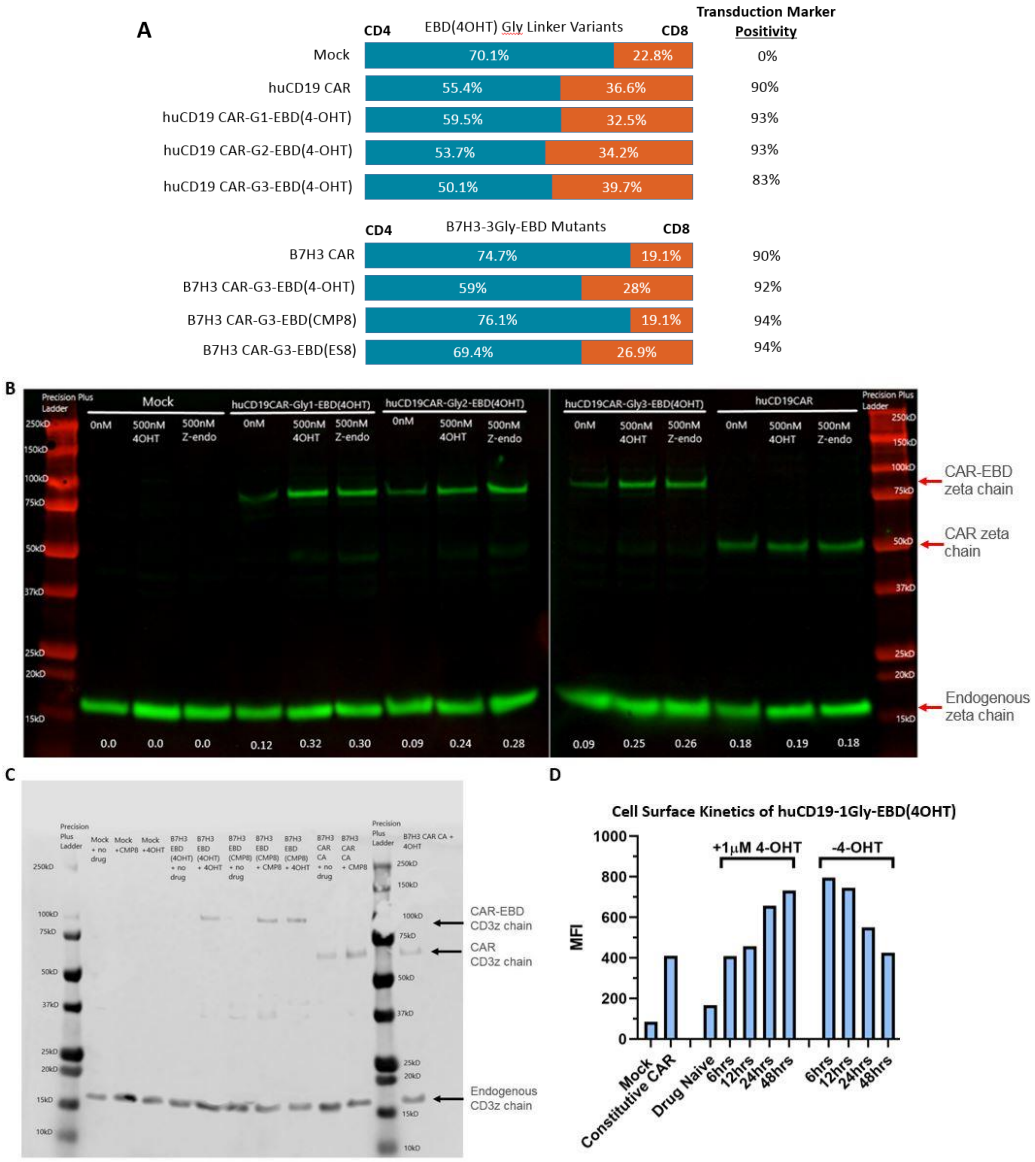

Figure 31. *The expression of CAR-EBD in primary T cells follows similar trends to expression observed in Jurkat T cells.*

A) Primary human CD4 and CD8 T cells were co-cultured at a ratio of 1:1 and transduced together (see Methods). Selection for transduction occurred in 100nM MTX. Cells were stained for CD4:CD8 ratio and transduction positivity by flow cytometry on Stim1, Day 7, and then were frozen and banked for use in future functional studies. B) Western blot of the huCD19CAR-XGly-EBD(4OHT) linker variants in the presence or absence of inducer molecules. Gels were stained with anti-CD3ζ enabling relative quantification of CAR transgenes through comparison with endogenous CD3ζ. C) Western blot of the B7H3CAR-3Gly-EBD(XXXX) EBD variants in the presence or absence of inducer molecules. Gel was stained with anti-CD3ζ Ab enabling relative quantification of CAR transgenes through comparison with endogenous CD3ζ. D) T cells in early culture (8 days post-stimulation) containing the huCD19-1Gly-EBD(4OHT) construct (or appropriate control) underwent a time series to explore changes in CAR-EBD expression observed upon drug addition. Cells were stained for CAR expression with an anti-human scFv antibody.

As previously discussed, the kinetics of protein expression change when working with a degron are generally rapid (~6 hours) and the increase in expression is usually large (~10x). To begin to probe the mechanics of our observed change in CAR-EBD expression, a time series was made of early-culture (8-days post-stimulation) T cells expressing the huCD19CAR-1Gly-EBD(4OHT) construct in 1 micromolar (Z)-4-OHT for various lengths of time up to 48 hours before staining with an antibody specific for the human scFv of the huCD19CAR. Also, CAR-EBD T cells cultured in (Z)-4-OHT for 48hrs were washed and the kinetics of the return to baseline expression were assessed. Consistent with previous data, the huCD19CAR-1Gly-EBD(4OHT) construct was detectable at baseline, though expression was low (Figure 13D). Surprisingly, the kinetics of expression change were slow in both directions. Return to baseline after drug washout was slower than the kinetics of increase upon drug addition, which may suggest protein turnover plays a significant role in this process, however this analysis may have been confounded by active division in the cells used. The role of active receptor dilution by division and protein turn-over will be evaluated further in Chapter 6.

4.2.2. CAR-EBD enables drug dose-titratable activation in response to antigen in primary human T cells

In order to assess whether the CAR-EBD functionality we observed in Jurkat T cells was transferable to primary T cells, we generated dose response curves for both the huCD19CAR-XGly-EBD(4OHT) linker variant cohort and B7H3CAR-3Gly-EBD(XXXX) EBD variant cohort of constructs. CAR-EBD T cells, constitutive CAR T cells or mock T cells were incubated in a range of inducer molecule concentrations over 3 orders of magnitude for 24 hours before being cocultured to K562+CD19 tumor cells expressing target antigen (K562 cells naturally express B7H3). These cultures were collected and stained for expression of

CD107a (LAMP-1), a marker of T cell degranulation, then run on a flow cytometer [46]. In contrast to our observations in Jurkat cells, all three gly linkers variants in the huCD19-XGly-EBD(4OHT) cohort generated similar dose response curves, with EC10s in the low single digit nanomolar range and EC90s in the high double digit nanomolar range to both (Z)-4-OHT and (Z)-endoxifen (Figure 14A). Importantly, maximal dose response was achieved at concentrations of (Z)-4-OHT that are an order of magnitude lower than serum concentrations achievable in the clinic [47]. As was noted in the Jurkats expressing the same construct, the EBD(4OHT) domain does not respond to CMP8. Also, while exhibiting some leakiness, each huCD19-XGly-EBD(4OHT) linker variant appeared to maintain good stringency compared to the same cells cocultured with K562s not expressing CD19 (Figure 14A, inset bar chart; see Supplemental Data SD3 for additional control and replicate donor data for this experiment). As will be seen in later functional studies, these differences in off-state stringency and the impact of linker may be due to differences in sensitivity of various T cell functional outputs.

The B7H3CAR-3Gly-EBD(XXXX) EBD variants were also tested in the same assay (Figure 14B). All three EBD variants succeeded in regulating activity of the B7H3CAR, with stringent off states and response to multiple inducer molecules. All three EBD variants respond to (Z)-4-OHT and (Z)-endoxifen (not shown for EBD(ES8)). Comparison of EC10s and EC90s in response to (Z)-4-OHT highlights the B7H3CAR-3Gly-EBD(4OHT) construct as significantly more sensitive to induction in T cells than the B7H3CAR-3Gly-EBD(CMP8) construct. Indeed, the full activation potential of the B7H3CAR-3Gly-EBD(CMP8) construct may be difficult to meaningfully assess as (Z)-4-OHT concentrations above 1 micromolar are difficult to sustain in a clinical environment. Additionally, while the B7H3CAR-3Gly-EBD(ES8) construct exhibits sensitivity to (Z)-4-OHT similar to EBD(4OHT) (responsiveness

to (Z)-4-OHT not previously reported), it is much more sensitive to induction its eponymous drug, but with a reduced maximum activation in response to target-antigen. Additionally, we showed that EBD(CMP8) does not respond to ES8 and EBD(ES8) does not respond to CMP8, while all three EBD variants respond to (Z)-4-OHT and (Z)-endoxifen. This demonstrates the potential for the fully orthogonal regulation of two transgene-EBD constructs with the added potential benefit of a "master" drug ((Z)-4-OHT) capable of regulating both (Figure 14B). Intriguingly, in the direct comparison case between the cohorts (where each CAR is regulated by -3Gly-EBD(4OHT)), the maximal degree of activation is significantly less with the B7H3CAR than the huCD19CAR, however, their relative CAR expression is inversely related (Figure 14C). This may be attributed to differences in the CARs – both in function and in their ability to be stained with the reagents used – but the differences in activation may also be due to differences in a nearly 10-fold difference in CD19 and B7H3 antigen density on the target tumor cells used (K562+CD19; not shown). This dose response data was used to inform future functional studies in which 0nM (OFF), 1nM (~EC10), 50nM (~EC50), and 500nM (~EC90) drug concentrations were used. See Supplemental Data SD2 for additional control data for this experiment

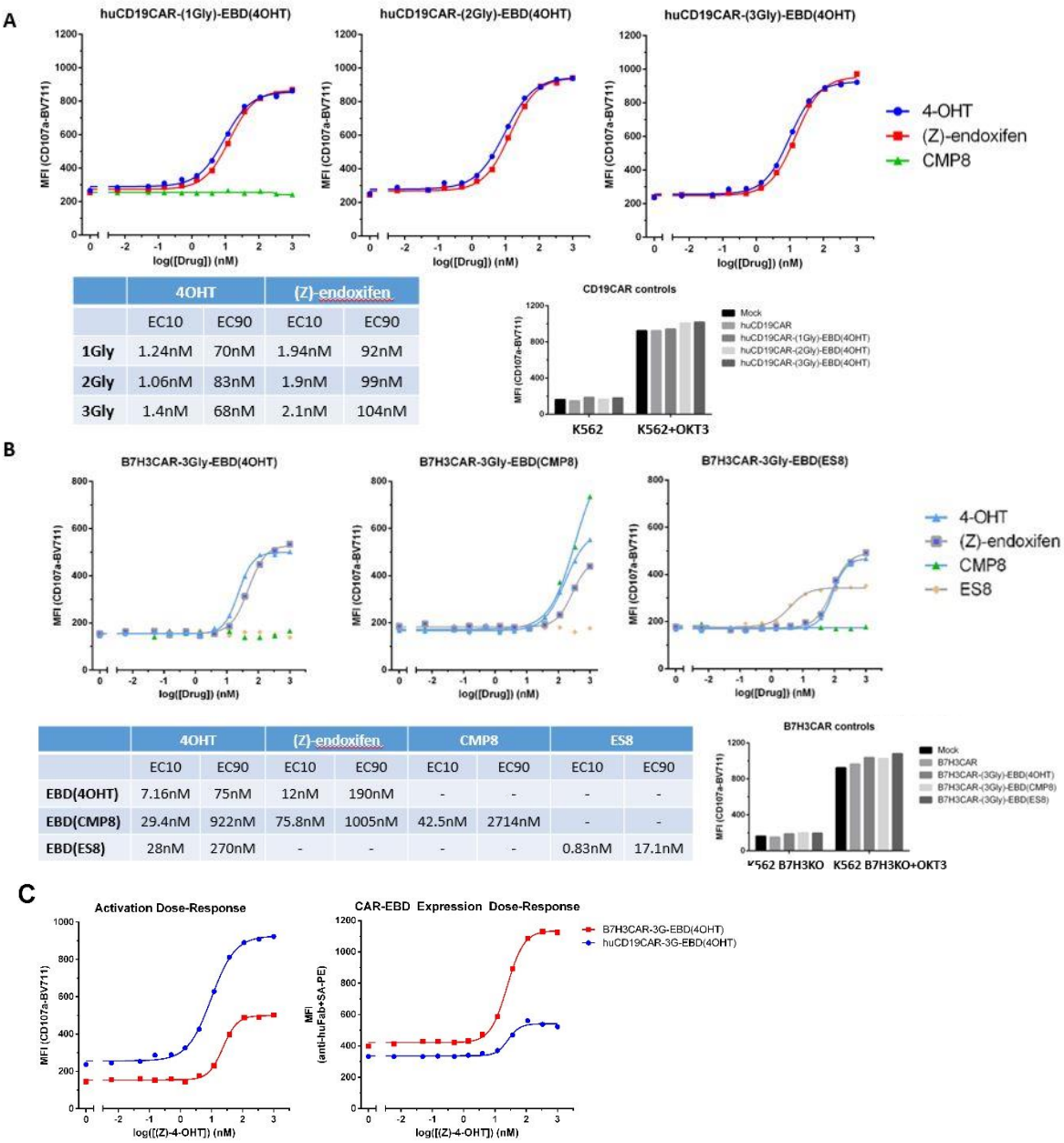

	4OHT		(Z)-endoxifen	
	EC10	EC90	EC10	EC90
1Gly	1.24nM	70nM	1.94nM	92nM
2Gly	1.06nM	83nM	1.9nM	99nM
3Gly	1.4nM	68nM	2.1nM	104nM

	4OHT		(Z)-endoxifen		CMP8		ES8	
	EC10	EC90	EC10	EC90	EC10	EC90	EC10	EC90
EBD(4OHT)	7.16nM	75nM	12nM	190nM	-	-	-	-
EBD(CMP8)	29.4nM	922nM	75.8nM	1005nM	42.5nM	2714nM	-	-
EBD(ES8)	28nM	270nM	-	-	-	-	0.83nM	17.1nM

Figure 34. *CAR-EBD enables drug dose-titratable activation in response to antigen in primary human T cells.*

A, B, C) Primary human T cells expressing constructs from the huCD19CAR-XGly-EBD(4OHT) linker variants cohort or the B7H3CAR-3Gly-EBD(XXXX) EBD variants cohort, or their respective caCARs, or none of the above (mock) were cultured for 24 hours in serial dilutions of a range of EBD inducer molecules (4-OHT, (Z)-endoxifen, CMP8, ES8) covering 3 orders of magnitude of drug concentration. These cells were subsequently cultured with K562 tumors either expressing target antigen for both CARs (K562+CD19) or neither CAR (K562 B7H3knockout) or a CAR independent activator (K562 B7H3knockout +OKT3) at a 2:1 ratio (Effector:Target) for 4 hours, stained for presence of CD107a, and analyzed by flow cytometry. huCD19CAR data: n=1, representative of data from 2 donors – see Supplemental Data SD3 for additional donor data. B7H3CAR data: n=1, representative data from 2 donors.

4.2.3. CAR-EBD enables pharmacologic control of cytokine production and activation in T cells.

As discussed previously, T cell activation has many components and outputs, and in order to understand the full functional impact of our manipulations, it is important to measure as many as is possible. The initial studies in T cells above used degranulation – primarily of CD8+ T cells – as a baseline metric for response to target antigen, as it is recognized as a sensitive marker for T cell effector function and activation [46]. Cytokine production and release into the environment are another hallmark of T cell activation in response to antigen stimulus, particularly of CD4+ T cells.

We performed intracellular cytokine staining (ICCS) on the B7H3CAR-3Gly-EBD(4OHT) and –EBD(CMP8) variants and the huCD19CAR-XGly-EBD(4OHT) linker variants cohort at a range of inducer molecule concentrations in order to determine if the CAR-EBD system is capable of regulating these important functional outputs (Figure 15A-H). Both the B7H3CAR-3Gly-EBD(4OHT) and B7H3CAR-3Gly-EBD(CMP8) constructs exhibited very stringent off states for cytokine production (IL-2, IFNγ, TNFα) and markers of activation (CD107a, 4-1BB, Nur77) when presented with B7H3-expressing K562 tumor cells in the absence of inducer molecule (Figure 15A and D). In line with the CD107a dose response data, addition of drug dramatically increased cytokine production and expression of markers of activation (Figure 15B&C, E&F, respectively). Of note, the drug exclusivity of EBD(4OHT) and EBD(CMP8) was maintained throughout, with B7H3CAR-3Gly-EBD(4OHT) remaining unresponsive to CMP8 across all measured marks of activation. In contrast to the CD107a only data set, most of the activation markers and cytokines expressed reached maximum production by 50nM drug, with few increases seen in the 500nM condition (identifying the sliver of pie-chart representing CD107a, one can observe that this increase between 50nM

and 500nM (Z)-4-OHT is preserved in this larger assay). As an exception to this observation, activation with the B7H3CAR-3Gly-EBD(CMP8) construct is less with 500nM (Z)-endoxifen than with (Z)-4-OHT, which is a unique feature of this method of measuring activation.

Furthermore, dose response to (Z)-4-OHT was also assessed by ICCS in the huCD19CAR-XGly-EBD(4OHT) linker variant cohort. In line with previous observations, all linker variants exhibit greater activation (CD107a, 4-1BB, Nur77) in the absence of inducer molecule than the B7H3CAR-based constructs (Figure 15H). This leakiness appears constrained to activation/degranulation, however, as cytokine production remained off until drug was added and each of the linker variants produced greater cytokine than the constitutive huCD19CAR at 500nM (Z)-4-OHT induction (Figure 15G; see Supplemental Data SD5 for additional control data for this experiment). It is notable that there did not appear to be meaningful differences between the linker variants in this assay.

Figure 37 *(Next Page). CAR-EBD enables control of cytokine production and activation in response to antigen stimulation in T cells.*

A-F) In brief, primary human T cells expressing either a construct in the B7H3CAR-3Gly-EBD(XXXX) EBD variants cohort, the B7H3CAR, or no CAR were cultured with or without inducer molecules for 24 hours before being placed in co-culture for 4 hours with K562 tumor lines expressing target antigen (B7H3), or no antigen (B7H3 knockout), or a CAR-independent activation molecule (B7H3 knockout +OKT3). Cells were then stained for extracellular markers (CD4, CD8, transduction marker, CD107a, 4-1BB) and intracellular markers (Nur77, IL-2, IFNg, TNFa). Representative data from 2 donors. See Supplemental Data 4 for additional control data for this experiment. G&H) primary human T cells expressing either a construct in the huCD19-XGly-EBD(4OHT) linker variants cohort, the huCD19CAR, or no CAR were cultured with or without inducer molecules for 24 hours before being placed in co-culture for 4 hours with K562 tumor lines transduced to express target antigen (+CD19), or no antigen (K562 parental line), or a CAR-independent activation molecule (+OKT3). Cells were then stained for extracellular markers (CD4, CD8, transduction marker, CD107a, 4-1BB) and intracellular markers (Nur77, IL-2, IFNg, TNFa). All data representative of 2 donors. See Supplemental Data 5 for additional control data for this experiment.

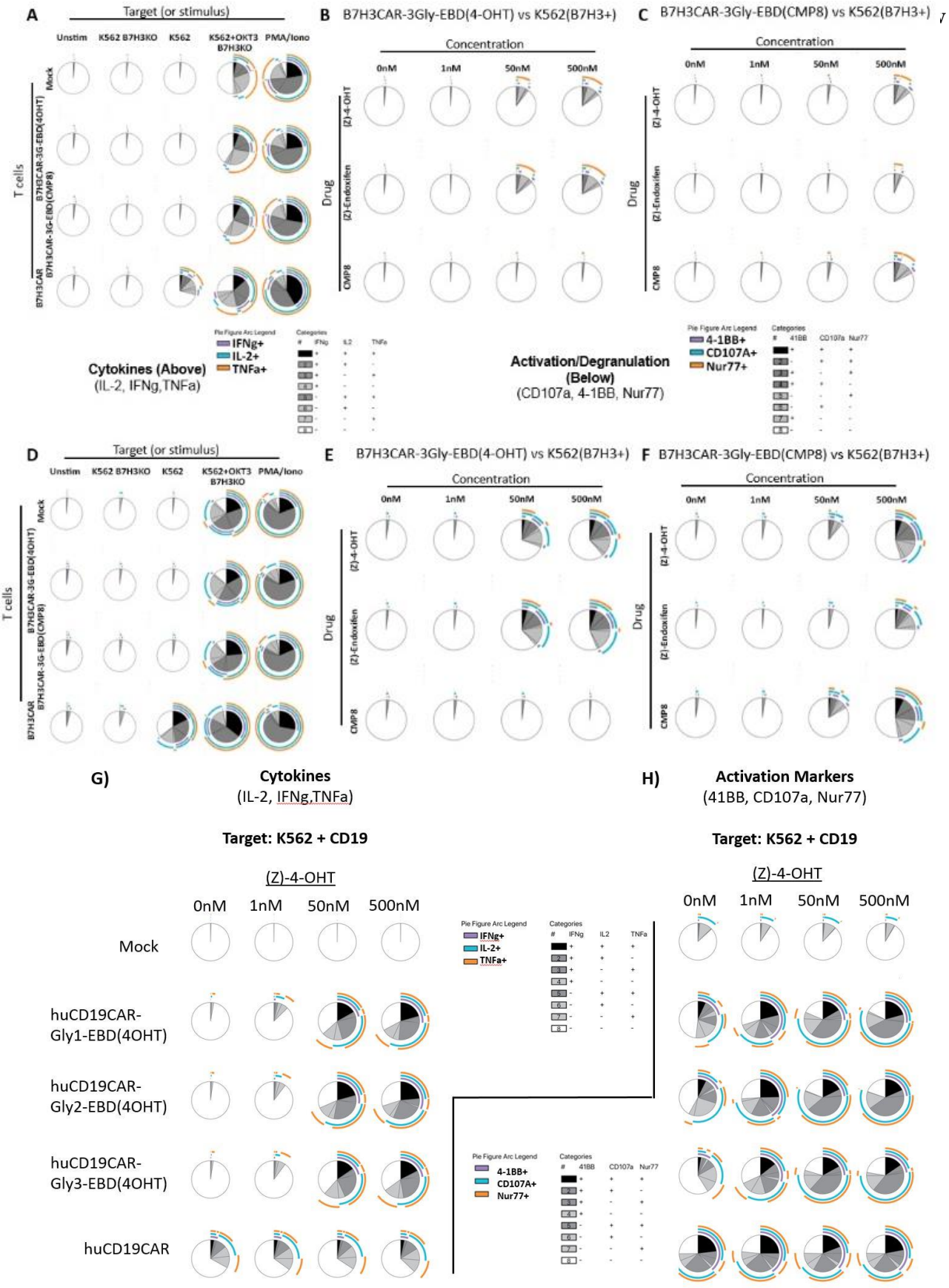
A
Target (or stimulus)
Unstim
K562 B7H3KO
K562
K562+OKT3 B7H3KO
PMA/Iono
T cells
Mock
B7H3CAR-3G-EBD(4OHT)
B7H3CAR-3G-EBD(CMP8)
B7H3CAR
B
B7H3CAR-3Gly-EBD(4-OHT) vs K562(B7H3+)
C
B7H3CAR-3Gly-EBD(CMP8) vs K562(B7H3+)
Concentration
0nM
1nM
50nM
500nM
Drug
(Z)-4-OHT
(Z)-Endoxifen
CMP8
Pie Figure Arc Legend
IFNg+
IL-2+
TNFa+
Categories
Cytokines (Above)
(IL-2, IFNg,TNFa)
4-1BB+
CD107A+
Nur77+
Activation/Degranulation (Below)
(CD107a, 4-1BB, Nur77)
D
E
F
G)
Cytokines
(IL-2, IFNg,TNFa)
H)
Activation Markers
(41BB, CD107a, Nur77)
Target: K562 + CD19
huCD19CAR-Gly1-EBD(4OHT)
huCD19CAR-Gly2-EBD(4OHT)
huCD19CAR-Gly3-EBD(4OHT)
huCD19CAR

cytometry, we also assessed CAR-EBD's ability to regulate T cell activation at the population level by measuring cytokine levels (IL-2, IFNγ, TNFα) in culture supernatant after coculture with target-antigen expressing tumor cells and a range of inducer molecules and concentrations (Figure 16). Similar to our ICCS observations, both the B7H3CAR-3Gly-EBD(4OHT) and B7H3CAR-3Gly-EBD(CMP8) constructs exhibited very stringent off states for cytokine release (Figure 16A; see Supplemental Data SD6 and SD7 for additional control and replicate donor data for this experiment). While the rates of cytokine production did not reach that of the caB7H3CAR, even in the 500nM condition, clear switching of activity was achieved and correlated well with other donors. (Note B7H3CAR-3Gly-EBD(4OHT)'s lack of response to CMP8, and the reduced sensitivity of B7H3CAR-3Gly-EBD(CMP8) to induction with (Z)-endoxifen.)

We also tested the cytokine production of the huCD19CAR-XG-EBD(4OHT) linker variants under increasing drug concentrations against multiple target tumors (Figure 16B and C). In contrast to the ICCS assay above, the huCD19CAR-XG-EBD(4OHT) constructs did not exhibit a clean off state for cytokine production, suggesting that while individual huCD19CAR-XG-EBD(4OHT) cells presented with target-antigen expressing tumor for 4hrs in the absence of drug induction will not produce cytokine, the longer incubation of this cytokine release assay (24hrs vs 4hrs for ICCS) provides sufficient stimulous in the off state to allow for small amounts of cytokine production. Because these longer incubation times are incompatible with the methods for ICCS (the protein transport inhibitor necessary for intracellular cytokine stain is toxic beyond a few hours), it remains unclear if particular sub-populations of huCD19CAR-XG-EBD(4OHT) T cells are responsible for this cytokine production leakiness, or if it is a low level expressed by the full culture. Of note, the huCD19CAR-XG-EBD(4OHT) T cells exhibited similar leaky behavior when presented with

a tumor which endogenously expresses the target antigen at physiological levels (opposed to forced expression under an EF1α promoter), highlighting that this leakiness is not exclusively dependent on high antigen density, and represents a fundamental difference in the control of the huCD19CAR-XG-EBD(4OHT) constructs (Figure 16D) [48]. Overall, the huCD19CAR-XGly-EBD(4OHT) linker variants cohort exhibited similar patterns of activation and regulatibility, though with increased leakiness and decreased control over the off state compared to the B7H3CAR-derived EBD constructs.

Finally, we further tested the applicability and transferability of the CAR-EBD platform, by testing the stringency of off state and cytokine production of CD22CAR-XG-EBD(4OHT) linker variant constructs [49]. All of these constructs exhibited great stringency of the off state, producing none of any of the measured cytokines when presented with target-expressing tumor, then titrating nicely up to maximum cytokine production in the 50nM condition, similar to the B7H3- and huCD19CAR-EBDs, and in line with the dose response observed in ICCS and other functional outputs.

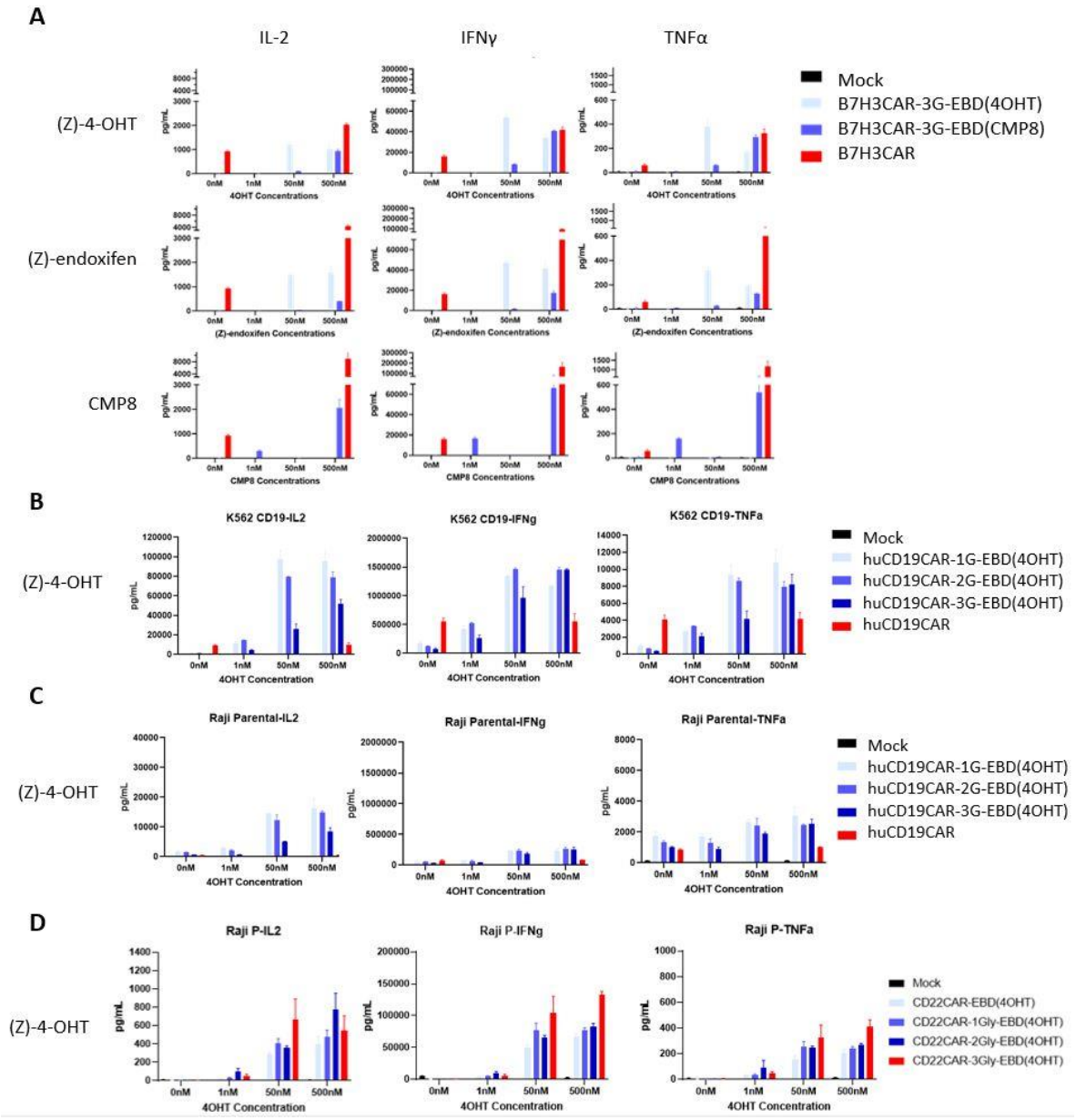

Figure 40. *CAR-EBD enables control of cytokine production and activation in response to antigen stimulation in T cells.*

A) primary human T cells expressing either a construct in the B7H3CAR-3Gly-EBD(XXXX) EBD variants cohort, the B7H3CAR, or no CAR were cultured with or without inducer molecules for 24 hours before being placed in co-culture for 24 hours with K562 tumor lines expressing target antigen (B7H3), or no antigen (B7H3 knockout), or a CAR-independent activation molecule (B7H3 knockout +OKT3). Supernatants were recovered from each well before being assessed for cytokine concentration by electrochemiluminescence. Representative data of 2 donors. see Supplemental Data SD6 for additional control data for this experiment. See Supplemental Data SD7 for additional replicate donor data for this experiment. B-D) similar to above, primary human T cells expressing either a construct in the huCD19CAR-XG-EBD(4OHT) or CD22CAR-XG-EBD(4OHT) cohorts, the huCD19CAR or CD22CAR, or no CAR were cultured with or without inducer molecules for 24hrs before being

placed in co-culture for 24hrs with K562 or Raji tumor lines expressing target antigen (CD19, CD22, respectively), or no antigen (K562 parental), or a CAR-independent activation molecule (K562 B7H3 knockout +OKT3). huCD19CAR data representative of 2 donors. CD22CAR data representative of 1 donor.

4.2.4. CAR-EBD enables pharmacological control of antigen-specific tumor cell killing.

Both the literature and our experience with the CAR-degron system suggest that degranulation is one of the most difficult T cell functional outputs to regulate [24]. This difficulty is made all the more important by the recognition that halting T cell activation and cytolytic activity is critical for a T cell regulatory platform, both for aborting runaway immune reactions (e.g. cytokine release syndrome) and providing sufficient rest to T cells to avoid exhaustion [20]. To test CAR-EBD's ability to regulate degranulation and target cell killing of CAR T cells, we performed chromium release assays on two of the constructs in the B7H3CAR-3Gly-EBD(XXXX) EBD variant cohort, all of the constructs in the huCD19CAR-XGly-EBD(4OHT) linker variants cohort, the CD22CAR-XGly-EBD(4OHT) linker variants cohort, and a second solid-tumor CAR-EBD, EGFR806CAR-3G-EBD(4OHT) (Figure 17).

Both B7H3CAR-3Gly-EBD(4OHT) and B7H3CAR-3Gly-EBD(CMP8) exhibit stringent off states for killing in the context of a chromium release assay against K562 tumor cells (4hr duration) (Figure 17A and B). This regulation is gated by inducer (i.e., induction with CMP8 does not cause killing in B7H3CAR-3Gly-EBD(4OHT) T cells), and nearly equivalent killing to the caB7H3CAR is achieved upon maximum induction. Similar to cytokine release and ICCS, nearly full induction of the B7H3CAR-3Gly-EBD(4OHT) construct is achieved by 50nM of drug, with little additional activity achieved by increasing the concentration to 500nM. Also in concordance with previous data, the B7H3CAR-3Gly-EBD(CMP8) construct appears less sensitive to drug, and sees increased killing with 500nM drug. In contrast to the cytokine release and ICCS data however, we see that induction of the B7H3CAR-3Gly-

EBD(CMP8) construct with (Z)-endoxifen produces nearly equivalent functional outputs to induction with (Z)-4-OHT. The reason for this discrepancy is unclear at present.

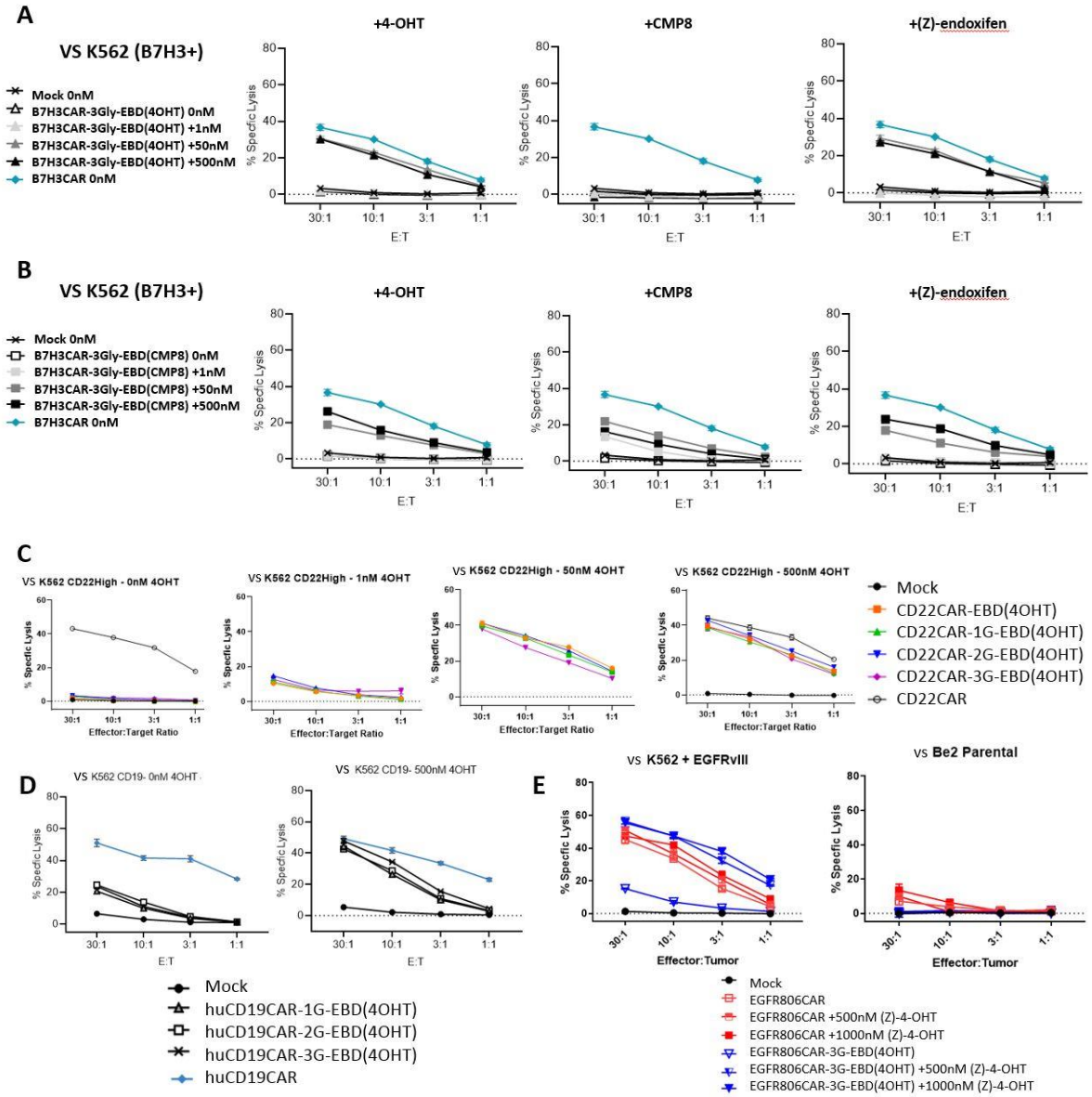

Figure 43. *CAR-EBD enables pharmacological control of antigen-specific tumor killing.*

A-E) Chromium release assays of B7H3-, CD22-, huCD19-, and EGFR806CAR-EBD constructs including varying linker or EBD variants against target antigen expressing K562 tumor lines which had been loaded with Cr51. T cells receiving drug treatment were are incubated with appropriate inducer molecule for 24hrs prior to exposure to target tumor at a range of effector:target ratios, then supernatants were collected and degree of lysis assessed by radioactive scintillation detection. B7H3CAR-EBD data is representative of 2 donors; See Supplemental Data SD8 for additional B7H3CAR-EBDdonor data. The huCD19CAR-EBD data is representative of 3 donors. See Supplemental Data SD10 and SD11 for additional huCD19CAR-EBD data

Next, we assessed the CD22CAR-XG-EBD(4OHT) linker variants for cytotoxic activity and stringency of offstate. All of these constructs exhibited extremely stringent off states which responded to increasing doses of (Z)-4-OHT until anti-tumor activity reached parity with the paired constitutive CAR at 50nM drug (Figure 17C; note – mock and CD22CAR were only treated with 0nM and 500nM (Z)-4-OHT). This aligns very closely with our previous findings with the B7H3CAR-3G-EBD(4OHT) construct, and further highlights, the ease with which the EBDs may be applied to new CARs and target antigens. Notably, there did not appear to be meaningful differences between the activity of the linker variants. (Please see Supplemental Data SD9 for additional controls and experimental chromium release data using the huCD22CAR-3Gly-EBD(4OHT) construct.)

We also performed chromium release assays with the huCD19CAR-XG-EBD(4OHT) linker variant cohort, as well as an EGFR806CAR-3G-EBD(4OHT) construct. The huCD19CAR-XG-EBD(4OHT) linker variants exhibited pronounced killing in the off state, especially at higher effector:target (E:T) ratios, further suggesting difficulty reaching a full off state (Figure 17D). However, killing was substantially increased upon drug addition. Notably, there did not appear to be meaningful differences between the activity of the linker variants. All of these findings align well with previous functional studies of the studies huCD19CAR-XG-EBD(4OHT) linker variant cohort. The EGFR806CAR-3G-EBD(4OHT) T cells also appeared to exhibit leakiness against both K562s transduced to express the EGFR806CAR target (EGFRvIII) and endogenous antigen expressing Be2s (Figure 17E). In spite of the leakiness in antigen-specific lysis observed, the EGFR806CAR-3G-EBD(4OHT) T cells did dramatically increase their killing upon drug addition, matching constitutive CAR activity in this assay. (Please see Supplemental Data SD10 and SD11 for more chromium release data utilizing the huCD19CAR-XGly-EBD(4OHT) linker variants across 3 donors.)

Chromium release assays are a very useful tool to examine degranulation in a limited, but extremely sensitive setting – displaying even minute changes in activation and degranulation potential that could be missed by CD107a staining. However, these assays are necessarily limited in duration and remain steps removed from the protracted cellular battles CAR T cells experience when targeting and killing a tumor *in vivo*.

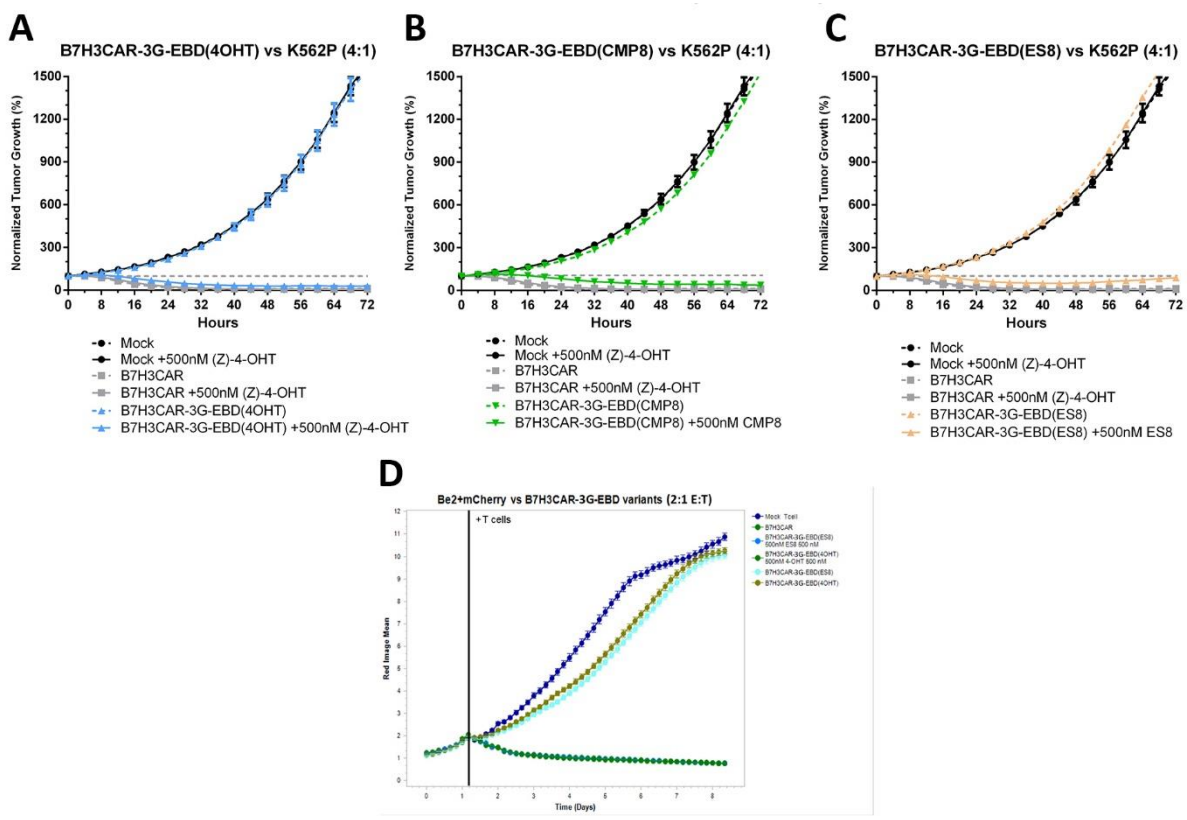

Figure 46. *B7H3CAR-3G-EBD variants demonstrate stringent off states in long-duration killing assays against multiple tumor targets.*

A-D) T cells containing either the constitutive B7H3CAR, one of the B7H3CAR-3Gly-EBD(XXXX) variants or neither (Mock) were either incubated with 500nM (Z)-4-OHT, CMP8, or ES8 for 24 hours prior to the initiation of the study or were not. At the initiation of the experiment, T cells were plated in triplicate and combined with K562 tumor cells expressing mCherry. Plates were imaged in an incucyte every 4 hours for 3 or more days and tumor growth was tracked using mCherry signal. Data is representative of 2 donors.

In order to gain additional insights into the functionality of our CAR-EBD systems, we utilized another T cell-extrinsic activity measure – Incucyte killing assays. The Incucyte is

an imaging system inside of an incubator, allowing for periodic imaging of co-cultures of fluorescently labelled target tumor cells with antigen-specific CAR T cells. All three of the B7H3CAR-3Gly-EBD(XXXX) EBD variants exhibited stringent off states and full switching of cytotoxic activity when presented with antigen-expressing targets in the context of an Incucyte killing assay (Figure 17A-D). These longitudinal assays are particularly sensitive to small degrees of activation, and we were very pleased to see both how stringent the off state is and how impactful the on state is for the B7H3CAR-3Gly-EBD(XXXX) EBD variants when dosed with their eponymous drugs (e.g., EBD(4OHT) received 500nM (Z)-4-OHT, EBD(CMP8) received 500nM CMP8, and EBD(ES8) received 500nM ES8) (Figure 18A-C). It is notable that while the B7H3CAR-3Gly-EBD(ES8) managed to control tumor growth effectively, it didn't eradicate it, and tumor was beginning to slowly grow out by the end of the 3 day study (Figure 18C). While more testing is needed, the dose-response curves presented earlier suggest that there may be limitations in the degree of activation possible inducing EBD(ES8) CARs with ES8 (see Figure 14B).

We also tested the B7H3CAR-3Gly-EBD(4OHT) and B7H3CAR-3Gly-EBD(ES8) constructs against a Be2 neuroblastoma tumor cell line (which endogenously express B7H3), and saw excellent switching activity as well (Figure 18D). We observed that against this tumor line, the B7H3CAR-3Gly-EBD(ES8) construct controlled tumor equally as well as the B7H3CAR-3Gly-EBD(4OHT) construct (which was the not the case against K562s). A full explanation of this effect is forthcoming, but it may involve differences in antigen density between K562s and Be2s.

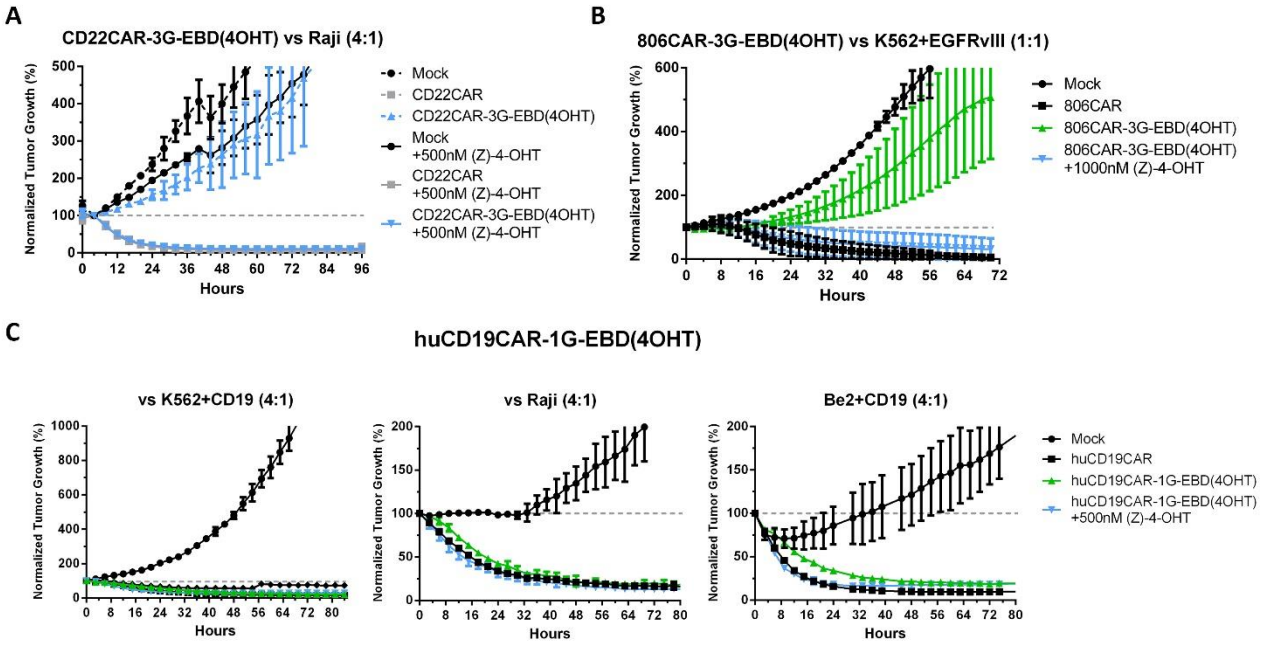

Figure 49. *Long-duration assays elucidate additional details about CAR-EBD function across different CARs and CAR targets.*

A-C) T cells containing either a CAR-EBD(4OHT) or a paired constitutive CAR (CD22CAR, EGFR806CAR, huCD19CAR), or neither (Mock) were either incubated with 500nM (Z)-4-OHT for 24hrs prior to the initiation of the study, or were not. At the initiation of the experiment, T cells were plated in triplicate and combined with tumor cells expressing mCherry as well as the appropriate target antigen (CD22, EGFRvIII, or CD19, respectively). Plates were imaged in an incucyte every 4 hours for 3 or more days, and tumor growth was tracked using mCherry signal.

With the CD22CAR-3G-EBD(4OHT) construct, we observed equivalent control of target-antigen expressing tumor to its paired constitutive CAR as well as very stringent off states resulting in equal growth kinetics to the mock T cell:tumor co-culture (Figure 19A). This was not the case, however, for the EGFR806-3G-EBD(4OHT) construct, which exhibited both inferior killing compared to the EGFR806CAR as well as an incomplete off state evidenced by substantially slower growing tumor (though it did eventually begin to grow out).

Finally, it is in the context of long-course Incucyte experiments that the huCD19CAR-1G-EBD(4OHT) construct shows the significance its consistent leakiness. While in many

previous functional outputs, the huCD19CAR-XG-EBD(4OHT) linker variants appeared to only have low levels of activation when presented with antigen expressing targets in the absence of inducer drug, we see here that this "low level" activation results in nearly identical tumor kill curves to the constitutive huCD19CAR over a longer timeline (Figure 18C). This effect is mitigated somewhat at lower effector:target (E:T) ratios, however, it largely persistents and is only removed at E:T ratios where the constitutive CAR fails to control tumor (data not shown).

4.3. Conclusions

Because the field's understanding of CAR biophysics and signal transduction is still limited, predicting the functional ramifications of altering the signaling domain of a CAR is a difficult problem. While not exhaustive, we have empirically demonstrated the functional characteristics of CAR-EBD from many important angles and highlighted many of the clinically valuable properties of this system. Chiefly, this technology is capable of gating the activity of a CAR T cell behind the presence of a small molecule drug. While not a new concept, previous endeavors have struggled with issues of transferability between CARs and with stringency of the off state [20, 50]. This novel means of regulation appears nearly agnostic to target, having demonstrated complete or significant reductions of a broad spectrum of CAR T cell activities in the absence of inducer drug for 4 unrelated CARs (B7H3CAR, CD22CAR, huCD19CAR, EGFR806CAR) targeting a wide range of tumor types and target antigen densities with minimal redesigns necessary. This technology is also highly modular, comprising multiple domains of similar, human-derived sequence that may be activated in concert (i.e., with (Z)-4-OHT or (Z)-endoxifen) or independently by small molecule

drugs orthogonal to each other and patient biology (e.g., CMP8 or ES8). Importantly, the core of this functionality occurs with FDA-approved drugs at serum concentrations well within clinically relevant limits [47].

While very encouraging, this surface-level description leaves many questions unanswered, chief among which are how does CAR-EBD achieve its regulatory capabilities, what are the on and off kinetics of the system, and whether or not these *in vitro* successes will translate *in vivo*. These questions will be addressed in chapters 5 and 6, respectively.

Chapter 5. Exploring CAR-EBD Kinetics and Mechanics.

5.1 Introduction

We have demonstrated our ability to regulate the activity of CARs using EBD across many functional outputs, however, several important questions remain regarding its underlying function, which may inform the future utility of this system. Why do both cell surface and total cell CAR-EBD increase when drug is added? Does this suggest that CAR-EBD is functioning as a degron? If so, is our ability to regulate CAR-EBD T cell activity solely predicated on this apparent change in CAR-EBD expression? How long, then, does it take for the increase in CAR-EBD expression to occur compared to the kinetics of gaining anti-tumor activity upon drug addition? Does this change in activity appear to be an analog or digital transition? Subsequently, how long does this increase in CAR-EBD expression last following removal of drug, and what happens to antigen-specific activity once drug has been removed from the culture or cleared from serum?

This rather simple but unexpected finding also leads to questions about the underlying mechanism(s) of control. The insight of the original design was to leverage endogenous protein-protein interactions between steroid hormone receptors (e.g., ER1α ligand binding domain) and heat shock proteins (e.g., HSP90) to provide steric blocking of CAR signal transduction until a hormone analog is administered. This transition – which would not rely on any DNA transcription, RNA translation, or proteasome machinery – is expected to be fast in both direction. While the exact kinetics would need to be defined, we would expect it to be faster than the slow changes in CAR-EBD expression we observed in Figure 13D.

Furthermore, while CAR-EBD has demonstrated its capacity for successfully regulating then activity of several CARs with minimal redesign or iteration needed, it remains unclear why it achieves superior off state stringency with some CARs (e.g., B7H3CAR and CD22CAR) compared to others (e.g., huCD19CAR and EGFR806CAR). Compounding this quandary further is the emergence of donor-specific effects for the huCD19CAR-XG-EBD(4OHT) system, the leakiest CAR-EBD we have tested to date (Figure 20; See Supplemental Data SD10 and SD11 for additional donor data with the huCD19CAR-1G-EBD(4OHT) construct.). In contrast to donors 1 and 2, donor 3 for these constructs demonstrates very stringent off states against target antigen expressing tumor cells, without sacrificing its ability to kill target tumor when induced with (Z)-4-OHT. While this illustrative chromium release assay data has been provided, a similar trend is seen for other functional outputs including ICCS and chromium release. It is notable that this is the only donor-specific effect we have observed across 7 donors and over a dozen CAR-EBD constructs, however, the truth remains that we lack a sufficient understanding of the underlying mechanics to troubleshoot issues of off-state stringency or donor-specific effects when they arise. To these ends, we endeavored to further explore the kinetics and mechanics of the CAR-EBD system in order to better inform its future use and fine-tuning.

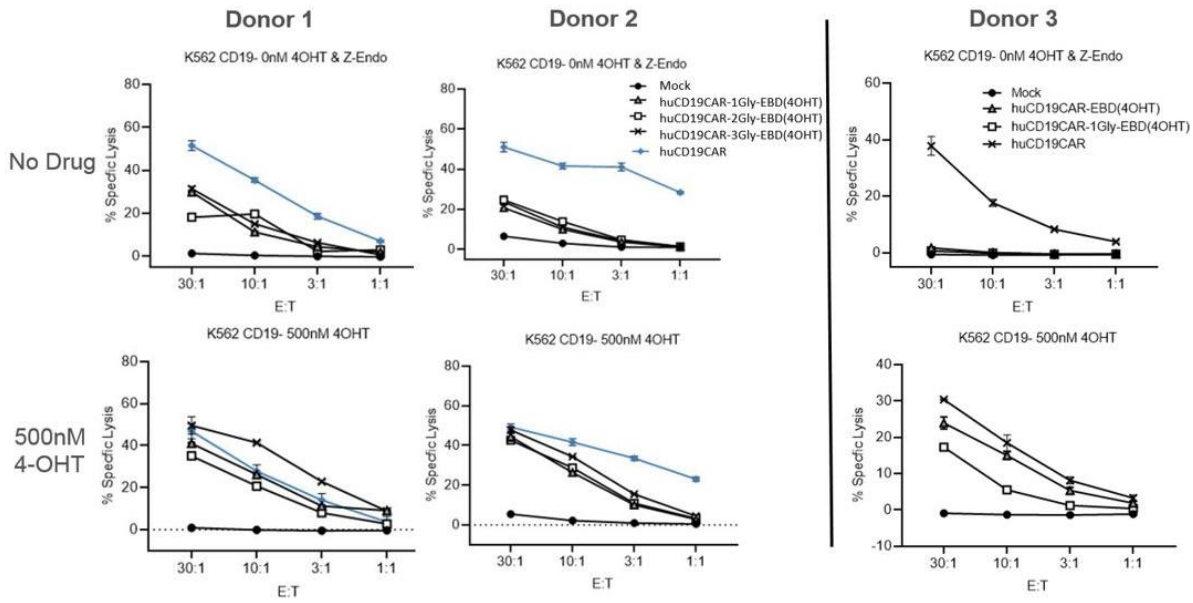

Figure 52. *huCD19-XGly-EBD(4OHT) linker variants exhibit donor-to-donor variation in its stringency of off-state, without impacting the inducibility of on-state.*

Chromium release assays from 3 donors expressing the huCD19CAR-XG-EBD(4OHT) linker variant construct cohort K562+CD19 tumor lines which had been loaded with Cr51. T cells receiving drug treatment were are incubated with appropriate inducer molecule for 24hrs prior to exposure to target tumor at a range of effector:target ratios, then supernatants were collected and degree of lysis assessed by radioactive scintillation detection. See Supplemental Data SD10 and SD11 for additional donor data with the huCD19CAR-1G-EBD(4OHT) construct.

5.2 Results

5.2.1. CAR-EBD does not appear to function as a degradation domain

Following up from our early findings that CAR-EBD expression increases upon inducer drug addition in both Jurkat T cells and primary T cells (see Figure 11 and Figure 13D), we wanted to investigate if this effect was limited to drug + EBD pairings that result in CAR-EBD activation, or was a feature of CAR-EBD in any estrogen-analog environments. Testing the dose response of CAR-EBD expression increase, we found that these increases are specific to drug + EBD pairs that produce activation and that the dynamics of this increase are highly

correlated with what is observed for activation, suggesting that this result is the product of CAR-EBD being bound by an inducer molecule (Figure 21A).

We next wanted to confirm that this increase was not the result of increases in CAR-EBD mRNA transcription in response to drug addition. To accomplish this, we performed qPCR for the CAR-EBD transcript and flow cytometry cell surface CAR-EBD on the same cell population with or without drug induction, and we found that there was no change in CAR-EBD transcription (Figure 21B). This aligns with previous findings that the transduction marker for the construct – which exists as a polycistron on the same mRNA separated from the CAR/CAR-EBD by a ribosomal skip sequence – does not experience a commensurate increase in expression upon drug induction (see Figure 11). This informs us that the increase in CAR-EBD expression upon drug addition is either due to an increase in translation-rates (an uncommon mechanism for increased protein expression) or an increase in CAR-EBD protein stability upon drug addition, leading to slower degradation rates.

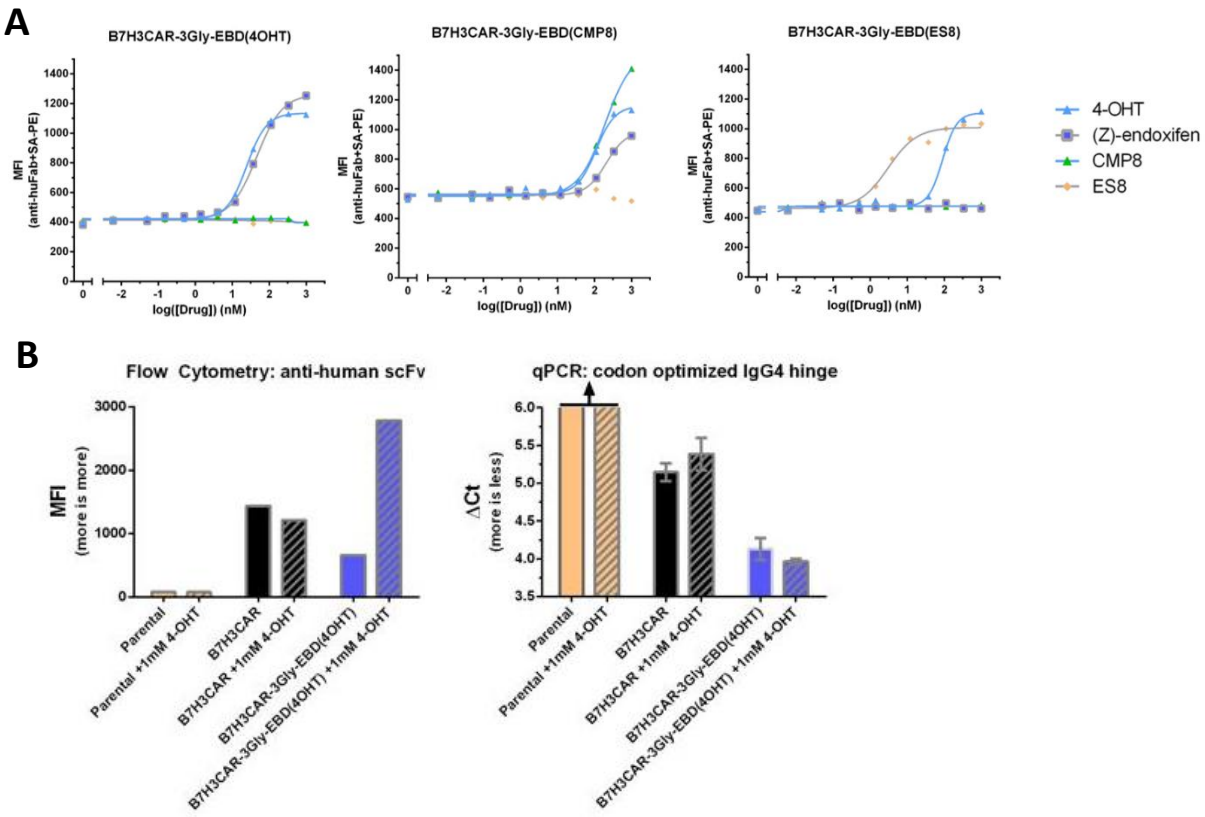

Figure 55. *Cell surface CAR-EBD receptor expression exhibits a dose-responsive increase to drug induction that is not a product of increased transcription.*

A) Primary human T cells expressing constructs from B7H3CAR-3Gly-EBD(XXXX) EBD variants cohort were cultured for 24 hours in serial dilutions of a range of EBD inducer molecules (4-OHT, (Z)-endoxifen, CMP8, ES8) covering 3 orders of magnitude of drug concentration. These cells were subsequently stained for CAR expression and analyzed by flow cytometry. Representative data from 2 donors. B) B7H3CAR-3G-EBD(4OHT), B7H3CAR, and Mock T cells were treated with 1000nM (Z)-4-OHT for 24hrs or not treated. These cells were subsequently split in half, and one half was stained for cell surface B7H3CAR and analyzed by flow cytometry, while the other half was used for RNA isolation. qPCR for an overlapping segment of the scFv and IgG4 hinge of the B7H3CAR enabled quantification of both B7H3CAR and B7H3CAR-3G-EBD(4OHT) transcripts from the same primer set. N=3.

These findings support the hypothesis that the CAR-EBD may be functioning as a cryptic degron, Classically, this is tested through the use of proteasome inhibitors, such as MG-132, which block the function of the proteasome, allowing for unstable proteins to better

accumulate in the cell[29]. However, when compared to a previous described (Z)-4-OHT-responsive degron, ER50dd, we did not observe the same kinetics of expression when exposed to (Z)-4-OHT and/or MG-132 (Figure 22A) [31]. Again, this aligns with previous data which suggests that this change in cell-surface CAR-EBD has a slow kinetic, in comparison to traditional degrons which rapidly lose expression once inducer drug is withdrawn, as is seen with the eBFP-ER50dd construct. Of interest, if the addition of inducer drug constitutes a stabilizing event for an unstable CAR-EBD, we would expect a commensurate increase in cell surface CAR-EBD when MG-132 is added to the cultures under each condition, however, this does not appear to be the case (however, even with eBFP-ER50dd, the change is small and does not reach statistical significance). This data strongly suggests that CAR-EBD is not functioning as a degron, however, it remains possible that the return to baseline after drug washout is slow enough that the length of this study was insufficient to elucidate this potential mechanism (6hrs).

Our next step was to directly evaluate our original hypothesis of CAR-EBD activity regulation by HSP90 sequestration and steric blocking of CD3ζ signaling. To achieve this, we utilized two previously described HSP90 inhibitors, 17-DMAG and Cucurbitacin D, that inhibit HSP90 by disparate means (N-terminal binder and C-terminal binder, respectively), but both inhibit binding to known HSP90 and reduce a cells total HSP90 expression [51, 52]. If the regulation of CAR-EBD function were a product of HSP90-binding, we would anticipate disruption of this event would lead to unregulated activity of the CAR-EBD, however, this was not the case: B7H3CAR-3G-CAR-EBD(4OHT) expression did not increase following administration of the HSP90 inhibitors (not shown), and most importantly, the stringency of the off state was not effected (Figure 22B).

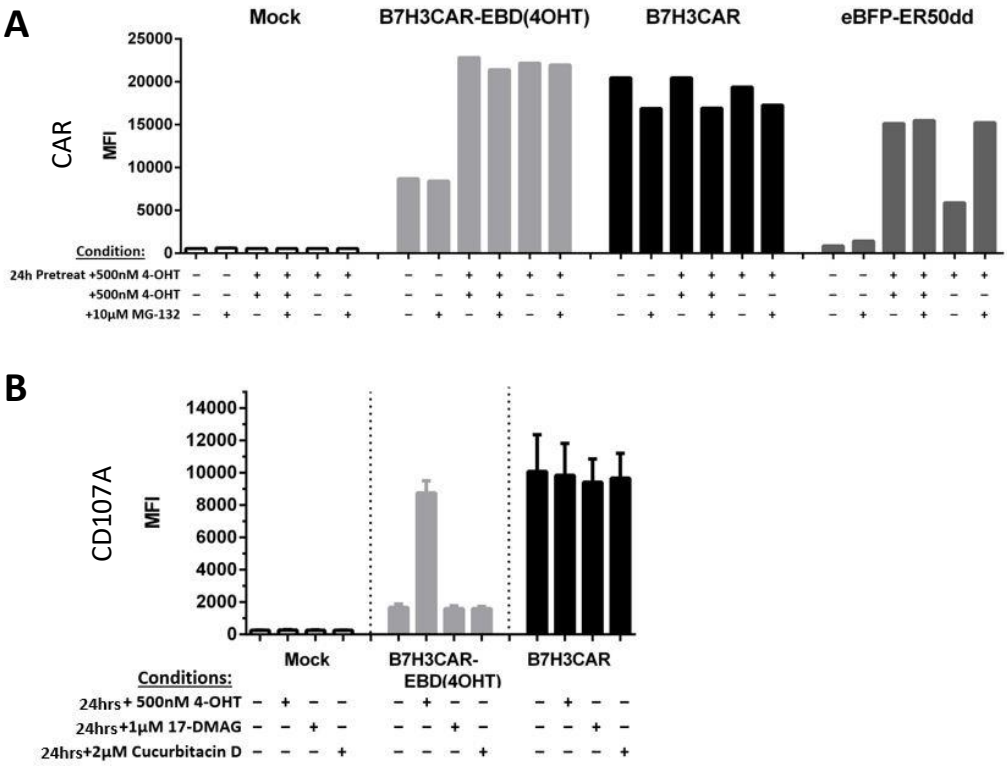

Figure 58. CAR-EBD does not appear to function as a degradation domain, though its mechanism of action remains unclear.

A) Jurkat T cells expressing the B7H3CAR-3G-EBD(4OHT) construct, the B7H3CAR, neither, or an eBFP-ER50dd fusion were treated with 500nM (Z)-4-OHT for 24hrs or not treated. These cells were subsequently washed thoroughly to remove drug from the media, and exposed to one, both, or neither of 500nM (Z)-4-OHT and 10uM MG-132 for 6 hours. Mock and CAR expressing cells were subsequently stained for the CAR and all cells were analyzed by flow cytometry. B) Primary T cells expressing B7H3CAR-3G-EBD(4OHT) construct, the B7H3CAR, or neither were exposed to nothing, 500nM (Z)-4-OHT, 1uM 17-DMAG, or 2uM Cucurbitacin for 24hrs, then were subsequently assessed for anti-tumor activity by co-culture with antigen-expressing K562 tumor cells, stained for CD107A, and analyzed by flow cytometry.

5.2.2 The on-kinetics of CAR-EBD anti-tumor activity are slower than the proposed mechanism would predict, however, drug induction is required for activation.

While we have investigated our findings regarding alteration to CAR-EBD expression upon drug addition, we have maintained a 24hour pre-incubation with applicable drug concentrations in all T cell functional assays. This is to ensure full and proper "switching" in the event that the CAR-EBD expression changes we have observed are related to activity or regulation. In order to investigate the kinetics of CAR-EBD activation directly, a time-series was compiled, comparing the CAR-directed degranulation of B7H3CAR-3G-EBD(4OHT) T cells exposed to 500nM (Z)-4-OHT for varying lengths of time (Figure 23A). Here we observe that the kinetic of CAR-EBD expression correlates closely with the kinetic of CAR-EBD antigen-specific activation following drug addition (spearman correlation: 0.95). With how the assay is performed (time incubated with drug + 2hr assay) it is also notable that the largest step-wise increases in both CAR-EBD receptor expression and activation in response to target antigen occurs between the 0hr and 2hr time points. The meaning of this finding is unclear, but it is inconsistent with a simple stability-increase model and may suggest that there are intracellular stores of translated CAR-EBD that are sequestered until drug induction. Replication of this finding, followed by further investigation into this possibility may provide valuable insights into the mechanics of CAR-EBD expression.

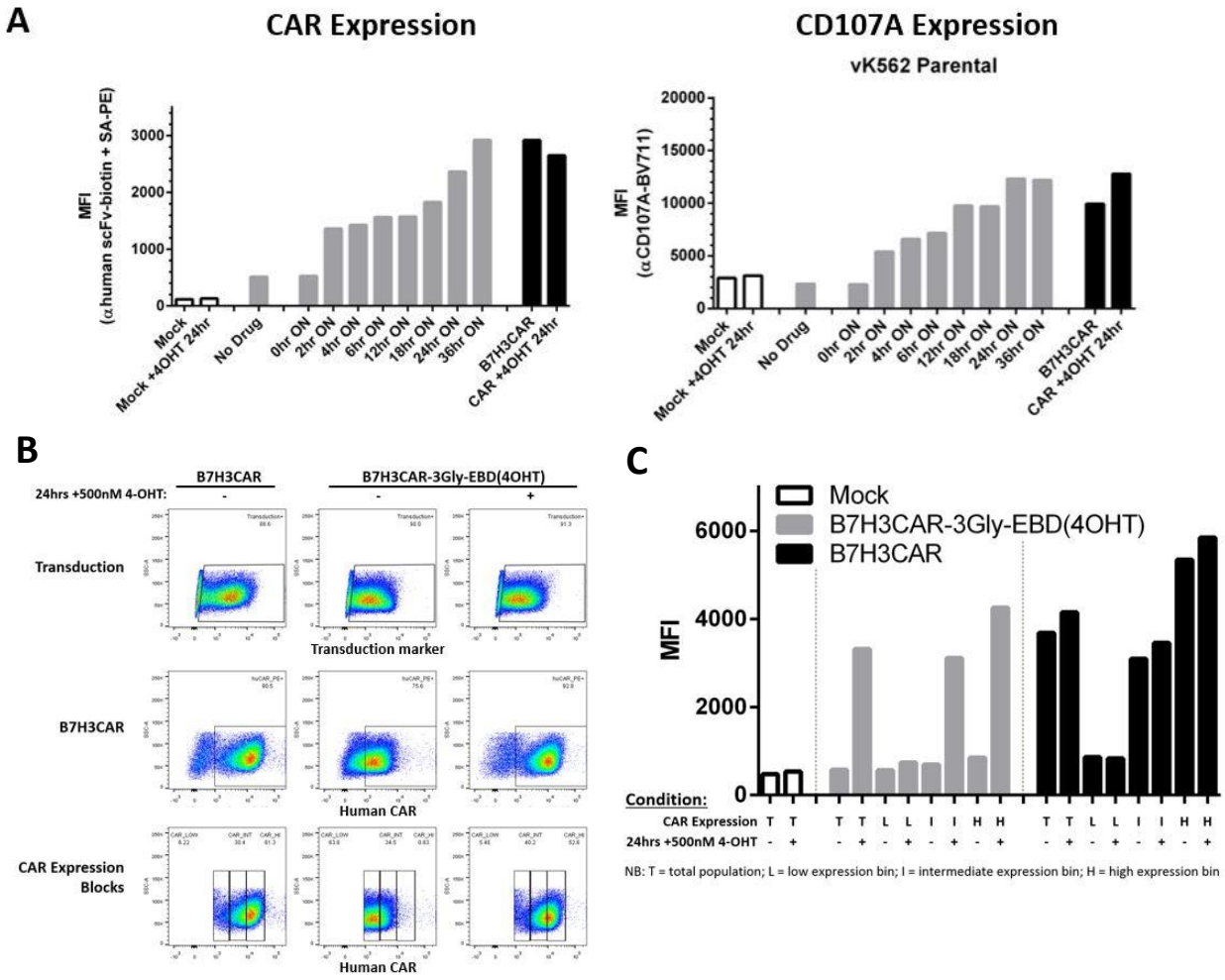

Figure 61. *CAR-EBD expression increases slowly after drug induction and correlates with capacity to degranulate in response to target antigen.*

T cells expressing the B7H3CAR or B7H3CAR-3Gly-EBD(4OHT) constructs or none (mock) were treated with 500nM 4OHT for 24hrs or not, then were cocultured with target-antigen expressing K562 tumor cells for 4 hours. They were then stained for CD107A and the CAR, and analyzed by flow cytometry. Each sample was subsequently segmented by low, intermediate, and high CAR expression, and the activation of each expression group was assessed.

While the close alignment between CAR-EBD expression and CAR-EBD activity certainly appears to be a smoking gun, it remains possible that receptor expression is necessary but insufficient for CAR-EBD activation. To test this, we assessed B7H3CAR-3G-EBD(4OHT) T cells ability to degranulate when presented with target-antigen expressing tumor cells with

and without inducer drug, but stratified our analysis into bins of differential CAR-EBD (or constitutive CAR) expression (Figure 23B). One can see clearly the increase in B7H3CAR-3G-EBD(4OHT) expression after 24hr incubation with 500nM (Z)-4-OHT, as well as the effect that that has on the proportion of the populations in each CAR expression bin. Specifically, the expression distribution of the B7H3CAR-3G-EBD(4OHT) receptor looks very similar – both in MFI and in population percentagess that fall in each bin – to the constitutive B7H3CAR following incubation with inducer drug. We next looked at the ability of each of these expression bins (labelled total, low, intermediate, and high) to degranulate when presented with target antigen (Figure 23C). Of great interest is the relationship between the CAR-EBD expression bins and whether they are capable of degranulating in response to antigen-expressing tumor in the presence vs absence of inducer drug. If the aforementioned hypothesis of CAR-EBD expression dictates response to antigen is true, one would expect high expression CAR-EBD cells to degranulate even in the absence of drug, however, we see the opposite – even the highest expression bin of B7H3CAR-3G-EBD(4OHT) T cells maintains a stringent off state in the absence of (Z)-4-OHT. Then, if drug has been added, cells with the same expression levels of B7H3CAR-3G-EBD(4OHT) become capable of degranulation when presented with target antigen. There is also an interesting trend seen in both the constitutive B7H3CAR and B7H3CAR-3G-EBD(4OHT) cells, namely that the lowest expression binned cells do not degranulate in response to target, even though they stain positive for transduction marker. Several attempts have been made in our lab and others to "detune" CAR activity through the use of promoters of reduced strength. This data suggests that these efforts are likely to work (see the stair step increases in constitutive CAR degranulation with increasing CAR expression), but only down to a point where the CAR density drops low enough that a meaningful percentage of cells will fail to exceed the signaling threshold necessary for activation. (Note: cell sorting was attempted to achieve a

similar, cleaner effect to this assay, however, CAR-EBD expression normalized between sorted populations after a few additional days in culture. There may be a clue here regarding CAR-EBD expression turnover, but it remains under investigation.)

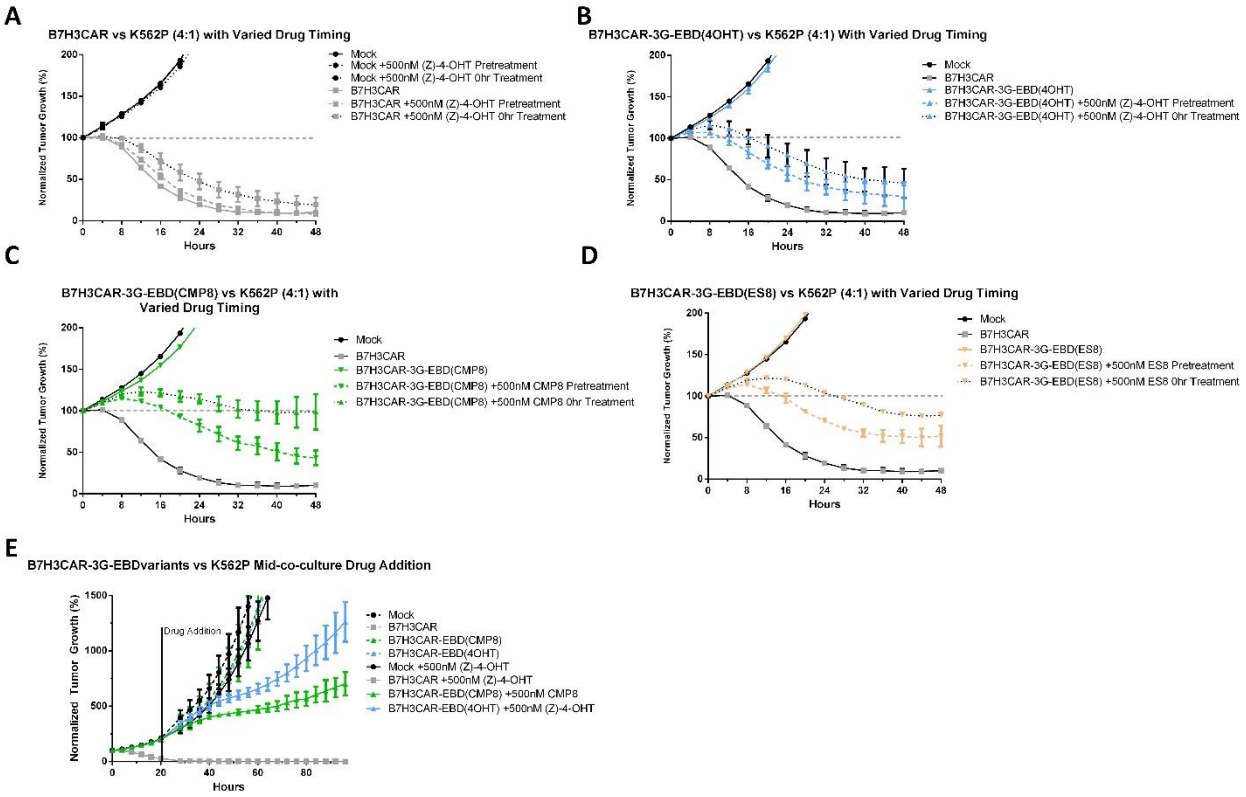

Figure 64. *Incucyte killing assays provide insight into the on-kinetics of the CAR-EBD system.*

T cells containing either the constitutive B7H3CAR, one of the B7H3CAR-3Gly-EBD(XXXX) variants or neither (Mock) were either incubated with 500nM (Z)-4-OHT for 24 hours prior to the initiation of the study or were not. T cells that were not pre-incubated with drug, were subsequently subdivided into two groups, one of which experienced drug for the first time during co-culture with tumor cells. At the initiation of the experiment, T cells were plated in triplicate and combined with K562 tumor cells expressing mCherry. Plates were imaged in an incucyte every 4 hours for 2 or more days and tumor growth was tracked using mCherry signal. Data is representative of 2 donors.

T cell-intrinsic methods – such as activation marker staining – are inherently difficult to use for the kinetic assaying of CAR-EBD activity due to the timelines involved. Fortunately, Incucyte killing assays allow us to infer the kinetics of switching more easily because the

result is T cell extrinsic, easily quantifiable, and the data acquisition is close to continuous. Because of this, we used an Inucyte killing assay to examine the differences in tumor killing kinetic between B7H3CAR-3G-EBD variant T cells pre-treated with (Z)-4-OHT ("Pretreatment" conditions) and those who experienced drug induction for the first time at the beginning of the assay ("0hr Treatment" conditions) (Figure 24). Drawing inference from previous kinetic work, these assays closely examine the first 24-48 hours after the assay begins to infer activation kinetic (opposed to longer timelines, which result in equivalent killing in nearly all cases). It is worth noting that this assay is inherently noisy, and there is some variation in kill kinetic of even the constitutive B7H3CAR between conditions due to small technical variations (Figure 23A). Even still, examination of individual EBD variants as well as cross comparison between the EBD variants produces some interesting findings. Of note, the EBD(4OHT) variant (Figure 24B) appears to acquire anti-tumor activity faster when exposed to drug compared to the EBD(CMP8) (Figure 24C) and EBD(ES8) (Figure 24D) variants. In contrast to this, a study was also performed where tumor and CAR-EBD T cells were co-cultured in an Inucyte in the absence of drug to allow for non-productive immunological synapse formation, followed by drug addition to the wells, which resulted in the on-rate of the EBD(CMP8) variant to beat the EBD(4OHT) variant (Figure 24E). While interesting, these analyses are still under development, and they should be interpreted lightly for the time being. This work does clearly highlight however, that the on-kinetic of the CAR-EBD system is rapid, but is not instant (as there are small, but meaningful and repeatable differences between the tumor controlling kinetic of CAR-EBD T cells pretreated with drug vs non-pretreated), and the process of CAR-EBD activation continues to evolve for up to 24 hours after drug induction.

5.2.3 The off-kinetics of CAR-EBD anti-tumor activity are slower than the proposed mechanism would predict.

The ability to turn off a regulated system is of nearly equal importance to its ability to turn on. Until this point, this has been an area of study for CAR-EBD that we have under explored (beyond the data presented in Figure 13D). In combination with our studies into the on-kinetics of CAR-EBD, we also performed time series exploring the loss of cell surface CAR-EBD and antigen-specific activity after the withdrawal of inducer drug from the culture medium. Of importance, the cells for these studies were allowed to reach a quiescent state in late culture (20-28 days post-stim) to avoid the dilution of active receptor through division events. In these studies, B7H3CAR-3G-EBD variants are induced with 500nM (Z)-4-OHT for 24 hours, thoroughly washed, returned to new, cytokine-supplemented media, and allowed to sit in culture for 1-6 days before being assayed for cell surface CAR-EBD expression and ability to degranulate in response to target antigen-expressing tumor lines. Notably, none of the B7H3CAR-3G-EBD variants returned to their original baseline CAR-EBD expression following drug washout (Figure 25A). In spite of this, it does appear that the EBD(CMP8) and EBD(ES8) variants return closer to baseline CAR-EBD expression, while the EBD(4OHT) generates both much greater quantities of CAR-EBD upon induction (graph scales held constant), and maintain it at a consistent level throughout the culture period. These same cells were also assessed for their ability to degranulate when presented with antigen-expressing tumor following drug washout and rest in drug-free media (Figure 25B). Again, none of the B7H3CAR-3G-EBD variants returned to baseline, but again, the EBD(CMP8) and EBD(ES8) variants returned closer to baseline, compared to the EBD(4OHT) variant which retained nearly equivalent activity out to 6 days after drug

washout. This is a very interesting finding, and one without precedent in the literature to our knowledge, highlighting a potentially novel form of regulation at hand. It is worth noting that EBD(4OHT) domain is derived from the ERT2 domain which was engineered to have much greater affinity for (Z)-4-OHT than the wildtype receptor (which was used to derive the EBD(CMP8) and EBD(ES8) domain variants) [37]. This difference in receptor sensitivity is reflected in the dose response we mapped in Chapter 4 (with the EBD(4OHT) being the most sensitive to drug induction of the three) and may influence receptor off-kinetic as well.

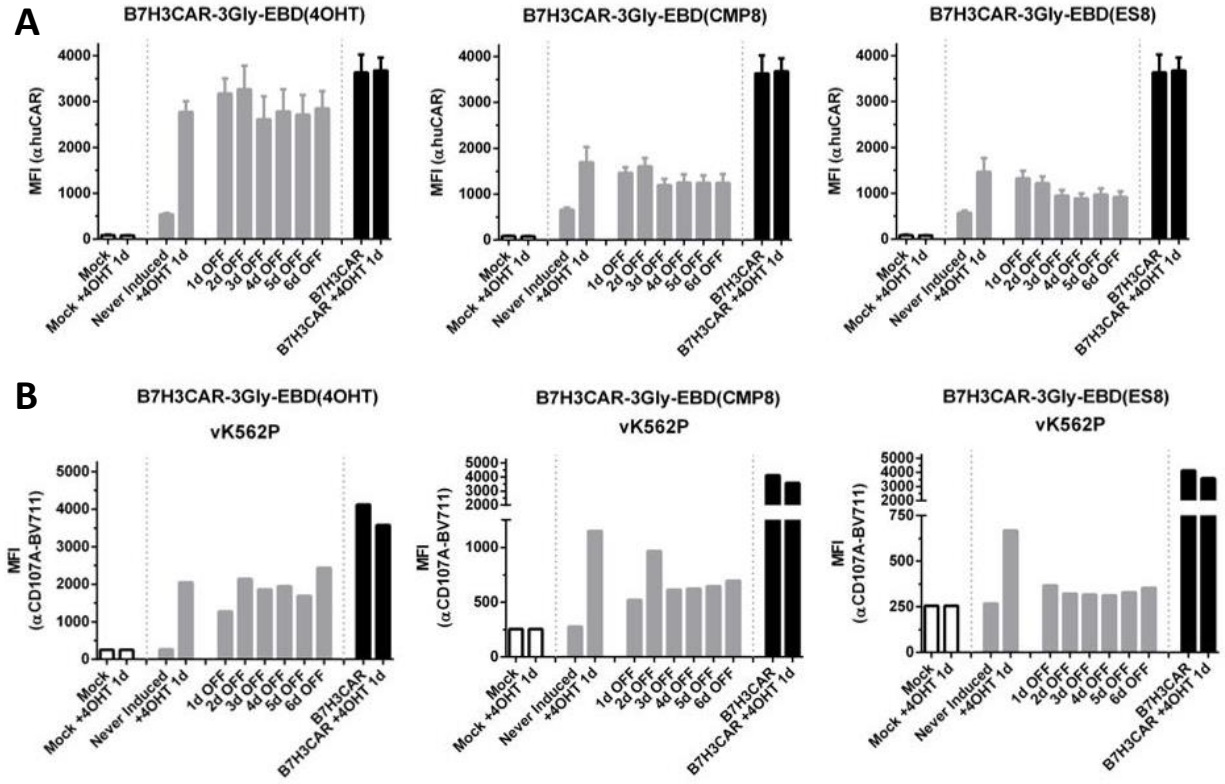

Figure 67. CAR-EBD retains increased expression and activity potential for many days following induction with inducer drug.

T cells expressing the B7H3CAR or B7H3CAR-3Gly-EBD(variant) constructs or none (mock) were treated with 500nM 4-OHT for 24hrs, then were thoroughly washed and returned to the incubator for up to 6 days. Cells at each time point were stained for CAR expression and were assessed for activation in the presence of antigen expressing cells by CD107A stain, then were analyzed on a flow cytometer.

The prior study was specifically performed in late-culture, quiescent T cells in order to minimize the effects of cell proliferation on activated receptor dilution. The fact remains, however, that we are less interested in how quiescent cells behave to drug withdrawal as we are in the response of proliferating CAR-EBD T cells engaged in protracted exposure to target antigen when drug is withdrawn. The best way to address this is through *in vivo* experiments, which is done in Chapter 6, however, we also utilized Incucyte killing assays with tumor rechallenges to probe the limits of CAR-EBD activation following drug washout. In this study, the experimental condition of each of the B7H3CAR-3G-EBD variants was pretreated with (Z)-4-OHT for 24 hours, before being washed thoroughly, and plated against target-antigen expressing tumor cells. Tumor growth was tracked with the Incucyte until the pretreated cells failed to control tumor. Importantly, this point is able to be differentiated from T cell senescence or exhaustion by the inclusion of a control condition of B7H3CAR-3G-EBD variant T cells that received both pre-treatment and additional drug during the experiment. As would be predicted by our previous findings in quiescent cells the B7H3CAR-3G-EBD(4OHT) took the longest to lose activity, continuing to control tumor for more than three days and likely proliferating through multiple generations of T cells before its drug-induced receptor diluted below the threshold for activation and tumor control (Figure 26A). In comparison, the B7H3CAR-3G-EBD(CMP8) T cells lost their ability to control tumor almost immediately (Figure 26B). This may in part be due to its reduced activation at the chosen drug concentration (see Figure 14B) requiring less dilution than the EBD(4OHT) variant, however, this difference in functionality remains an important distinction between the variants that may influence future design and therapy inclusion decisions. The EBD(ES8) variant lands in the middle, exhibiting moderate tumor control for 24-48 hours, before losing tumor control completely upon tumor rechallenge on day 3 (Figure 26C).

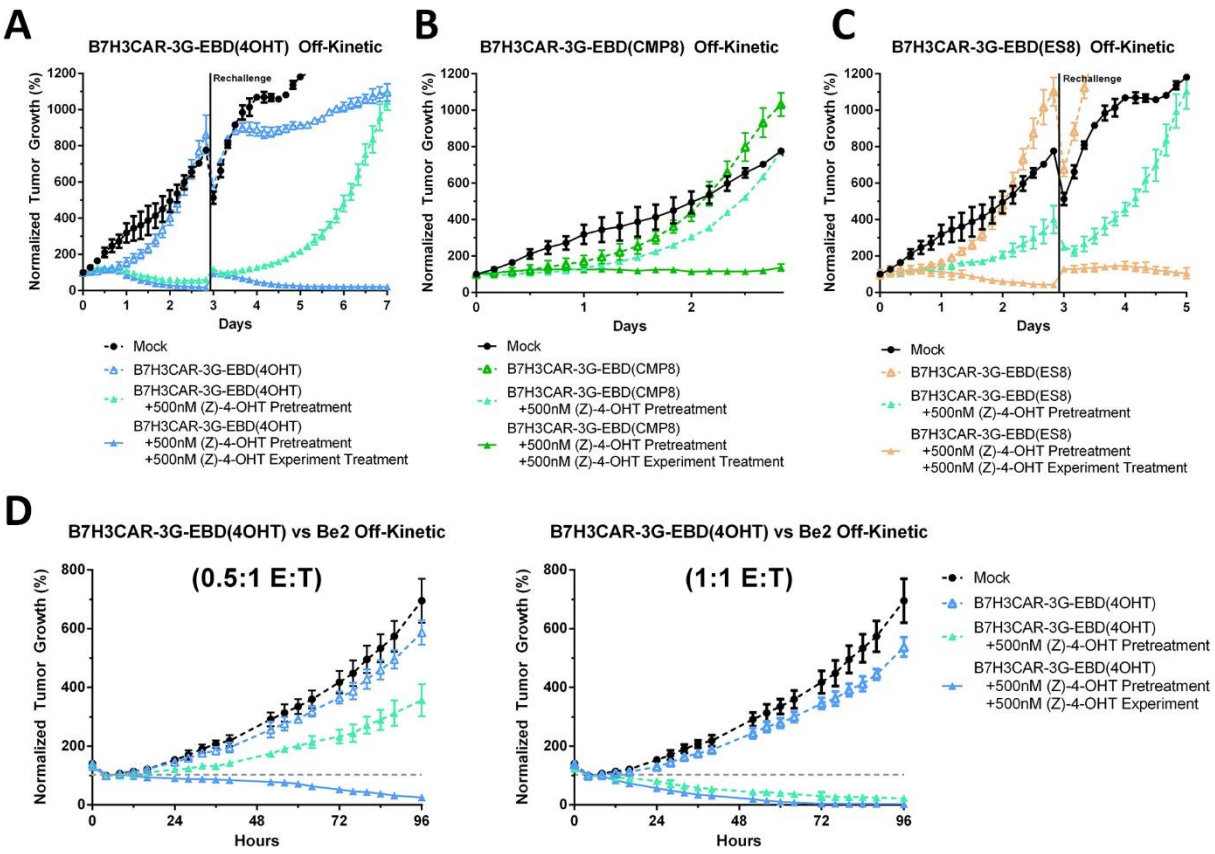

Figure 70. CAR-EBD T cells induced with (Z)-4-OHT, then washed, lose activity under activating, proliferative conditions.

A-D) T cells containing one of the B7H3CAR-3Gly-EBD variants or no transgene (Mock) were incubated with 500nM (Z)-4-OHT for 24 hours prior to the initiation of the study or were not. T cells that received drug pretreatment were thoroughly washed and subsequently subdivided into two groups, one of which received drug in the tumor killing assay (+Pretreatment, +Experiment), and the other did not receive additional drug treatment (+Pretreatment). At the initiation of the experiment, T cells were plated in triplicate and combined with K562 or Be2 tumor cells expressing mCherry. Plates were imaged in an incucyte every 4 hours for 3 or more days and tumor growth was tracked using mCherry signal. For D), serial dilutions of the same T cell preparations were used to achieve the stated E:T ratios.

Finally, there is evidence that there are meaningful differences in the quality of anti-tumor activity of B7H3CAR-3G-EBD(4OHT) T cells that have been pre-incubated with drug, then washed, compared to those that maintain consistent drug exposure through the tumor killing assay (Figure 26D). This difference appears when tuning experiments by adjusting

effector:target (E:T) ratios, and may highlight an important element of CAR-EBD biology as loss of tumor control occurs well before T cell proliferation occurs (counts of non-red objects in an incucyte analysis; data not shown). This variation appears to ride a knife's edge and has proven resistant to replication (i.e, in most experiments a drop from 1:1 E:T to 0.5:1 E:T results in every condition failing to control tumor).

5.3 Conclusions

Understanding the kinetics and mechanics of CAR-EBD functionality is critical for its future use in clinical products. As a whole, we have learned a lot about how it functions (and how it doesn't function), but still have much to uncover. Namely, while CAR-EBD does not function as a traditional degron, it retains elements of such systems, and it appears likely that the increases in cell-surface receptor we observe over the first 24 hours of drug induction are required for activation through a CAR-EBD. If drug induction does represent a CAR-EBD stabilization event allowing for greater accumulation in the T cells, it may make sense then that the EBD variants, which have differential affinity for (Z)-4-OHT, have differential loss of cell surface CAR-EBD.

That said, the kinetic of CAR-EBD accumulation upon drug induction is itself unusual, as it appears steeply asymptotic, suggesting a burst increase in cell surface CAR-EBD following drug induction. This may be more consistent with the intracellular-sequestration hypothesis than a simple stabilization hypothesis, these questions readily suggest running a protein stability study (e.g., pulse-chase) in the presence and absence of inducer drug to double check.

While the on and off kinetics of CAR-EBD appear inconsistent with our original hypothesis of a simple protein:protein interaction system, it also seems likely that this paradigm is a part of the truth in that high cell surface receptor expression is insufficient to produce antigen-specific activity. This finding represents the first of its kind to our knowledge, which has the potential to open up many new engineering opportunities in the future.

The kinetic data we've generated here is extremely important in helping us understand that while quiescent CAR-EBD T cells may not readily lose activity, a CAR-EBD T cell in a clinically-relevant, inflammatory, proliferative environment is likely to lose its antitumor activity (and likely its "sight" of tumor) after drug is withdrawn. Additional studies will need to be performed to understand how the receptor expression degranulation potential changes over these time courses in each of these cell cultures, but knowing that they do turn off is the first step.

Unfortunately, we are not much closer to understanding the relationship between donor and stringency of the off state of the huCD19CAR-1G-EBD(4OHT) construct, but we have gained considerable understanding and built a number of tools that will allow us to continue to investigate this interaction further in the future.

Chapter 6. In Vivo Testing of CAR-EBD.

6.1 Introduction

Our investigations into the function and mechanics of the CAR-EBD system *in vitro* have been a powerful proof of concept of a new technology for the regulation of CAR T cell activity. However, these cellular and protein engineering endeavors are advanced with the explicit goal of generating novel therapeutics for use in the clinic, and they are of limited utility without demonstrating that these systems can function *in vivo*. To this end, we have performed several studies to demonstrate this technology and understand its function in the context of animal models of human diseases.

6.2 Results

6.2.1 huCD19CAR-1G-EBD(4OHT) turns on *in vivo* and is capable of targeting tumor.

In order to demonstrate the functionality of CAR-EBD *in vivo*, we first selected the huCD19CAR-1G-EBD(4OHT) construct. While this construct has exhibited some degree of activity leakiness in previous *in vitro* studies (see Figure SXX), it is a very potent CAR that targets well characterized tumor lines with long track records, both in our lab and in the literature. NSG (NOD-scid IL2Rgamma^{null}) mice bearing Raji +ffluc tumors were administered T cells expressing the huCD19CAR-1G-EBD(4OHT) construct, the huCD19CAR, or neither (mock) and injected qMWF with (Z)-4-OHT or with vehicle only.

Tumor progression was measured by photon flux of a luciferase transgene present in the Raji tumor cell. Animals that received mock-transduced T cells were sacrificed on day 18 post-tumor injection (day 11 post-T cell injection) due to complications from tumor overgrowth (Figure 27A). Animals that received constitutive huCD19CAR lost detectable tumor signal as early as day 11 post-tumor injection (day 4 post-T cell injection), however a few animals did experience small recurrences in the femur head or submandibular gland (Figures 27A and B). While unusual, these recurrences are not unheard of in this model, and the tumor outgrowth was quickly controlled by remaining engrafted huCD19CAR T cells without additional intervention. Notably, the administration of (Z)-4-OHT appears to have had no impact on the growth of tumor in mock T cell treated animals and no impact on the eradication of tumor from huCD19CAR treated animals. Animals that received T cells transduced with the huCD19CAR-1G-EBD(4OHT), but did not receive (Z)-4-OHT survived

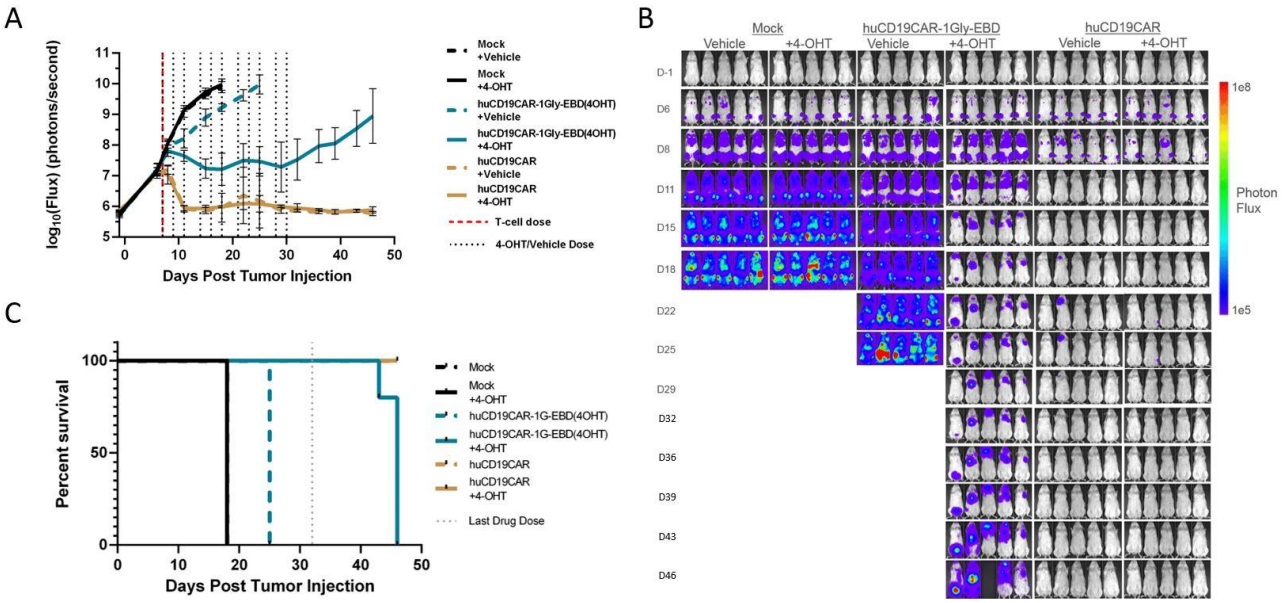

Figure 73. *huCD19CAR-1G-EBD(4OHT) demonstrated anti-tumor functionality and activity switching in vivo.*

A-C) NSG mice were inoculated intravenously with 0.5e6 Raji tumor cells expressing ffluc for imaging purposes. 7 days later, groups of 10 mice were administered 10e6 T cells transduced either with the constitutive huCD19CAR, the huCD19CAR-1G-EBD(4OHT) construct, or no transgene (mock). Groups were then subdivided into animals that receive qMWF 150mg/kg (Z)-4-OHT drug injections and animals that receive qMWF vehicle only for the duration of the study. N=5 per condition.

longer that the mock T cell treated animals ($p<0.05$), highlighting the leakiness of the huCD19CAR under the control of EBD(4OHT). Animals that received T cells transduced with the huCD19CAR-1G-EBD(4OHT) in addition to injections with (Z)-4-OHT managed to hold their disease stable until day 30 post-tumor inoculation ($p<0.001$ compared to huCD19CAR-1G-EBD(4OHT) treated animals receiving vehicle only). At this point, qMWF (Z)-4-OHT injections were withdrawn, the huCD19CAR-1G-EBD(4OHT) appears to turn off, and tumor grew out in every animal until they were euthanized due to complications from tumor overgrowth.

6.2.2 CD22CAR-3Gly-EBD(4OHT) turns on in vivo and is capable of controlling tumor

One of the proposed advantages of the CAR-EBD system is its portability to new CARs and targeting domains with minimal re-engineering required. We have demonstrated this capacity in vitro, with similar experimental results between CARs, but it remains to be seen if this is also possible *in vivo*. Furthermore, while the huCD19CAR-1G-EBD(4OHT) construct was investigated first for its prodigious antitumor activity, it was already known to exhibit greater leakiness than several of our other constructs. Finally, the huCD19CAR-1G-EBD(4OHT) experiment referenced above experienced technical limitations with drug injections, delaying the first injection of (Z)-4-OHT until several hours after T cell administration, potentially leading to some kinetic difficulties given the rapid growth of the Raji tumor. To address all of these concerns simultaneously, we proceeded to test the regulatibility of the huCD22-3Gly-EBD(4OHT) construct *in vivo*.

To this end, we again inoculated NSG mice with Raji +ffluc tumors allowed them to gestate for 7 days before administering T cells. For this study, animals were provided with their first

dose of (Z)-4-OHT or vehicle on day 6, and the T cells administered were pre-incubated with (Z)-4-OHT overnight prior to injection. In contrast to the huCD19CAR-1G-EBD(4OHT) *in*

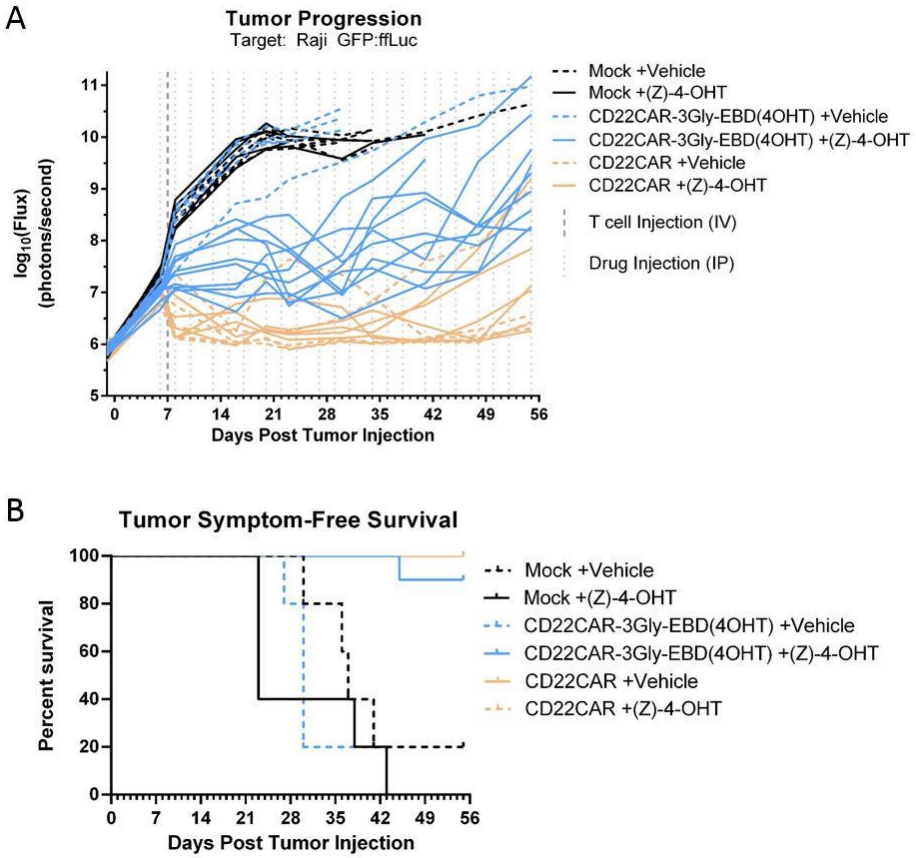

Figure 76. *huCD22-3Gly-EBD(4OHT) demonstrates anti-tumor functionality and activity switching in vivo.*

A-C) NSG mice were inoculated intravenously with 0.5e6 Raji tumor cells expressing ffluc for imaging purposes. 7 days later, groups of 10 mice were administered 10e6 T cells transduced either with the constitutive huCD19CAR, the huCD19CAR-1G-EBD(4OHT) construct, or no transgene (mock). Groups were then subdivided into animals that receive qMWF 150mg/kg (Z)-4-OHT drug injections and animals that receive qMWF vehicle only for the duration of the study. N=5 per condition; CD22-3Gly-EBD(4OHT) +(Z)-4-OHT condition N=10.

vivo study, the huCD22-3Gly-EBD(4OHT) construct exhibited little to no leakiness *in vivo*, demonstrated by the animals that received CAR-EBD T cells, but vehicle only injections, exhibiting tumor growth and survival kinetics similar the mock treated animals (Figure 28A and B)(tumor growth, p=0.87; survival, p= 0.41). Additionally, animals that received both

huCD22CAR-3Gly-EBD(4OHT) T cells and (Z)-4-OHT experienced reduced tumor burdens compared to their vehicle-receiving counterparts, demonstrating switching activity *in vivo* with a second CAR-EBD construct ($p<0.05$). Similar to the huCD19CAR-1G-EBD(4OHT) construct however, the huCD22CAR-3Gly-EBD(4OHT) construct exhibited reduced capacity for tumor control compared to the constitutive CD22CAR, an especially intriguing finding in light of the "optimized" drug dosing regimen of this study. Additionally, while the study is ongoing, administration of (Z)-4-OHT has not been withdrawn from these animals, allowing for the full kinetic of anti-tumor activity to be observed over time. Of note, the huCD22CAR-3Gly-EBD(4OHT) T cell treated animals that received (Z)-4-OHT begin to experience a significant increase in the speed of tumor outgrowth around day 40. This trend is also observed in many of the animals that received constitutively active huCD22CAR, in spite of many of these animals nearly clearing tumor earlier in the study (Figure 28A).

6.3 Conclusions

The most important conclusions to be drawn from this data are that we are able to achieve both on and off switching activity of the CAR-EBD system *in vivo*, and that this switching activity is possible with multiple CAR-EBDs. On-switching requires both sufficient serum concentrations of (Z)-4-OHT to be attained, and for us to detect this switching, the CAR-EBD T cells must produce sufficient anti-tumor activity to slow tumor growth in comparison to the mock-transduced T cell groups. Off-switching, as demonstrated for the huCD19-1Gly-EBD(4OHT) construct in Figure 27, requires that our inducer drug, (Z)-4-OHT, be cleared from the animals in a reasonable time frame (opposed to accumulating in significant quantities in or fluxing through fat stores), and that the CAR-EBD is able to turn off, once

activated, if (Z)-4-OHT is removed. Indeed, we observed in the huCD19-1Gly-EBD(4OHT) study, that immediately following withdrawal of drug administration, the tumor held in check by huCD19CAR-1G-EBD(4OHT) T cells began to grow out, and ultimately resulted in the demise of this group by day 46 after tumor inoculation (Figure 27A). This observation coincides with our assessment from Chapter 5 that CAR-EBD T cells exposed to an activating environment will lose activity as they proliferate and dilute the active CAR-EBD receptor from their cell surfaces. Furthermore, it seems that the off-state behavior of CAR-EBDs *in vitro* (whether stringent or leaky) is conserved in the *in vivo* Raji model. This is an important demonstration due to the significant differences between the experimental systems – we had predicted early that the small amount of leakiness observed in the huCD19CAR-1G-EBD(4OHT) system *in vitro* would prove immaterial *in vivo* due to the added complexity of the animal model (e.g., no exogenous cytokine, competing cell types, tissue compartmentalization, tumor microenvironment and 3D structure), this however has proven not to be the case.

The *in vivo* studies we have performed to date have also highlighted another intriguing hurdle, namely, the anemic anti-tumor effect of CAR-EBD T cells compared to their derivative constitutively active CARs (including the B7H3CAR-3Gly-EBD(4OHT); data not shown). Several interpretations of these data are possible. The first is that the switching kinetics of the CAR-EBD system are such that we do not achieve full activation of our CAR-EBD T cells until after the tumor had progressed to a point where it could no longer be fully controlled. The second is that we are not able to achieve the necessary serum concentrations of (Z)-4-OHT to achieve maximal activation of our CAR-EBD T cells. The third is that the CAR-EBD constructs generate inferior per cell anti-tumor activity, and the CAR-EBD cell dose administered to these animals was insufficient to overcome their tumor burden.

We attempted to address the first concern with the huCD22CAR-3Gly-EBD(4OHT) experiment. While the animals in the huCD19CAR-1G-EBD(4OHT) experiment received T cells straight from thaw and only received their first dose of (Z)-4-OHT ~2 hours after T cells were administered, the animals from the huCD22CAR-3Gly-EBD(4OHT) experiment were first dosed with (Z)-4-OHT the day before they were administered T cells (day 6) and the T cells administered were pre-incubated with (Z)-4-OHT for 24hrs prior to injection in order to avoid any potential activity switching kinetic issues the first study may have introduced. While this staging introduced its own confounds (specifically, low viability of the injected T cell product since they were rested for 24hrs out of thaw without stimulation), it clearly did not address the underlying issue (compare CAR vs CAR-EBD in Figure 27A and Figure 28A).

The second consideration – that of our actual achieved serum concentration of (Z)-4-OHT – has not been tested in our hands, but is well established in the literature. Multiple sources suggest that our method of drug preparation and frequency of administration (qMWF) should achieve peak drug concentrations in excess of 1 micromolar (over 10x the EBD(4OHT) EC90) and troughs in the 50nM range (approximately the EBD(4OHT) EC50) [53-56]. Given the slow off-kinetic of the EBD(4OHT) domains, these temporary drops in serum concentration to the EC50 should have little to no effect on the CAR-EBD T cells ability to maintain activity. However, given the evidence we are observing, it is incumbent upon us to validate that our methods are achieving both our expected serum (Z)-4-OHT concentrations and if not, the serum concentrations necessary to activate our constructs. This work in ongoing.

The third consideration, that a CAR-EBD is less potent than the CAR it is derived from, remains possible (and is an effect demonstrated in other regulated CAR T cell systems [50]), but would be surprising since there is little to no evidence of this from our *in vitro* data. Once we have confirmed that our current drug dosing scheme achieves the level of CAR-EBD

activation we expect, we intend to explore this possibility more fully with a dose-titration experiment to determine the *in vivo* CAR:CAR-EBD anti-tumor equivalence ratio.

Finally, it remains possible that further experimental optimization may help us attain the effects and knowledge needed to move this technology forward. Indeed, there are several experimental optimizations and expansions that we aim to pursue once we understand the results from these early experiments better. Chief among these is a study to explore the off-kinetic of the EBD(4OHT) domain *in vivo*. In such an experiment, CAR-EBD T cells would be pre-incubated with inducer drug (e.g., (Z)-4-OHT) and then administered to CAR-target-expressing-tumor-bearing mice that do not receive drug. Similar to the Incucyte-based experiments presented in 5.2.3, we would expect the CAR-EBD T cells to dilute their active receptor as they become activated and divide, resulting in a similar kinetic curve. Additionally, once our drug and T cell dosing have been optimized, we aim to explore rechallenge experiments *in vivo*, wherein, CAR-EBD and CAR T cells which clear tumor are provided with a second challenge with tumor in the presence or absence of (Z)-4-OHT. Our motivations for these studies and our initial findings in this space are explored in more depth in Chapter 7.

Chapter 7. The Future of CAR-EBD: Applications, Advantages, and Novel Engineering Strategies.

7.1 Introduction

We have demonstrated that CAR-EBD is a powerful platform for the control of CAR T cell activity with small molecule drugs. These initial forays into construct development, optimization, and characterization are just the beginning – once fully established, and well defined, this technology has enormous potential to revolutionize the field of cellular therapies. As we transitions from CAR-EBD platform design to CAR-EBD applications, I wanted to highlight some of the most interesting results we've had in this space, as well as discuss what the future of this technology could be.

7.2 Results and Ongoing Work

7.2.1. CAR-EBD may enhance CAR T cell potency through improved persistence in chronic antigen environments

We have hypothesized that modulation of CAR T cell activity through cyclical CAR-EBD induction will enhance therapeutic potency and/or T cell persistence by sparing CAR T cells from the dysfunction associated with chronic antigen exposure and subsequent immunological exhaustion. In the course of testing cycling schemes, however, we have discovered clear anti-tumor persistence advantages associated with CAR-EBD compared to caCARs, even when kept consistently in the on state (Figure 28). While all B7H3CAR and

B7H3CAR-3Gly-EBD(XXXX) EBD variant lines successfully control tumor upon initial challenge, the groups begin diverging upon tumor rechallenge. In both donors tested, the first cell line to fail to control tumor is the constitutively active B7H3CAR, while both B7H3CAR-3Gly-EBD(4OHT), B7H3CAR-3Gly-EBD(CMP8), and B7H3CAR-3Gly-EBD(ES8) each maintains tumor control much longer (Figure 28). This is a striking result, suggesting that the mere inclusion of an EBD domain on a CAR improves CAR T cell fitness. We have several hypotheses regarding why this may be the case which will require additional testing to elucidate, but our current favorite is that by blocking CAR signaling in the absence of an inducer drug, we are saving the CAR-EBD T cells from chronic tonic signaling known to occur with some CARs and has been associated with early T cell exhaustion and poor clinical outcomes [57]. We are in the process of validating this hypothesis, and if true, it could be enormously beneficial to the field of CAR T cell therapies, independent of our ability to cycle T cell activity.

A related prediction currently under testing is that the inclusion of an EBD on a CAR during production produces CAR T cells with a less differentiated state and superior phenotype for use in fighting cancer. These stem cell-like memory T cells have long lifespan, are self-renewing, are capable of rapid differentiation into effector T cells, and have increased resistance to immune-checkpoints [58]. Furthermore, they have been identified as important contributors to successful CAR T cell engraftment and the antitumor activity of CAR T cells [59]. To this end, a series of experiments assessing CAR T cell vs CAR-EBD T cell tonic signaling and molecular phenotypes following manufacturing and antigen exposure have been planned.

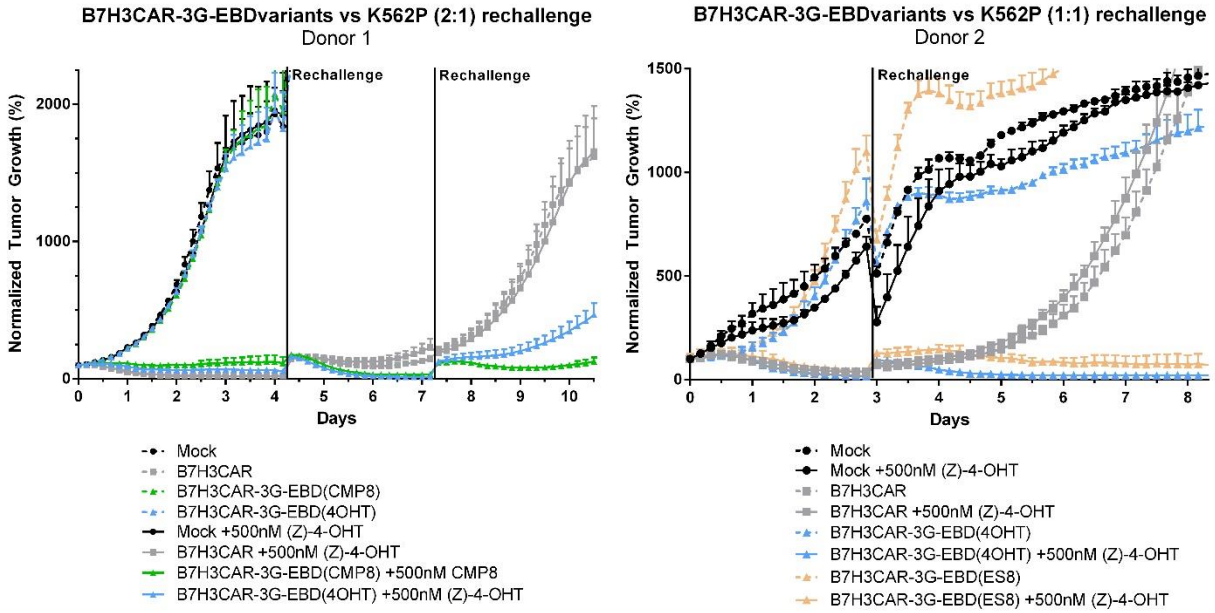

Figure 79. *CAR-EBD may enhance CAR T cell potency through improved persistence in chronic antigen environments.*

To assess their resistance to functional decline, the B7H3CAR-3Gly-EBD(XXXX) EBD variants were exposed to chronic antigen by serial rechallenge with antigen-expressing tumor. As an extension of the experiment in Figure 16C, additional K562 tumor was added on day 3 or 4 and day 7, depending on the donor. (Additional challenges are initiated once the previous round of tumor has been eradicated by at least one condition.).

7.2.2 Combining multiple CAR-EBDs enables multiplexed targeting under differential drug regulation.

One design specification of the CAR-EBD system that confers enormous potential to future engineering strategies is its theoretical capacity for integrated multiplexing through the use of multiple, independently regulatable EBD domains. While early studies examining antigen-specific degranulation in the presence of various estrogen analogs, we have only recently begun to directly demonstrate the potential for multiplexed regulation of CAR-EBDs against different targets. In a co-culture Incucyte tumor killing assay, K562+GFP tumor cells (B7H3+CD22-) were mixed with Raji+mCherry tumor cells (B7H3-CD22+). This tumor combination was subsequently plated with B7H3CAR-3G-EBD(CMP8) T cells and

CD22CAR-3G-EBD(4OHT) T cells from the same donor. This combination of two tumors and two CAR-EBDs were then treated with (Z)-4-OHT, CMP8, or no drug and the growth of each tumor was independently tracked. The result demonstrates the power of this technology (Figure 29). When treated with (Z)-4-OHT, both CAR-EBDs turn on, killing both tumors, but when the culture is treated with CMP8, only the B7H3CAR-3G-EBD(CMP8) T cells are activated, killing the K562 tumor, while the Raji tumor grows out. Finally, in the absence of drug, both tumors grow out, as if they were treated with the Mock T cells. This toy model functioned perfectly and demonstrates the potential of this platform for the independent regulation of multiple transgenes – not just CARs – at once.

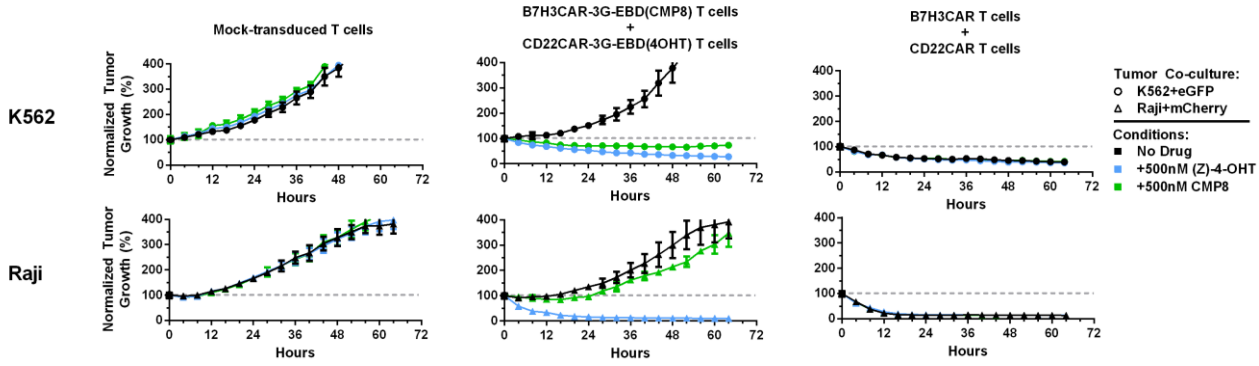

Figure 82. Combining multiple CAR-EBDs enables multiplexed targeting under differential drug regulation.

Donor-matched T cells expressing the B7H3CAR-3G-EBD(CMP8), CD22CAR-3G-EBD(4OHT), B7H3CAR, CD22CAR, or no transgene were plated on a 1:1 combination of K562+GFP tumor cells and Raji+mCherry tumor cells. Cultures were then treated with 500nM (Z)-4-OHT, 500nM CMP8, or no drug. Red and green Incucyte chennels were used to track the growth of each tumor line in each condition. Tumor growth was normalized to study start and plotted. Columns represent the independent tumor tracking data from the same wells.

7.3. Summary and Future Directions

We have demonstrated that CAR-EBD possesses many of the desirable traits we enumerated at the beginning of this journey. While there is some variability between the CARs we've chosen to regulate and between specific T cell functional outputs, CAR-EBD has shown immense promise as a potential clinical tool with stringent on and off states, rapid switching kinetics, that it is contained within a small genetic payload, that it is human derived, that it is regulated by FDA-approved drugs (in addition to non-approved drugs if multiplexing), that it can be used with multiple CARs or other transgenes, and has the potential to be multiplexed for the simultaneous parallel or orthogonal regulation of multiple transgenes. The success of this work has resulted in a recent patent application [60].

These studies represent just a sliver of what may be possible with a fully explored and elucidated CAR-EBD regulation platform. Many additional targets for regulation are also being cloned including inducible suicide genes and potency enhancers [61]. To date, the B7H3CAR and CD22CAR has been the biggest successes for CAR-EBD, with the most stringent off states, and inducible on states with functional potency nearing their constitutively active parent CARs. However, the underlying determinants of this success are less clear, and understanding this better is a major goal of the project moving forward.

As this may suggest, future directions for the project are numerous and divergent. In the immediate future, better understanding the mechanism of action of CAR-EBD regulation will likely lead to greater success in its application to novel CARs or other proteins of interest as well as the first publication on this topic. The work necessary to reach these milestones include a thorough investigation of proteasome and HPS90 inhibitors to validate or disprove our original mechanism theory (or elucidate a new one). Simultaneous testing of the

functional impact of HSP90 under and over expression on the stringency of regulation is also underway in an attempt to better understand the donor to donor variability seen with the huCD19CAR-1Gly-EBD(4OHT) construct. Furthermore, a superior understanding of the mechanics and kinetics of CAR-EBD could better inform clinical applications (e.g., if it takes days for EBD(4OHT) to turn off, alternative controls, such as dasatinib, would need to be used in an emergency, and planned CAR-EBD activity cycling would need to run several days behind the intended schedule.)

It will also be extremely important to follow up in detail on the apparent advantages of CAR-EBD on functional persistence. We have many theories what may be occurring here, but the current front runner is that reduction in tonic signaling during therapy manufacturing results in a less differentiated product with a longer therapeutic lifespan. Testing this will involve the use concurrent use of single cell functional genomics and flow cytometry on caCAR and CAR-EBD cells throughout the manufacturing process in the presence and absence of drug induction.

Additionally, initial *in vivo* studies to validate CAR-EBD functionality in animal models are ongoing and seem promising. Once proof of concept experiments have completed, demonstrating capacity for switching activity *in vivo* and the potential for therapeutic enhancement will be a high priority. Humanized mouse models developed in our lab also have the potential to underscore the benefits of this system.

Further into the future, things appear very bright. The advent of an easily adaptable transgene regulation technology such as CAR-EBD could enable many groundbreaking technologies, including the use of implantable, drug eluting hydrogels for the spatiotemporal control of CAR-EBD T cell activity, enable the use of previously identified "immunity boosters" that have been deemed by the field as too unsafe to allow without strict expression

regulation, or create platforms of multiplexed CARs and CAR-EBDs for selective synergistic use.

In conclusion, it has been an incredible experience and honor working to bring such an interesting and powerful technology to fruition. I look forward to seeing what the world will do with it once it is released.

Materials and Methods

Construct Designs

Construct designs were produced in Benchling from existing construct sequences in the Jensen lab, NCBI, and literature. Plasmids were constructed through a combination of Gibson assembly and custom synthesis. EBD variant sequences are provided in Supplemental SXX

Lentivirus Production

Recombinant lentivirus was generated by transiently transfecting a 293T producer cell line with lentiviral packaging plasmids alongside a transfer plasmid containing the transgenes of interest. Transfection was performed using Lipofectamine 2000 (Life Technologies, Cat. # 11668-500). Four days after transfection, lentivirus was isolated from the 293T cell culture supernatant via ultracentrifugation and stored at -80° C until the day of transduction.

iSynPro GFP:ffluc Reporter Jurkat T cells

A synthetic promoter specific to T cell activation ("iSynPro") was identified by members of the Jensen Lab through the bio-panning of a large custom library of combined T cell transcription factor binding sites (manuscript in preparation). A CAR activation reporter Jurkat cell line was generated by transducing Jurkats with lentivirus housing this promoter upstream from GFP:ffluc. Clonal populations of iSynPro_GFP:ffluc expressing Jurkats were isolated by flow assisted cell sorting (FACS) and clonal dilution.

Western Blot

Western blot is used to verify or quantify the expression of a protein of interest in a cell population. 1-5e6 cells are collected and washed before being lysed in RIPA buffer

containing protease inhibitors and incubated on ice for an hour. Samples are spun at 15k RPM and supernatants are collected. A Micro BCA Protein Assay Kit (Thermo Scientific, Cat# 23235) is used using the manufacturer's instructions to quantify and normalize the total protein loaded into each well of the gel. Quantified samples are then mixed with LDS sample buffer (Invitrogen, Cat# NP0007) and reducing agent (Invitrogen, Cat# NP0009) to a final volume less than 20uL per sample. Load gel and follow manufacturer's instructions in the operation of the gel box (Mini Gel Electrophoresis Tank, ThermoFischer Cat# B4478641, with recommended buffers and a gel appropriate to your anticipated protein product) to run your sample down the gel, and transfer it to a nitrocellulose membrane. Block the nictorcellulose membrane with Odyssey blocking buffer for 1 hour. Add primary antibody (anti-human CD3ζ) at a pre-optimized dilution (1:500 for CD3ζ) and incubate at room temperature for 1 hours. Wash membrane twice in 1x TTBS. In a light-proof box, add 1uL of anti-mouse IRDye 800CW in 10mL odyssey blocking buffer and incubate for 30min. Washing the membrane 4x in 1xTTBS, and 1x in TBS. Image your gel on a Licor Odyssey CLx Scanner, using the included software to quantify protein expression. Quantified protein bands within a lane are then compared to a housekeeping gene (e.g., endogenous CD3ζ) for comparisons between samples.

T cell Production and Culture (Chapter 2)

Protocols to acquire human cells were approved by the institutional review board of Seattle Children's Hospital. CD4+ and CD8+ T cells were isolated from human peripheral blood mononuclear cells (PBMCs) by magnetic activated cell sorting with a CD4+ or CD8+ T cell isolation kit (Miltenyi Biotech, Cat. # 130-096-495). The cells were immediately subjected to a bead-based CD3/CD28 stimulation using Dynabeads (Thermo Fisher Scientific, Cat. # 11131D) at a bead to cell ratio of 1:1. Unless otherwise indicated, T cell culture media

consisted of RPMI 1640 (Gibco, Cat. # 22400-089) supplemented with 10% FBS (Hyclone, Cat. # SH30071.03), and 2mM L-glutamine (Gibco, 25030-081). CD4 T cell culture media was supplemented with 0.5 ng/mL IL-7 and 0.05 ng/mL IL-15 (Miltenyi, Cat. # 130-095-765) throughout the culture period. CD8 T cell culture media was supplemented with 50 U/mL IL-2 (Chiron, Cat. # 53905-991-01) and 0.05 ng/mL IL-15 (Miltenyi, Cat. # 130-095-765). Two days post-stimulation, cells were transduced with lentivirus containing construct of interest. Dynabeads were removed on day 7, and the cells were allowed to expand until day 12 before being MACs sorted for transduction marker (e.g., EGFRt/Her2tG), and frozen on D14. Thawed cells underwent Rapid Expansion Protocol (REP) as previously described [62]. Flow cytometry was used to confirm the purity of T cell populations expressing our construct(s) of interest prior to functional studies. Functional studies were performed between Day 7 and 21 of REP.

T cell Production and Culture (Chapters 3-7)

Prior to the start of the CAR-EBD project, CAR T cell manufacturing in the Jensen lab migrated to a 7 day protocol in X-VIVO 15 media (Lonza, Cat# BE02-060Q) supplemented with 2% KnockOut Serum Replacement (Gibco, Cat# 10828028), IL2, IL7, IL15, and IL21, and utilizing methotrexate for selection (in interaction with the selection transgene, DHFRdm) T cells which were successfully transduced. In brief, fresh or frozen CD4+ and CD8+ T cells are counted and mixed at a 1:1 ratio, targeting 2.5e6-10e6 total T cells per transduction. If cells are frozen, rest for 3-4hrs before proceeding. Stimulate cells using CTS stim beads (ThermoFischer, Cat# 40203D) using the manufacturer's protocol. For each intended transduction, place the cells in 4mL of media in an incubator at 37C overnight. The next day remove and reserve 3mL of the media, leaving the cells undisturbed. Calculate the amount of each titered virus required to reach an MOI of 1. Add this much

virus and 4uL of protamine sulfate to the appropriate cultures and incubate over night. The next day, media should be added to the cultures and they may be moved to a larger vessel, depending on anticipated expansion. 100nM methotrexate is added to the cultures on day 2 after transduction. On day 7, remove beads, and remove an aliquot of cells for counting and flow cytometry to determine CD4:CD8 ratio (which may drift after time in culture – supplemented cytokines may be adjusted to promote CD4 or CD8 outgrowth over the other) and transduction efficiency/culture purity. Cells may be used for assays at this point (S1D7), frozen down, or placed into rapid expansion protocol (as previously described [62]) for later use in assays.

Flow Cytometry

Flow cytometric analysis was performed to determine transduction marker expression and phenotypic marker expression. Cells were removed from culture and placed into 96-well round-bottom plates, washed twice with PBS (Gibco, Cat. # 10010-023), stained with pre-titered quantities of antibody, washed three more times with PBS and finally fixed with 0.5% paraformaldehyde (Electron Microscopy Sciences, Cat. # 15713) in PBS before analysis. Flow cytometric data was collected using a BD LSRFortessa flow cytometer and later analyzed using FlowJo software. Final flow plots were populated by cell populations remaining after the following gating strategy was performed. First, a "lymphocyte" gate was generated by drawing a polygon within the forward scatter vs side scatter scatterplot to isolate events with size and granularity characteristic of lymphocytes and remove debris and dead cell events. Within the lymphocyte gate, a second "single cell" gate was generated by gating on events that followed a linear relationship between forward scatter in the height and area dimensions to remove cell doublets from downstream analysis. If

applicable, a “live cells” gate was generated using the live dead stain to exclude cells with compromised membranes.

Chromium Release Assay

Chromium release assays are used to assess the cytolytic potential of CAR T cells by measuring the amount of radioactive Chromium 51 released from target tumor cells as they are killed. The day before the assay, target tumor cells are labelled with 51Cr (Perkin Elmer, Cat# NEZ030010MC). For assays testing T cells containing drug regulated domains (such as CD19CAR-huERdd or huCD19CAR-1Gly-EBD(4OHT)) T cells are incubated in their final drug concentrations for 24hrs prior to the start of the assay. On the day of the assay, 51Cr-loaded target lines (including positive and negative controls) are counted and plated in a 96 well plate at 5000 cells per well. Effector T cells are plated with the target effectors at ratios of 30:1, 10:1, 3:1, and 1:1. Tumor controls for no killing and maximum killing are added to wells with no T cells and wells containing 2% SDS, respectively. Plates are briefly spun to settle cells, and incubated at 37C for 4 hours. Supernatants are subsequently taken and transferred to white LUMA plates (Perkin Elmer, Cat# 6006633) and allowed to dry overnight. Dry plates are read on a Perkin Elmer Topcount machine and the data is analyzed in Microsoft Excel and Prism.

Cytokine Release Assay

Cytokine release assays are used to determine the quantity of inflammatory cytokine (IL2, IFNg, TNFa) released into the culture medium by T cells in response to target tumor antigens. For assays testing T cells containing drug regulated domains (such as CD19CAR-huERdd or huCD19CAR-1Gly-EBD(4OHT)) T cells are incubated in their final drug concentrations for 24hrs prior to the start of the assay. T cells and target tumor line(s) are

then plated together at the desired drug concentrations at an effector:target ratio of 2:1, and allowed to incubate at 37C for 24hours. Then, supernatants are saved and frozen. Thawed samples may then be diluted 1:20-1:50 before cytokine quantification using the V-PLEX Proinflammatory Panel 1 Human Kit for the detection of IL2, IFNg, and TNFa using the manufacturers protocol and run on a MESO QuickPlex SQ120 instrument. Analysis of results was performed in Graphpad Prism.

Intracellular Cytokine Staining (including CD107a T cell Activation Assay)

Production of cytokine and markers of activation in response to stimulation was assayed using intracellular cytokine staining (ICCS). Four hours prior to staining, a transport inhibitor cocktail (Thermo Fisher Scientific, Cat. # 00-4980-03) was added to prevent T cell release of secretory proteins. One hour later, anti-CD107a antibody is added to culture wells at a pretitered concentration. Following completion of the study, cells are then stained with Live Dead Fixable Aqua viability dye (Thermo Cat # L34957) and relevant surface markers to allow gating of live, modified T cells. Next, samples were fixed and permeabilized using the Fixation/Permeabilization Kit (BD, Cat. # 554714) according to the manufacturer's protocol. The cells were then stained with antibodies for IL2, IFNg, TNFa, 4-1BB, and Nur77. After additional washing, cells were run on an LSR fortessa and analyzed in flowjo.

IncuCyte Cytotoxicity Assay

Incucyte cytotoxicity assays are used to visualize the cytolytic ability of CAR T cells against target tumors longitudinally. Tumor lines expressing mCherry are seeded alone into an Incucyte compatible plate at a range of densities to determine the ideal tumor density for the desired length of study. For assays testing T cells containing drug regulated domains

(such as CD19CAR-huERdd or huCD19CAR-1Gly-EBD(4OHT)) T cells are incubated in their final drug concentrations for 24hrs prior to the start of the assay, unless otherwise noted. On the day of the assay, effectors are plated with targets in triplicate and at a range of effector:target ratios including 4:1, 2:1, 1:1, and 0.5:1 to address variable effector potency between donors, REPs, and CARs. Assays using specific concentrations of inducer molecules were performed in edge-well plates filled with PBS to avoid inadvertent increases in drug concentration due to media evaporation. Incucyte software is used to take phase and red fluorescence images of each well every 3-4 hours for the duration of the study. Data analysis may be performed in IncuCyte software, or raw data may be exported and analyzed in Graphpad Prism.

Serial Tumor Challenge Assay

Serial tumor challenge is an extension of an IncuCyte Cytotoxicity assay wherein additional tumor challenges are made to the T cells once they have cleared tumor (or at a set schedule) until they fail to control tumor. It is important to avoid too much time between challenges to avoid allowing the T cells time to rest, invalidating the experiment. Challenges are performed on a consistent number of tumor cells during each round, even though the tumor-specific T cells will be multiplying throughout the experiment. It is worth noting that while the dysfunction, may replicate some of the functional characteristics of immunological exhaustion, it does not, strictly speaking, producing “exhausted” T cells. Results are analyzed similarly to the Incucyte Cytotoxicity Assay.

Acknowledgements

None of this work would have been possible without the decades of guidance, instruction, patience, care, and affection I have received from my community of friends, family, coworkers, and advisors. I would like to extend a heartfelt thanks too al the members of the Jensen Lab through the years. I would especially like to thank the folks who have worked with me to bring CAR-EBD to life including (but not limited to), Ryan Koning, Adam Johnson, Jason Yokoyama, Blake Baxter, Aquene Reid, Piper Cramer, Josh Gustafson, Michael Baldwin, Mike Fitzgerald, and the springboard team. I would also like to thank many other members of the lab (in no particular order): Chris Saxby, Ben Curtis, Clint Heinz, Ian Cardle, Taylor Ishida, James Matthaei, Josh Gustafson, Adam Johnson, Jia Wei, James Rosser, Niels Rekers, Elle Curinga, Leanne Rubin, and an enormous thank you to Dr. Jensen. It has been a long road we have had together, and it hasn't always been easy. Thank you for always believing in me and for your continued support and advising throughout.

I would like to acknowledge my committee. Dr. Suzie Pun, both for her sage advice, and for immediately accepting much more responsibility on my committee than she signed up for when it was needed. Also Drs. Pat Stayton, Hao Yuan Kueh, and Jim Olson for your patience during my time off from UW, and your excitement for the work once I returned.

I would also like to acknowledge my friends, both local to Seattle, and around the world, who helped keep me sane and grounded throughout my time as a graduate student at UW. I would like to call out David Peeler, Zak Wescoe, and Kristian Eschenburg, in particular – living with you was one of the best decisions I ever made, and I will remember our time at Treewalla fondly for the rest of my life. Too many others played an important role in my

journey to the finish line to mention by name, but needless to say, I am looking forward to continuing to adventure and grow with you all, and I thank you for your endless support.

I would like to acknowledge my family, Ann Blumenthal, Tico Blumenthal, Nadia Hanafy, Naia Blumenthal, Talia Blumenthal, and Teo Blumenthal for your endless support and love throughout. Graduate school was a more complicated path for me than any of us could have imagined, and I am extremely thankful to have some of the smartest, most compassionate people I've ever known on my side to work through it all. While my father, Julius Blumenthal, didn't live to see me graduate, he remains my largest inspiration and role model, and it makes me proud to know how much he enjoyed the thought of me getting a doctorate.

I would also like to acknowledge my new family, Tarek Elabbady and Engy Fahmy, for welcoming me into your home, feeding me, supporting me, and providing me with advice when my own family was far away. Not only is your daughter the greatest good that has ever happened to me, but I feel doubly blessed to have in-laws who care about me so much.

Finally, I would like to acknowledge my wife, Leila Elabbady. When we met, neither of us could have known that I had so much further to go in my degree. I know how difficult this has been for you as well, and I thank you for trusting me, thank you for believing in me, and thank you for staying by my side. You inspired me to accomplish this work, and truly, it would not have been possible without you.

It is difficult for me to express how indebted I am to all of you. This is as much your accomplishment as it is mine, and I thank each of you from the bottom of my heart for your support through the years. I'm excited to share what we have accomplished and to see what comes next.

References

1. Allison, J.P., B.W. McIntyre, and D. Bloch, *Tumor-specific antigen of murine T-lymphoma defined with monoclonal antibody.* J Immunol, 1982. **129**(5): p. 2293-300.
2. Fitch, F.W., *T-cell clones and T-cell receptors.* Microbiol Rev, 1986. **50**(1): p. 50-69.
3. Gross, G., T. Waks, and Z. Eshhar, *Expression of immunoglobulin-T-cell receptor chimeric molecules as functional receptors with antibody-type specificity.* Proc Natl Acad Sci U S A, 1989. **86**(24): p. 10024-8.
4. Kershaw, M.H., J.A. Westwood, and P.K. Darcy, *Gene-engineered T cells for cancer therapy.* Nat Rev Cancer, 2013. **13**(8): p. 525-41.
5. Hudecek, M., et al., *The nonsignaling extracellular spacer domain of chimeric antigen receptors is decisive for in vivo antitumor activity.* Cancer Immunol Res, 2015. **3**(2): p. 125-35.
6. Sheykhhasan, M., H. Manoochehri, and P. Dama, *Use of CAR T-cell for acute lymphoblastic leukemia (ALL) treatment: a review study.* Cancer Gene Ther, 2022.
7. Maude, S.L., et al., *Tisagenlecleucel in Children and Young Adults with B-Cell Lymphoblastic Leukemia.* N Engl J Med, 2018. **378**(5): p. 439-448.
8. Neelapu, S.S., et al., *Axicabtagene Ciloleucel CAR T-Cell Therapy in Refractory Large B-Cell Lymphoma.* N Engl J Med, 2017. **377**(26): p. 2531-2544.
9. Rafiq, S., C.S. Hackett, and R.J. Brentjens, *Engineering strategies to overcome the current roadblocks in CAR T cell therapy.* Nat Rev Clin Oncol, 2020. **17**(3): p. 147-167.
10. Wherry, E.J. and M. Kurachi, *Molecular and cellular insights into T cell exhaustion.* Nat Rev Immunol, 2015. **15**(8): p. 486-99.
11. Bengsch, B. and E.J. Wherry, *The importance of cooperation: partnerless NFAT induces T cell exhaustion.* Immunity, 2015. **42**(2): p. 203-205.
12. Gennert, D.G., et al., *Dynamic chromatin regulatory landscape of human CAR T cell exhaustion.* Proc Natl Acad Sci U S A, 2021. **118**(30).
13. Weber, E.W., et al., *Pharmacologic control of CAR-T cell function using dasatinib.* Blood Adv, 2019. **3**(5): p. 711-717.
14. Sterner, R.C. and R.M. Sterner, *CAR-T cell therapy: current limitations and potential strategies.* Blood Cancer J, 2021. **11**(4): p. 69.
15. McLellan, A.D. and S.M. Ali Hosseini Rad, *Chimeric antigen receptor T cell persistence and memory cell formation.* Immunol Cell Biol, 2019. **97**(7): p. 664-674.
16. Tantalo, D.G., et al., *Understanding T cell phenotype for the design of effective chimeric antigen receptor T cell therapies.* J Immunother Cancer, 2021. **9**(5).
17. Spiegel, J.Y., et al., *CAR T cells with dual targeting of CD19 and CD22 in adult patients with recurrent or refractory B cell malignancies: a phase 1 trial.* Nat Med, 2021. **27**(8): p. 1419-1431.
18. Si, S. and D.T. Teachey, *Spotlight on Tocilizumab in the Treatment of CAR-T-Cell-Induced Cytokine Release Syndrome: Clinical Evidence to Date.* Ther Clin Risk Manag, 2020. **16**: p. 705-714.
19. Moon, E.K., et al., *Multifactorial T-cell hypofunction that is reversible can limit the efficacy of chimeric antigen receptor-transduced human T cells in solid tumors.* Clin Cancer Res, 2014. **20**(16): p. 4262-73.
20. Weber, E.W., et al., *Transient rest restores functionality in exhausted CAR-T cells through epigenetic remodeling.* Science, 2021. **372**(6537).
21. Kobold, S., et al., *Impact of a New Fusion Receptor on PD-1-Mediated Immunosuppression in Adoptive T Cell Therapy.* J Natl Cancer Inst, 2015. **107**(8).
22. Roybal, K.T., et al., *Precision Tumor Recognition by T Cells With Combinatorial Antigen-Sensing Circuits.* Cell, 2016. **164**(4): p. 770-9.

23. Lienert, F., et al., *Synthetic biology in mammalian cells: next generation research tools and therapeutics.* Nat Rev Mol Cell Biol, 2014. **15**(2): p. 95-107.
24. Francois, P., et al., *Phenotypic model for early T-cell activation displaying sensitivity, specificity, and antagonism.* Proc Natl Acad Sci U S A, 2013. **110**(10): p. E888-97.
25. Salter, A.I., et al., *Comparative analysis of TCR and CAR signaling informs CAR designs with superior antigen sensitivity and in vivo function.* Sci Signal, 2021. **14**(697).
26. Ghosh, S., *T Cell Receptor Signaling.* 2020.
27. Qian, D., M.N. Mollenauer, and A. Weiss, *Dominant-negative zeta-associated protein 70 inhibits T cell antigen receptor signaling.* J Exp Med, 1996. **183**(2): p. 611-20.
28. Ramos, J.A., et al., *Rapid degradation of auxin/indoleacetic acid proteins requires conserved amino acids of domain II and is proteasome dependent.* Plant Cell, 2001. **13**(10): p. 2349-60.
29. Banaszynski, L.A., et al., *A rapid, reversible, and tunable method to regulate protein function in living cells using synthetic small molecules.* Cell, 2006. **126**(5): p. 995-1004.
30. Wandless, T., Chen, L., *ESTROGEN-RECEPTOR BASED LIGAND SYSTEM FOR REGULATING PROTEIN STABILITY.* United States Patent Office, 2014.
31. Miyazaki, Y., et al., *Destabilizing domains derived from the human estrogen receptor.* J Am Chem Soc, 2012. **134**(9): p. 3942-5.
32. Iwamoto, M., et al., *A general chemical method to regulate protein stability in the mammalian central nervous system.* Chem Biol, 2010. **17**(9): p. 981-8.
33. Trump, D.L., et al., *High-dose oral tamoxifen, a potential multidrug-resistance-reversal agent: phase I trial in combination with vinblastine.* J Natl Cancer Inst, 1992. **84**(23): p. 1811-6.
34. Gallinari, P., et al., *A functionally orthogonal estrogen receptor-based transcription switch specifically induced by a nonsteroid synthetic ligand.* Chem Biol, 2005. **12**(8): p. 883-93.
35. Lopez, C.L., et al., *Arming Immune Cell Therapeutics with Polymeric Prodrugs.* Adv Healthc Mater, 2021: p. e2101944.
36. Patrick S. Stayton, A.C., Debobrato DAS, Hye-Nam Son, Selvi Srinivasan, Katherine MONTGOMERY, Ian BLUMENTHAL, Courtney Crane, Michael Jensen, James MATTHAEI, John Chiefari, Maarten DANIAL, Fei Huang, James Macdonald, Almar Postma, Kathleen Turner, *Cell-based methods and compositions for therapeutic agent delivery and treatments using same. WO2018165198A1.* US Patent Office, 2018.
37. Indra, A.K., et al., *Temporally-controlled site-specific mutagenesis in the basal layer of the epidermis: comparison of the recombinase activity of the tamoxifen-inducible Cre-ER(T) and Cre-ER(T2) recombinases.* Nucleic Acids Res, 1999. **27**(22): p. 4324-7.
38. Shi, Y. and J.T. Koh, *Selective regulation of gene expression by an orthogonal estrogen receptor-ligand pair created by polar-group exchange.* Chem Biol, 2001. **8**(5): p. 501-10.
39. Yajima, I., et al., *Spatiotemporal gene control by the Cre-ERT2 system in melanocytes.* Genesis, 2006. **44**(1): p. 34-43.
40. Dhamad, A.E., et al., *Systematic Proteomic Identification of the Heat Shock Proteins (Hsp) that Interact with Estrogen Receptor Alpha (ERalpha) and Biochemical Characterization of the ERalpha-Hsp70 Interaction.* PLoS One, 2016. **11**(8): p. e0160312.
41. Fuentes, N. and P. Silveyra, *Estrogen receptor signaling mechanisms.* Adv Protein Chem Struct Biol, 2019. **116**: p. 135-170.
42. Pratt, W.B. and D.O. Toft, *Regulation of signaling protein function and trafficking by the hsp90/hsp70-based chaperone machinery.* Exp Biol Med (Maywood), 2003. **228**(2): p. 111-33.
43. Sommermeyer, D., et al., *Fully human CD19-specific chimeric antigen receptors for T-cell therapy.* Leukemia, 2017. **31**(10): p. 2191-2199.

44. Majzner, R.G., et al., *CAR T Cells Targeting B7-H3, a Pan-Cancer Antigen, Demonstrate Potent Preclinical Activity Against Pediatric Solid Tumors and Brain Tumors.* Clin Cancer Res, 2019. **25**(8): p. 2560-2574.
45. Ravanpay, A.C., et al., *EGFR806-CAR T cells selectively target a tumor-restricted EGFR epitope in glioblastoma.* Oncotarget, 2019. **10**(66): p. 7080-7095.
46. Betts, M.R. and R.A. Koup, *Detection of T-cell degranulation: CD107a and b.* Methods Cell Biol, 2004. **75**: p. 497-512.
47. Kisanga, E.R., et al., *Tamoxifen and metabolite concentrations in serum and breast cancer tissue during three dose regimens in a randomized preoperative trial.* Clin Cancer Res, 2004. **10**(7): p. 2336-43.
48. Haso, W., et al., *Anti-CD22-chimeric antigen receptors targeting B-cell precursor acute lymphoblastic leukemia.* Blood, 2013. **121**(7): p. 1165-74.
49. Fry, T.J., et al., *CD22-targeted CAR T cells induce remission in B-ALL that is naive or resistant to CD19-targeted CAR immunotherapy.* Nat Med, 2018. **24**(1): p. 20-28.
50. Leung, W.H., et al., *Sensitive and adaptable pharmacological control of CAR T cells through extracellular receptor dimerization.* JCI Insight, 2019. **5**(11).
51. Mellatyar, H., et al., *Targeted cancer therapy through 17-DMAG as an Hsp90 inhibitor: Overview and current state of the art.* Biomed Pharmacother, 2018. **102**: p. 608-617.
52. Sikander, M., et al., *Cucurbitacin D exhibits potent anti-cancer activity in cervical cancer.* Sci Rep, 2016. **6**: p. 36594.
53. Reid, J.M., et al., *Pharmacokinetics of endoxifen and tamoxifen in female mice: implications for comparative in vivo activity studies.* Cancer Chemother Pharmacol, 2014. **74**(6): p. 1271-8.
54. Koubek, E.J., et al., *Bioavailability and Pharmacokinetics of Endoxifen in Female Rats and Dogs: Evidence to Support the Use of Endoxifen to Overcome the Limitations of CYP2D6-Mediated Tamoxifen Metabolism.* Drug Metab Dispos, 2023. **51**(2): p. 183-192.
55. Binkhorst, L., et al., *Circadian variation in tamoxifen pharmacokinetics in mice and breast cancer patients.* Breast Cancer Res Treat, 2015. **152**(1): p. 119-128.
56. Lien, E.A., et al., *Distribution of tamoxifen and metabolites into brain tissue and brain metastases in breast cancer patients.* Br J Cancer, 1991. **63**(4): p. 641-5.
57. Ajina, A. and J. Maher, *Strategies to Address Chimeric Antigen Receptor Tonic Signaling.* Mol Cancer Ther, 2018. **17**(9): p. 1795-1815.
58. Connolly, K.A., et al., *A reservoir of stem-like CD8(+) T cells in the tumor-draining lymph node preserves the ongoing antitumor immune response.* Sci Immunol, 2021. **6**(64): p. eabg7836.
59. Arcangeli, S., et al., *Next-Generation Manufacturing Protocols Enriching T(SCM) CAR T Cells Can Overcome Disease-Specific T Cell Defects in Cancer Patients.* Front Immunol, 2020. **11**: p. 1217.
60. Blumenthal, I., Jensen, MCV, Johnson, A, Koning, R, Reid, A., *Activity-Inducible Fusion Proteins Having a Heat Shock Protein 90 Binding Domain*, P. Pending, Editor. 2022.
61. Panneerselvam, P., et al., *T-cell death following immune activation is mediated by mitochondria-localized SARM.* Cell Death Differ, 2013. **20**(3): p. 478-89.
62. Wang, X., et al., *Phenotypic and functional attributes of lentivirus-modified CD19-specific human CD8+ central memory T cells manufactured at clinical scale.* J Immunother, 2012. **35**(9): p. 689-701.

Supplemental Data

SD1. Selected additional donor cell and manufacturing data.

SD2. Selected controls for B7H3CAR-3Gly-EBD(variant) CD107A dose response curves (Figure 14B)

SD3. huCD19CAR-XGly-EBD(4OHT) linker variants are dose responsive to drug induction. Donor 2 data.

SD4. Additional control data for the B7H3CAR-3Gly-EBD(variant) ICCS experiment (Figure 15A-F).

SD5. Additional control data for the huCD19CAR-XGly-EBD(4OHT) linker variant ICCS experiment (Figure 15G-H).

SD6. Additional control data for B7H3CAR-3G-EBD variant cytokine release assay (Figure 16A).

SD7. Cytokine release data for B7H3CAR-3Gly-EBD(4OHT) donor 2.

SD8. Chromium Release Assay data of the B7H3CAR-3Gly-EBD(4OHT) construct. Donor 2.

SD9. The huCD22CAR-3Gly-EBD(4OHT) construct enables full control over the killing of primary tumors expressing a common leukemia antigen.

SD10. huCD19CAR-1G-EBD(4OHT) chromium release data from three donors demonstrates anomalous donor to donor variation of this construct.

SD11. Donor to donor variation of the huCD19CAR-1Gly-EBD(4OHT), extends across targets and experiments.

Figure SD1. Selected additional donor cell and manufacturing data.

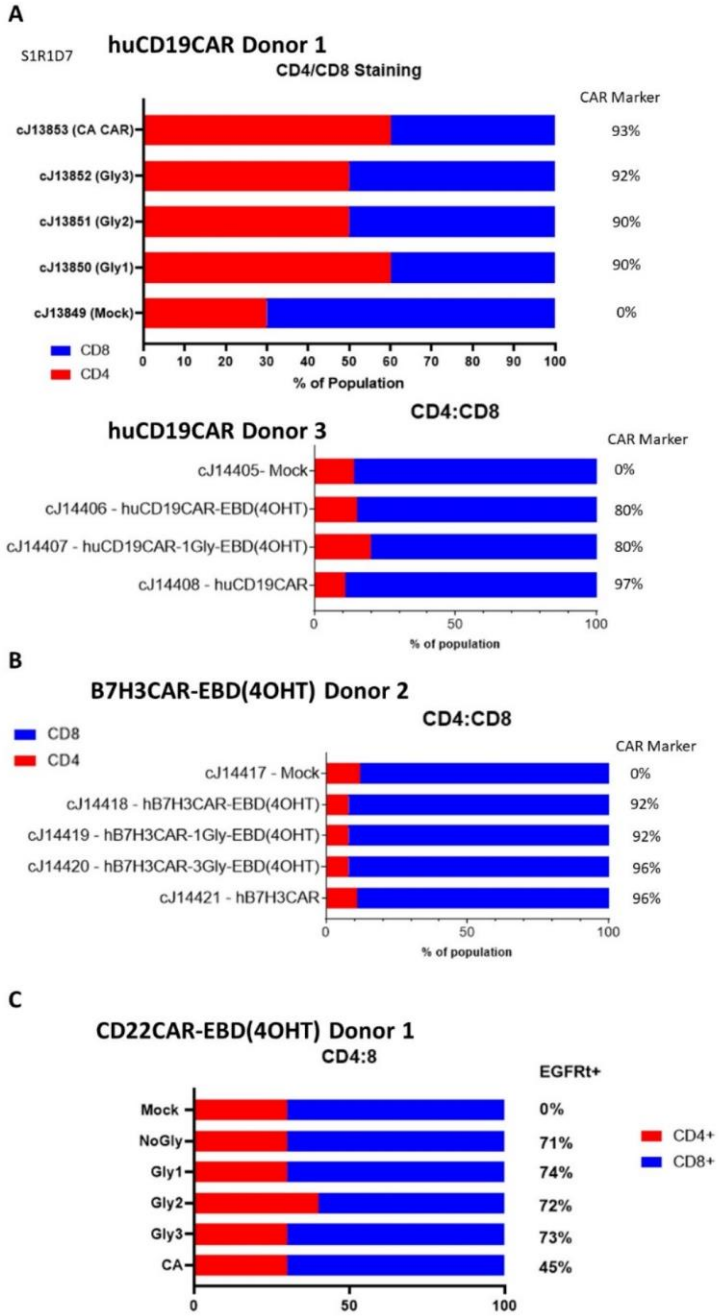

Selected additional donor data. Construct positivity and CD4/CD8 split after production and REP1. Data represents cells between REP1 day 7 and REP1 day 12. Cell manufacturing is described in detail in the methods section. In brief, isolated CD4 and CD8 T cells are mixed at a 60:40 ratio, stimulated with CD3/CD28 beads, transduced with virus containing a construct, and grown in fully cytokine-supplemented defined media for 7-14 days. Note that many donors skew, with the majority (but not all) skewing to CD8s. Supplemental cytokine (e.g., IL-2 or IL-7) may be added to help correct for skew, though broadly, we have not seen significant differences between donors or lines with one skew vs another.

Figure SD2. Selected controls for B7H3CAR-3Gly-EBD(variant) CD107A dose response curves (Figure 14B)

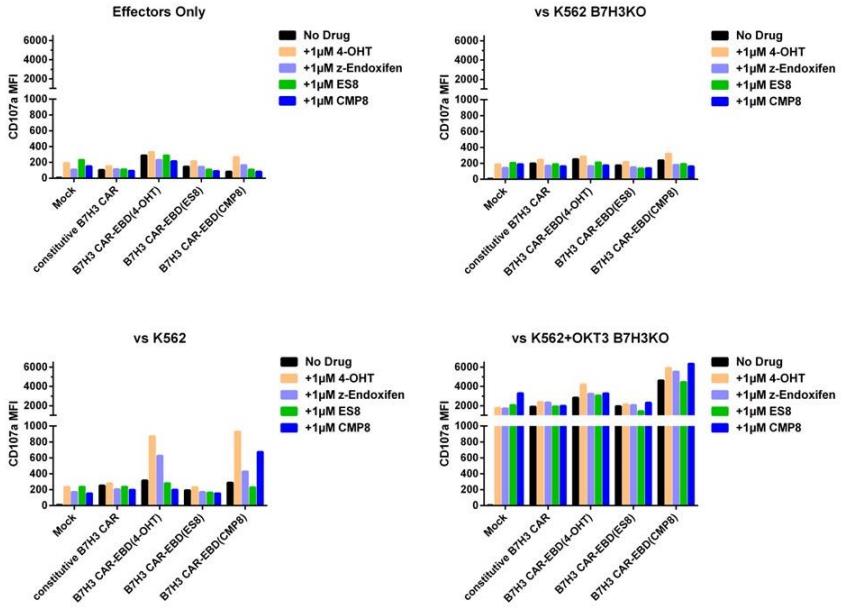

Additional controls for the experiment presented in Figure 14B highlighting the negative control conditions (Effectors only, vs K562 B7H3KO), the positive control condition (vs K562+OKT3 B7H3KO), and the experimental condition which defines the parameters of the dose response curve ultimately generated.

Figure SD3. huCD19CAR-XGly-EBD(4OHT) linker variants are dose responsive to drug induction. Donor 2 data.

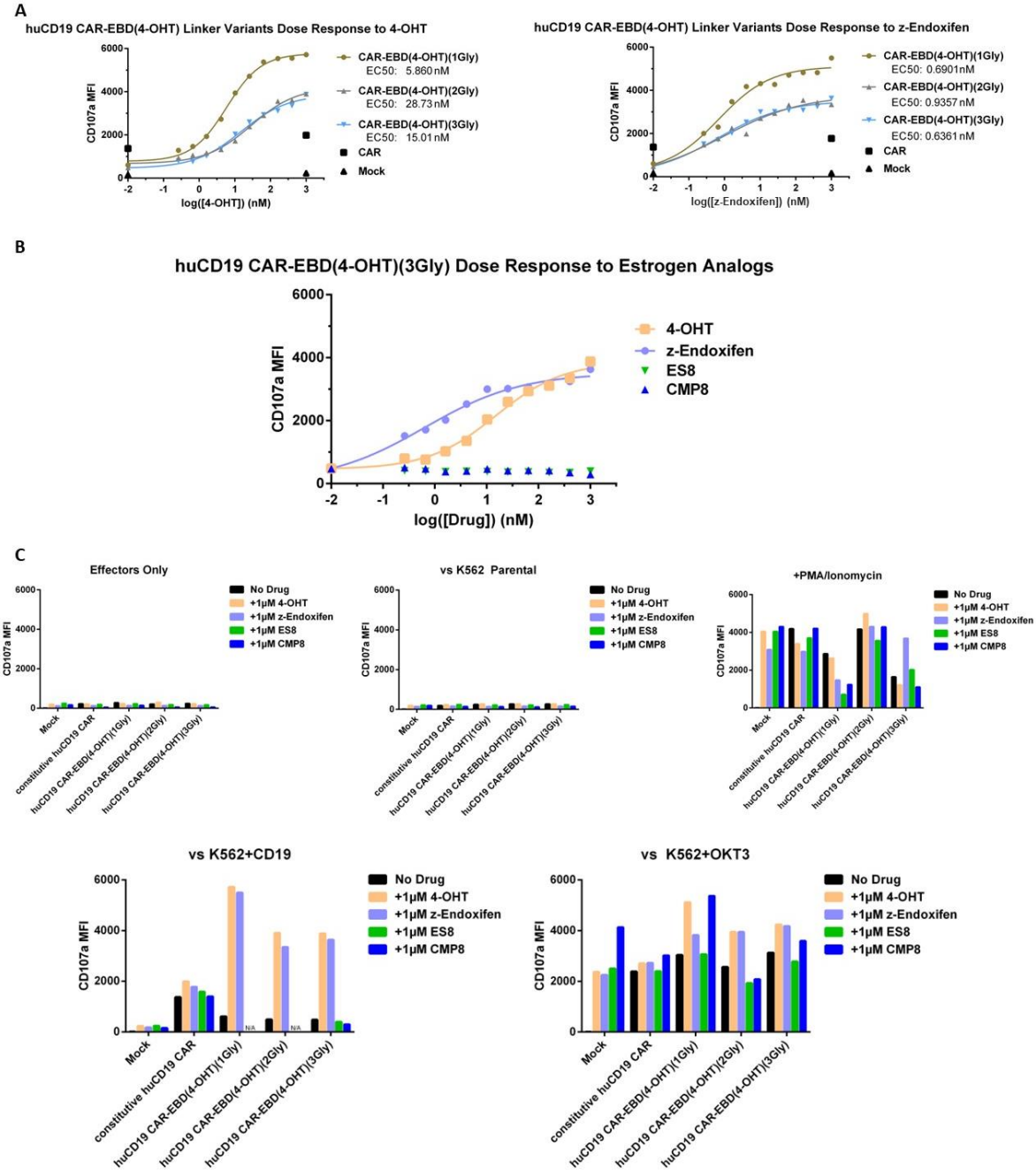

A) linker variant dose response curves to (Z)-4-OHT and (Z)-endoxifen. B) 3Gly linker variant dose response to drug induction with four different estrogen analogs. C) Experiment control data (left to right, top to bottom – T cells only, T cells vs antigen negative tumor cells, T cells stimulated with PMA/Ionomycin, experimental condition T cells vs antigen expressing with no drug induction or maximum drug induction, T cells vs tumor cells expressing an anti-CD3 antibody).

Figure SD4. Additional control data for the B7H3CAR-3Gly-EBD(variant) ICCS experiment (Figure 15A-F).

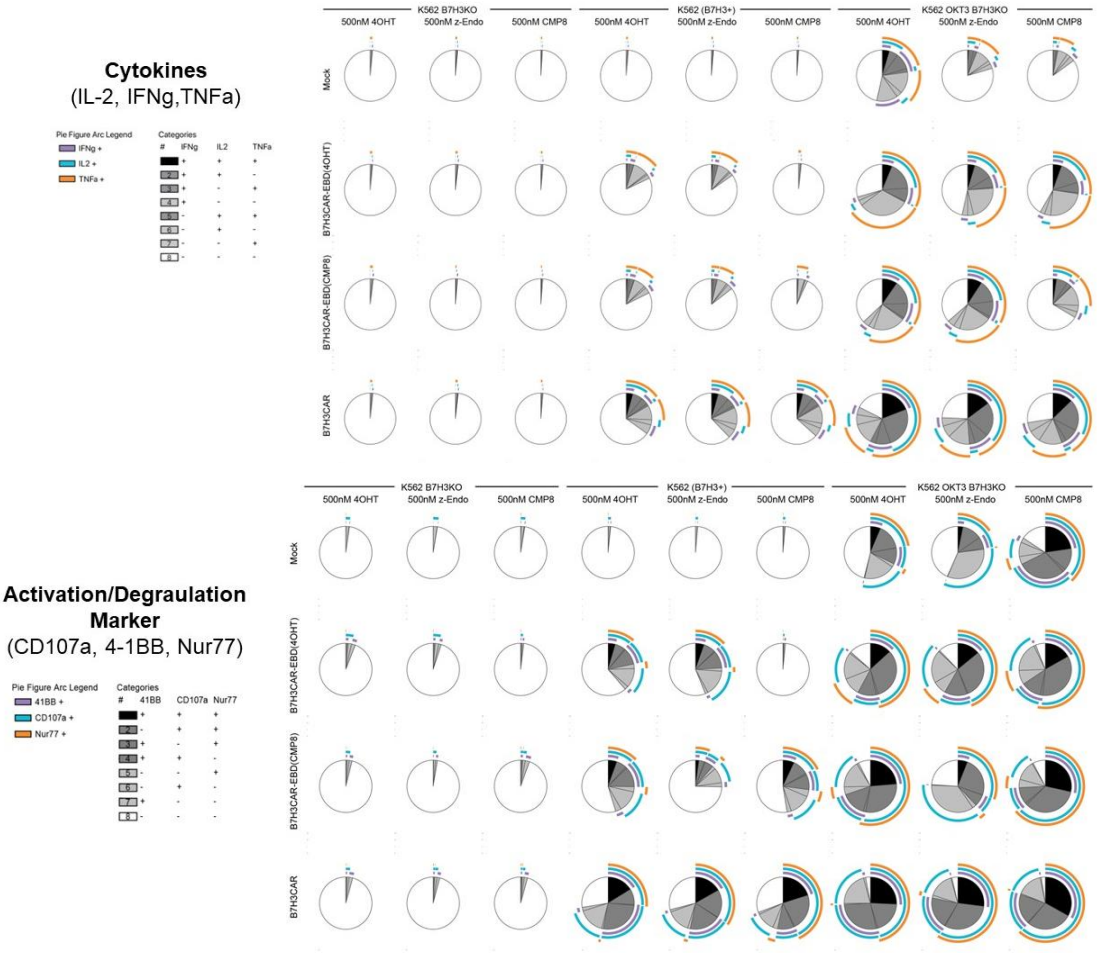

Complete controls for the ICCS experiment presented in Figure 15A-F. Cytokine production above and Activation/Degranulation markers below. In brief, primary human T cells expressing either a construct in the B7H3CAR-3Gly-EBD(XXXX) EBD variants cohort, the B7H3CAR, or no CAR were cultured with or without inducer molecules for 24 hours before being placed in co-culture for 4 hours with K562 tumor lines expressing target antigen (B7H3), or no antigen (B7H3 knockout), or a CAR-independent activation molecule (B7H3 knockout +OKT3). Cells were then stained for extracellular markers (CD4, CD8, transduction marker, CD107a, 4-1BB) and intracellular markers (Nur77, IL-2, IFNg, TNFa). Representative data from 2 donors. G&H) primary human T cells expressing either a construct in the huCD19-XGly-EBD(4OHT) linker variants cohort, the huCD19CAR, or no CAR were cultured with or without inducer molecules for 24 hours before being placed in co-culture for 4 hours with K562 tumor lines transduced to express target antigen (+CD19), or no antigen (K562 parental line), or a CAR-independent activation molecule (+OKT3). Cells were then stained for extracellular markers (CD4, CD8, transduction marker, CD107a, 4-1BB) and intracellular markers (Nur77, IL-2, IFNg, TNFa).

Figure SD5. Additional control data for the huCD19CAR-XGly-EBD(4OHT) linker variant ICCS experiment (Figure 15G-H).

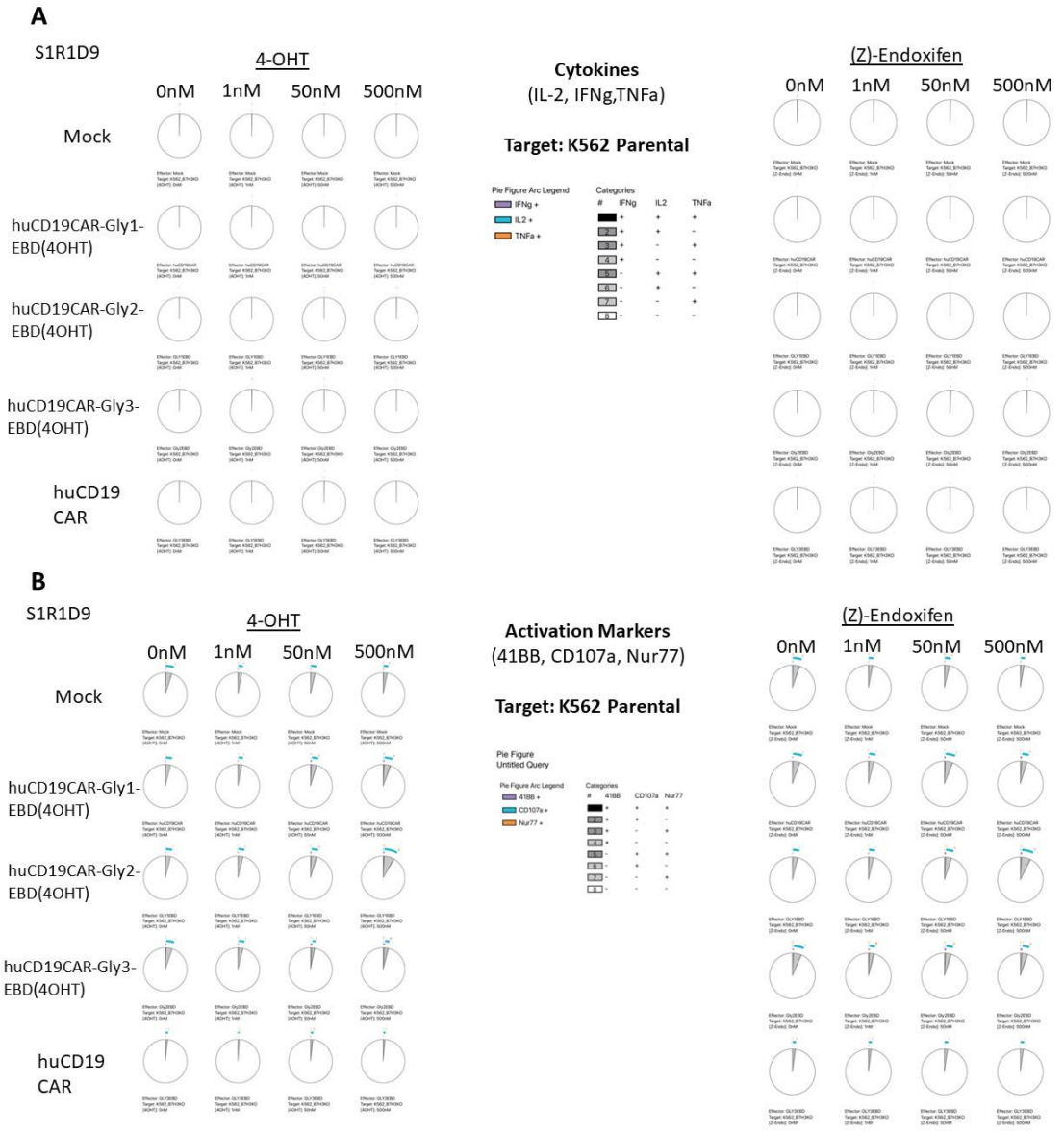

Full set of controls for the experiment presented in Figure 15G-H. A) Cytokine production, B) Activation/Degranulation markers below. (Z)-4-OHT data presented on the left, (Z)-endoxifen data presented on the right. Experimental description available in the methods and the description of Figure S3.

Figure SD6. Additional control data for B7H3CAR-3G-EBD variant cytokine release assay (Figure 16A).

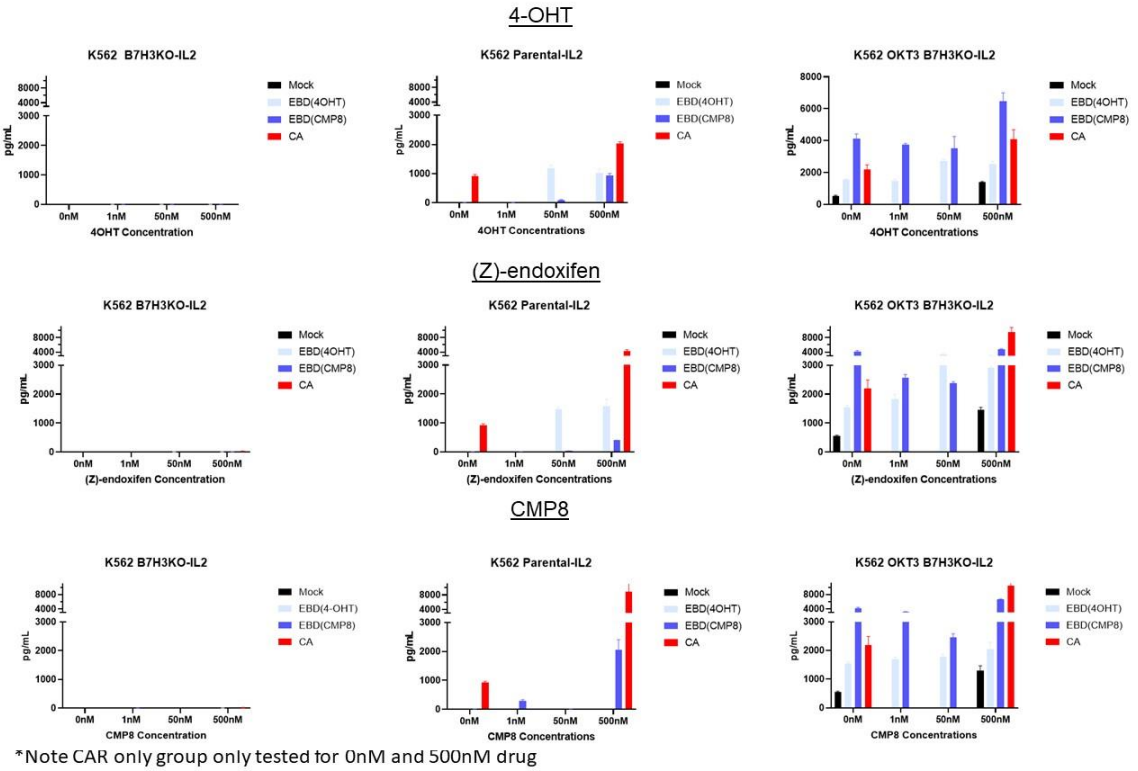

Additional control data for the B7H3CAR-3G-EBD variant cytokine release assay presented in Figure 16A, highlighting the negative controls (left column) where the T cells are cocultured with K562s that have had a genetic knockout of the B7H3 protein and positive controls (right column) where the T cells are exposed to K562s engineered to express an anti-CD3 antibody. Sample data from IL-2 is presented, however trends were very similar for TNFα and IFNγ.

Figure SD7. Cytokine release data for B7H3CAR-3Gly-EBD(4OHT) donor 2.

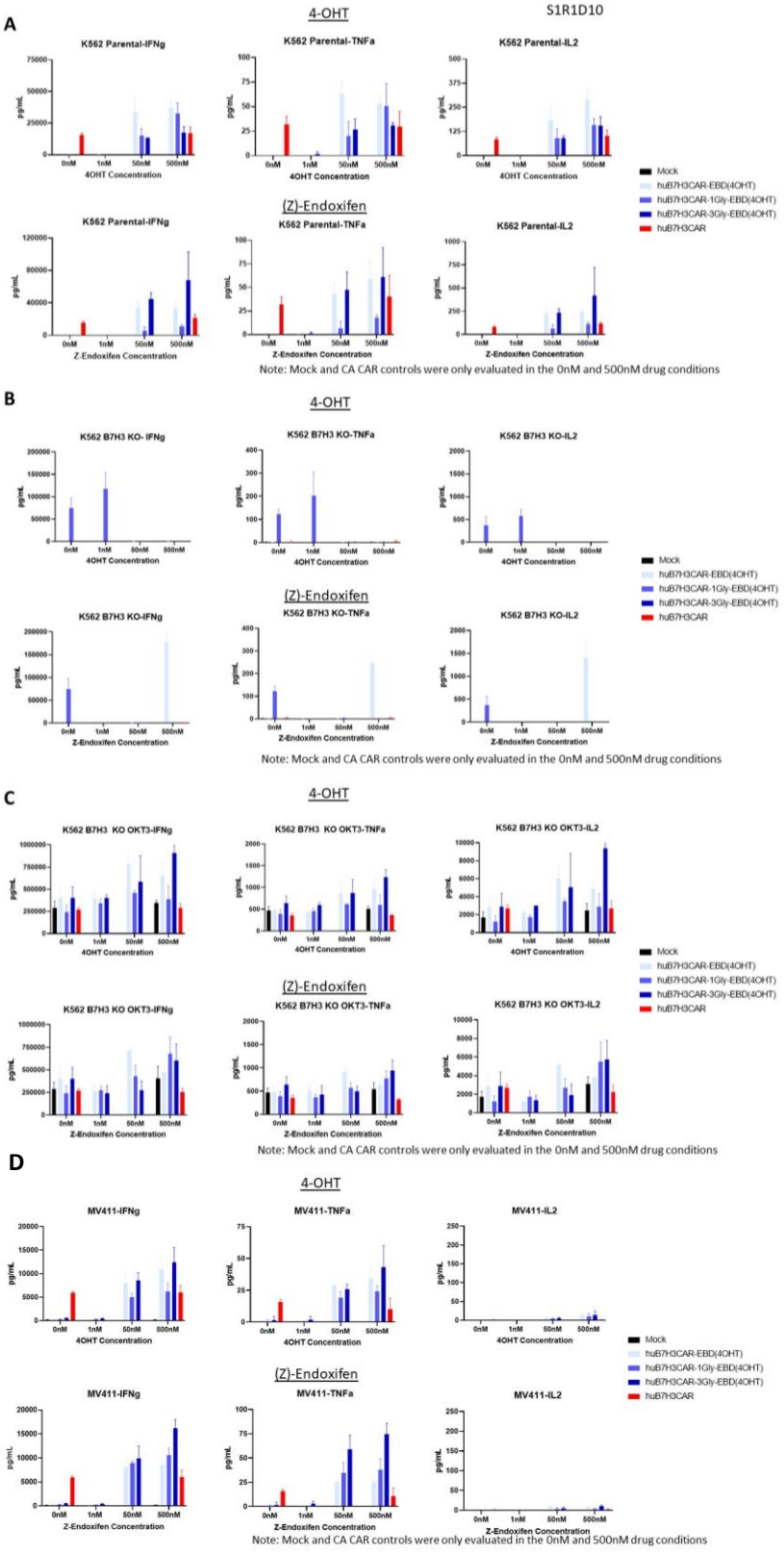

(Previous Page) Cytokine release data for B7H3CAR-3Gly-EBD(4OHT) donor 2. Primary human T cells expressing either a construct in the B7H3CAR-3Gly-EBD(XXXX) EBD variants cohort, the B7H3CAR, or no CAR were cultured with or without inducer molecules for 24 hours before being placed in co-culture for 24 hours with K562 tumor lines expressing target antigen (B7H3), or no antigen (B7H3 knockout), or a CAR-independent activation molecule (B7H3 knockout +OKT3). Supernatants were recovered from each well before being assessed for cytokine concentration by electrochemiluminescence. Trends in this data are consistent with those seen in donor 1. A) and D) represent experimental conditions against two different targets (K562 and MV411 tumor cells). B) and C) represent control conditions (negative and positive, respectively). Where there were some issues with the negative controls, it did not appear to meaningfully alter the data from the experimental conditions, and may represent user error in prepping the analysis.

Figure SD8. Chromium Release Assay data of the B7H3CAR-3Gly-EBD(4OHT) construct. Donor 2.

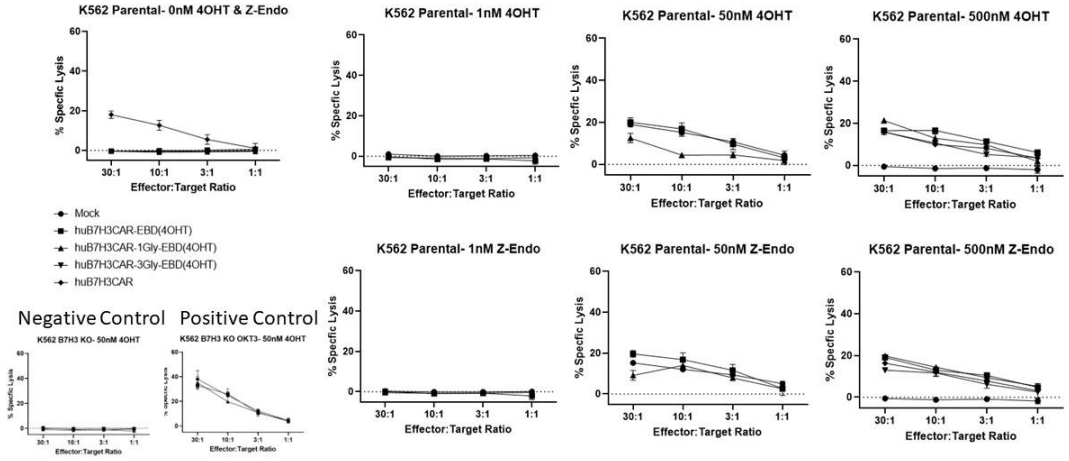

Chromium release assays of B7H3CAR-3Gly-EBD(4OHT) construct including a linker varitation were plated with target antigen expressing K562 tumor lines which had been loaded with Cr51. T cells receiving drug treatment were are incubated with appropriate inducer molecule for 24hrs prior to exposure to target tumor at a range of effector:target ratios, then supernatants were collected and degree of lysis assessed by radioactive scintillation detection. This data aligns well with the B7H3CAR-3Gly-EBDvariant donor 1 data presented in Figure 17A and B.

Figure SD9. The huCD22CAR-3Gly-EBD(4OHT) construct enables full control over the killing of primary tumors expressing a common leukemia antigen.

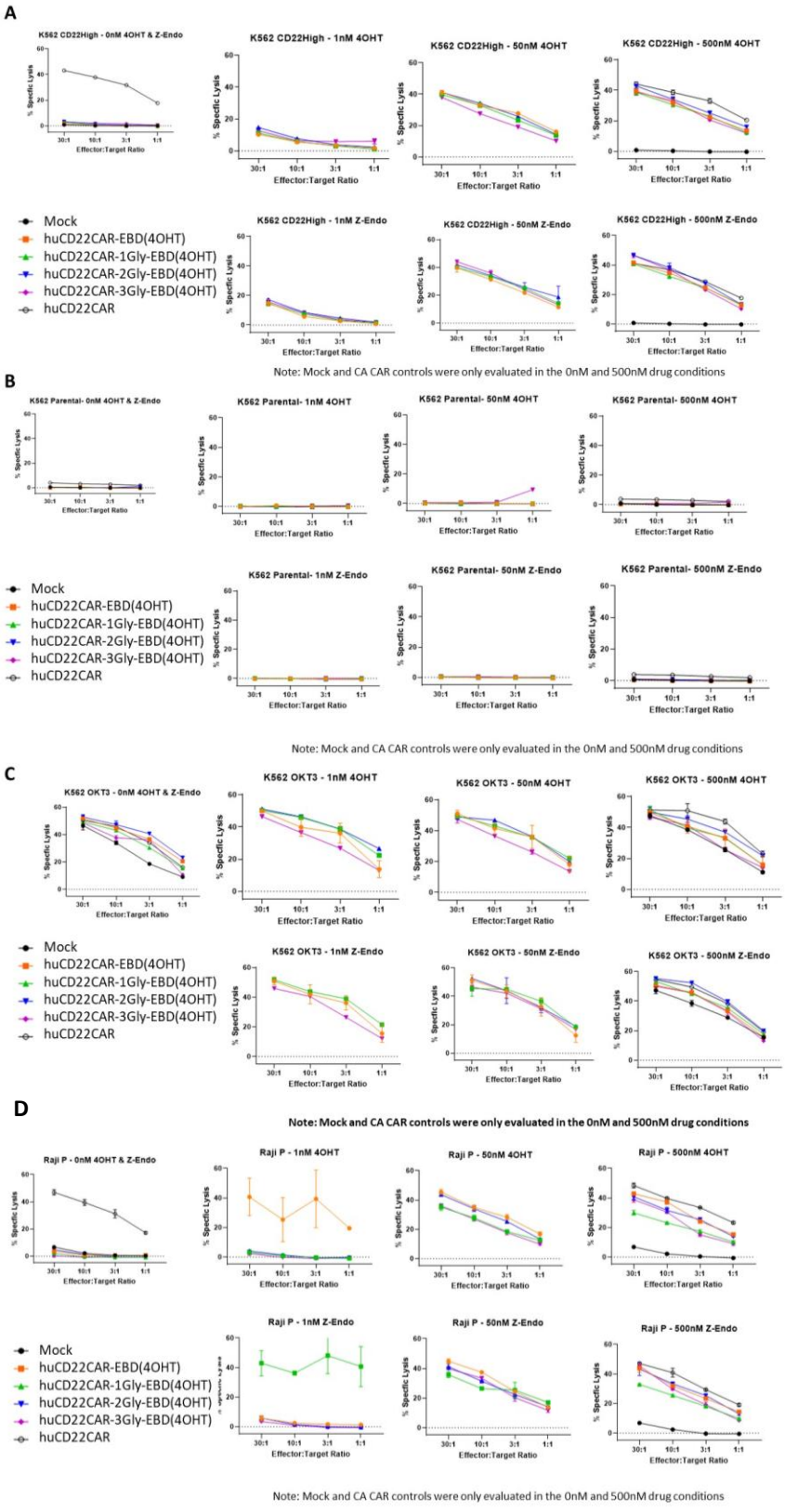

(Previous page) Chromium release assays of CD22CAR-3Gly-EBD(4OHT) constructs including varying linker or EBD variants against target antigen expressing K562 tumor lines which had been loaded with Cr51. T cells receiving drug treatment were are incubated with appropriate inducer molecule for 24hrs prior to exposure to target tumor at a range of effector:target ratios, then supernatants were collected and degree of lysis assessed by radioactive scintillation detection. This data supplements the abbreviated results provided in Figure 17C.

Figure SD10. huCD19CAR-1G-EBD(4OHT) chromium release data from three donors demonstrates anomalous donor to donor variation of this construct.

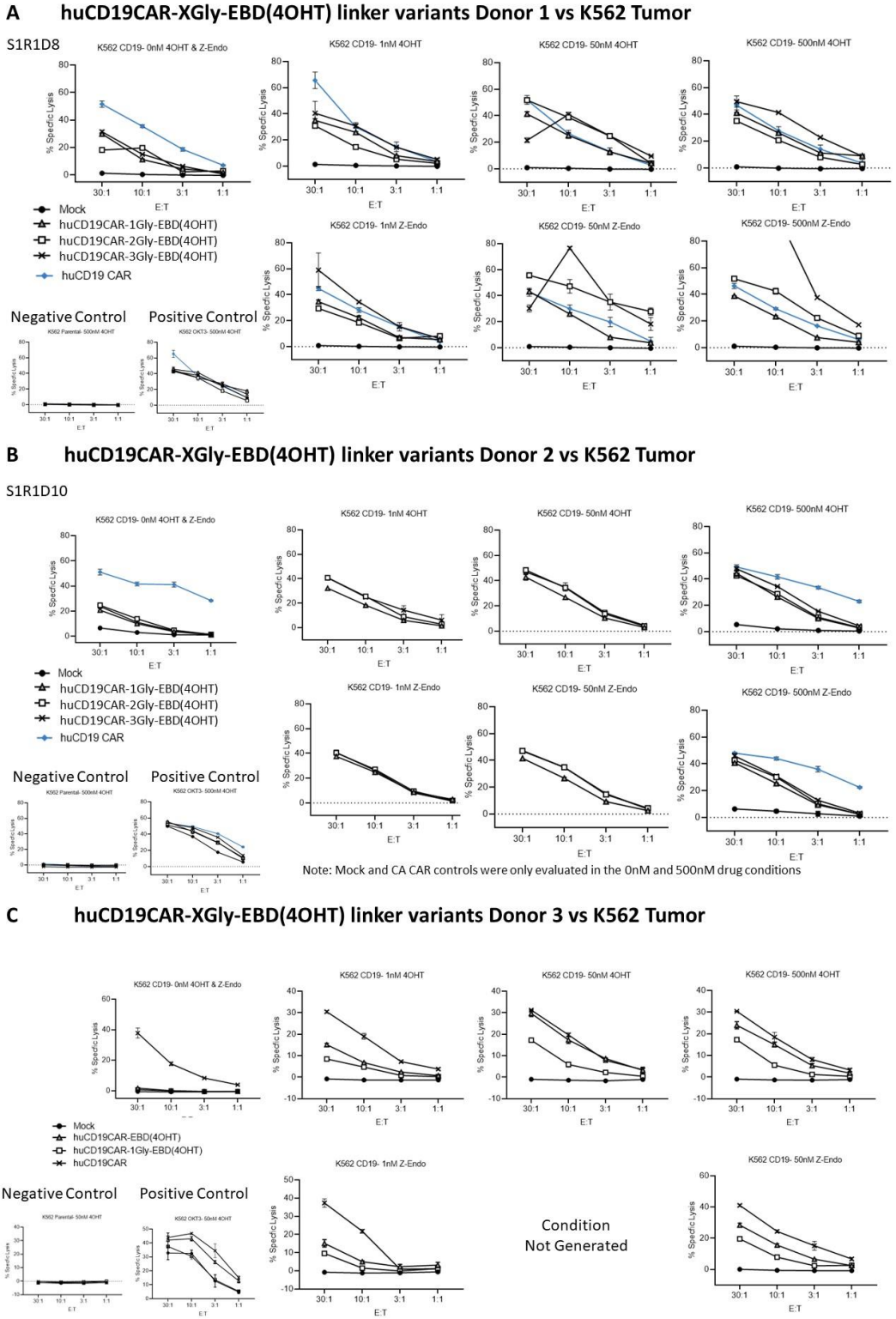

(Previous page) Chromium release assays of huCD19CAR-1Gly-EBD(4OHT) constructs including varying linker or EBD variants against target antigen expressing K562 tumor lines which had been loaded with Cr51. T cells receiving drug treatment were are incubated with appropriate inducer molecule for 24hrs prior to exposure to target tumor at a range of effector:target ratios, then supernatants were collected and degree of lysis assessed by radioactive scintillation detection. This data provides context for the abbreviated data sets presented in Figure 17D and Figure 20. Of particular importance is this data set represents one of the few instances we have experienced meaningful donor-to-donor variation with the CAR-EBD system. A) donor 1 data, B) donor 2 data, C) donor 3 data.

Figure SD11. Donor to donor variation of the huCD19CAR-1Gly-EBD(4OHT), extends across targets and experiments.

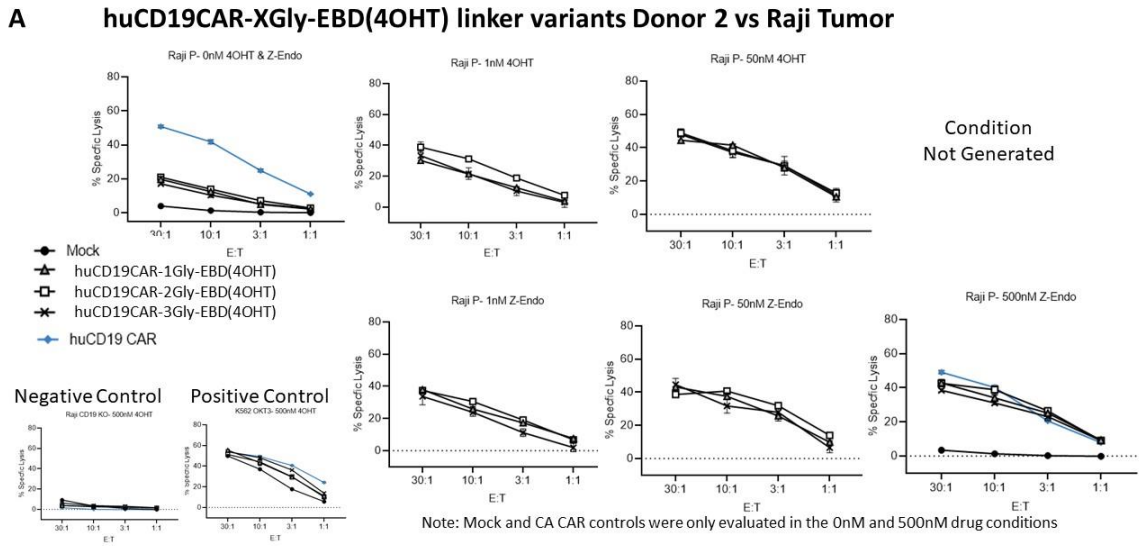

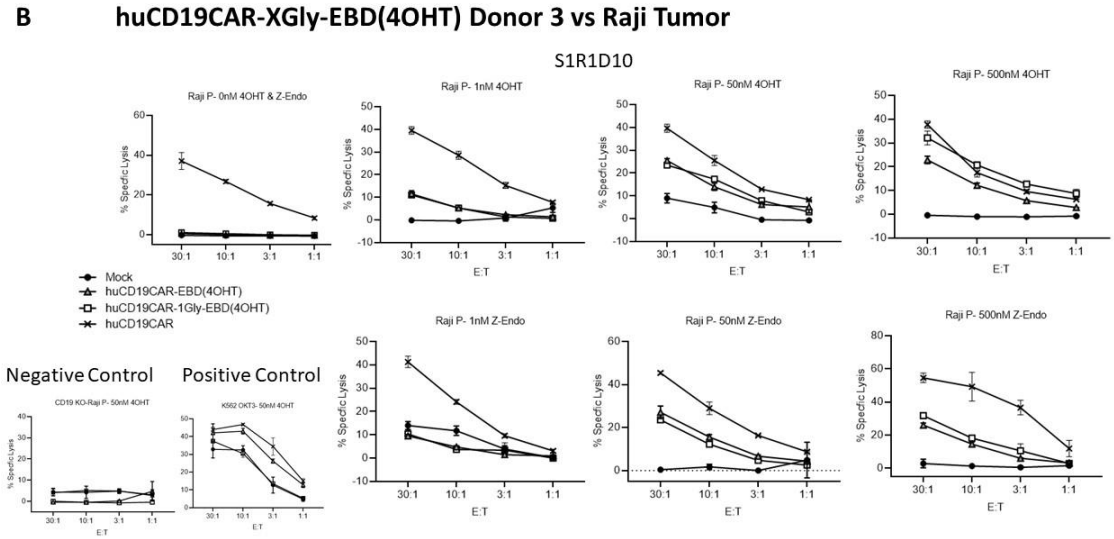

As an extension of the above data set, we looked at the a tumor cell line with a much lower antigen expression to see if and how it influenced both the leakiness of the huCD19CAR-1G-EBD(4OHT) construct as well as the donor to donor variation we were observing.